
Masters Theses

Student Theses and Dissertations

Summer 2011

Categorization and experimental evaluation of anchorage systems for fiber-reinforced polymer laminates bonded to reinforced concrete structures

Stephen V. Grelle

Follow this and additional works at: https://scholarsmine.mst.edu/masters_theses



Part of the [Civil Engineering Commons](#)

Department:

Recommended Citation

Grelle, Stephen V., "Categorization and experimental evaluation of anchorage systems for fiber-reinforced polymer laminates bonded to reinforced concrete structures" (2011). *Masters Theses*. 5152.
https://scholarsmine.mst.edu/masters_theses/5152

This thesis is brought to you by Scholars' Mine, a service of the Missouri S&T Library and Learning Resources. This work is protected by U. S. Copyright Law. Unauthorized use including reproduction for redistribution requires the permission of the copyright holder. For more information, please contact scholarsmine@mst.edu.

CATEGORIZATION AND EXPERIMENTAL EVALUATION OF ANCHORAGE
SYSTEMS FOR FIBER-REINFORCED POLYMER LAMINATES BONDED TO
REINFORCED CONCRETE STRUCTURES

by

STEPHEN VINCENT GRELLE

A THESIS

Presented to the Faculty of the Graduate School of the
MISSOURI UNIVERSITY OF SCIENCE AND TECHNOLOGY

In Partial Fulfillment of the Requirements for the Degree

MASTER OF SCIENCE IN CIVIL ENGINEERING

2011

Approved by

Lesley H. Sneed, Advisor
John J. Myers
K. Chandrashekhara

ABSTRACT

While externally-bonded fiber-reinforced polymer (FRP) composites are commonly used for the strengthening of structurally deficient reinforced concrete (RC) members, the topic of anchoring FRP to concrete to achieve higher design strengths has not been addressed. Many innovative systems have been developed to anchor FRP to concrete, but the research involving these anchorage systems is not centralized and is therefore difficult to access. Additionally, systematic testing procedures for evaluating the strength of an anchorage system have not been widely used. To aid in the organization of anchorage system research and facilitate a better understanding of anchorage system behavior, a categorization system was developed based on the understood behavior of the FRP anchorage systems, as well as their potential applications. This new categorization system was used to discuss the applicability of anchorage testing procedures to various types of anchorage. Experimental research involving anchorage systems used for the emergency repair of severely damaged bridge columns was also performed. The anchorage systems included a novel anchorage system that was the focus of the experimental portion of this research. Results from the experimental program show that while the novel anchorage has promise for use in FRP strengthening applications, the assumed behavior of the novel anchorage was inconsistent with the observed behavior. Because detailed design procedures could not be developed using the experimental data, future testing of this anchorage system should be performed in the absence of the large number of variables that affected the anchorage's performance during the column tests.

ACKNOWLEDGMENTS

First and foremost, I would like to express my sincere gratitude to my advisor, Dr. Lesley Sneed, for giving me the opportunity to study with her at Missouri S&T. My experience both as a graduate student and research assistant has been outstanding and I owe much of my success to her unwavering commitment to me and the rest of her students. I would also like to thank the other members of my graduate committee, Dr. John Myers and Dr. K. Chandrashekhara for their support during my graduate studies.

I am extremely grateful for the opportunity to work with Ruili He, Yang Yang, and Corey Grace. I was fortunate enough to spend a large amount of time working with them on this project, during which time they have become my good friends. Their hard work and companionship were essential in making the long days and nights spent working on this project more enjoyable.

I would also like to thank the many others who contributed to this project, including Jason Cox, John Bullock, Gary Abbott, Brian Swift, Steve Gabel, and Bill Frederickson. Without their assistance, the column repair would not have been possible. Additionally, thanks are due to Dr. Abdeldjelil Belarbi for his donation of the columns to our research group and to Qian Li for teaching me how to set up and test the columns. Thank you also to Carlos Ortega, whose expertise on the topic of FRP anchorage was a valuable resource.

I am also very grateful to the sources of funding that helped me finance my graduate studies at Missouri S&T. In addition to the generous funding provided to me by Dr. Sneed, I was fortunate to receive the Missouri S&T Chancellor's Fellowship from the Office of Graduate Studies which has helped me immensely during the course of my graduate education.

Finally, I would like to thank my mother, Debbie Grelle, my father, Vince Grelle, and my sisters, Andrea and Melissa Grelle for their quiet but constant support of my graduate education. I would also like to express gratitude to my girlfriend of over eight years, Emilie Lueker, for her patience and support of my decision to pursue this degree.

TABLE OF CONTENTS

| | Page |
|--|------|
| ABSTRACT..... | iii |
| ACKNOWLEDGMENTS | iv |
| LIST OF ILLUSTRATIONS..... | x |
| LIST OF TABLES..... | xiv |
| NOMENCLATURE | xv |
| SECTION | |
| 1. INTRODUCTION..... | 1 |
| 1.1. GENERAL..... | 1 |
| 1.2. BACKGROUND | 2 |
| 1.2.1. Overview of FRP Composite Systems..... | 2 |
| 1.2.2. Externally Bonded FRP in Civil Engineering..... | 3 |
| 1.2.3. Rapid Repair of Earthquake Damaged Structures..... | 4 |
| 1.2.4. FRP-to-Concrete Anchorage Systems..... | 4 |
| 1.3. PROBLEM DEFINITION..... | 6 |
| 1.3.1. General Challenges for Anchorage System Research..... | 6 |
| 1.3.2. Anchorage Systems for Repaired Bridge Columns..... | 7 |
| 1.4. OBJECTIVES..... | 8 |
| 1.5. SCOPE AND LIMITATIONS OF RESEARCH..... | 8 |
| 1.6. THESIS ORGANIZATION..... | 9 |
| 2. LITERATURE REVIEW..... | 10 |
| 2.1. GENERAL..... | 10 |
| 2.2. TYPES OF ANCHORAGE SYSTEMS..... | 10 |
| 2.2.1. Anchor Spikes..... | 10 |
| 2.2.1.1 90° Anchor Spikes..... | 10 |
| 2.2.1.2 180° Anchor Spikes..... | 13 |
| 2.2.2. Transverse Wrapping..... | 15 |
| 2.2.3. U-Anchors..... | 18 |
| 2.2.4. Longitudinal Chase..... | 20 |

| | |
|--|----|
| 2.2.5. FRP Strips..... | 22 |
| 2.2.6. Plate Anchors. | 23 |
| 2.2.7. Bolted Angles. | 23 |
| 2.2.8. Cylindrical Hollow Section (CHS) Anchorage. | 27 |
| 2.2.9. Ductile Anchorage System. | 27 |
| 2.3. APPLICATIONS FOR ANCHORAGE SYSTEMS | 28 |
| 2.3.1. Flexural Strengthening. | 29 |
| 2.3.1.1 Beams, Girders, and Slabs. | 29 |
| 2.3.1.2 Columns. | 30 |
| 2.3.1.3 Shear Walls. | 30 |
| 2.3.2. Shear Strengthening. | 30 |
| 2.3.3. Other Strengthening Schemes. | 31 |
| 2.4. EXPERIMENTAL PERFORMANCE OF ANCHORAGE SYSTEMS | 31 |
| 2.4.1. Anchor Spikes. | 32 |
| 2.4.1.1 90° Anchor Spikes. | 32 |
| 2.4.1.2 180° Anchor Spikes. | 32 |
| 2.4.2. Transverse Wrapping. | 33 |
| 2.4.3. U-Anchors. | 34 |
| 2.4.4. Longitudinal Chase..... | 35 |
| 2.4.5. FRP Strips..... | 35 |
| 2.4.6. Plate Anchors. | 36 |
| 2.4.7. Bolted Angles. | 36 |
| 2.4.8. Cylindrical Hollow Section (CHS) Anchorage. | 37 |
| 2.4.9. Ductile Anchorage Systems. | 38 |
| 2.4.10. Anchorage Summary. | 38 |
| 2.5. ANCHORAGE TEST PROCEDURES | 44 |
| 2.5.1. Shear Type Anchorage Tests..... | 44 |
| 2.5.2. Pull-Out Type Anchorage Tests. | 47 |
| 2.5.3. Bending Type Anchorage Tests. | 47 |
| 2.6. CONCLUDING REMARKS..... | 49 |
| 3. ANCHORAGE SYSTEM CATEGORIZATION | 50 |

| | |
|--|----|
| 3.1. GENERAL | 50 |
| 3.2. DEFINITION OF ANCHORAGE SYSTEM CATEGORIES | 50 |
| 3.2.1. Type I Anchorage Definition. | 51 |
| 3.2.2. Type II Anchorage Definition. | 51 |
| 3.2.3. Type III Anchorage Definition..... | 51 |
| 3.3. CATEGORIZATION OF EXISTING ANCHORAGE SYSTEMS | 52 |
| 3.3.1. Anchor Spikes. | 53 |
| 3.3.1.1 90° Anchor Spikes. | 53 |
| 3.3.1.2 180° Anchor Spikes. | 53 |
| 3.3.2. Transverse Wrapping. | 54 |
| 3.3.3. U-Anchors and Longitudinal Chases. | 55 |
| 3.3.4. FRP Strips..... | 56 |
| 3.3.5. Plate Anchors. | 57 |
| 3.3.6. Bolted Angles. | 57 |
| 3.3.7. CHS Anchorage and Ductile Anchorage Systems. | 58 |
| 3.4. APPLICABILITY OF ANCHORAGE TESTING PROCEDURES | 58 |
| 3.4.1. Type I and Type II Testing Procedures. | 60 |
| 3.4.2. Type III Testing Procedures. | 60 |
| 3.5. CONCLUDING REMARKS..... | 61 |
| 4. EXPERIMENTAL PROGRAM..... | 63 |
| 4.1. GENERAL..... | 63 |
| 4.2. BACKGROUND OF DAMAGED COLUMNS | 64 |
| 4.2.1. Testing Program. | 64 |
| 4.2.2. Original Column Design. | 65 |
| 4.2.3. Damage Review of Original Columns. | 66 |
| 4.3. REPAIR GOALS | 67 |
| 4.4. MATERIAL PROPERTIES | 68 |
| 4.4.1. Composite Repair Materials..... | 68 |
| 4.4.2. Concrete Properties..... | 70 |
| 4.4.3. Anchorage Materials. | 71 |
| 4.5. REPAIR DESIGN..... | 71 |

| | |
|---|-----|
| 4.5.1. Column #1 Design..... | 71 |
| 4.5.2. Column #2 Design..... | 72 |
| 4.5.3. Column #3 Design..... | 73 |
| 4.6. ANCHORAGE DESIGN AND CONSTRUCTION | 74 |
| 4.6.1. Design Philosophies. | 75 |
| 4.6.2. Anchor Rod Arrangement. | 76 |
| 4.6.3. Anchorage System Concept and Design. | 77 |
| 4.6.4. Other Anchorage. | 83 |
| 4.7. REPAIR PROCEDURE..... | 85 |
| 4.7.1. Pre-Repair Work..... | 85 |
| 4.7.2. Removal of Loose Concrete. | 86 |
| 4.7.3. Placement of Repair Mortar. | 87 |
| 4.7.4. Concrete Surface Preparation. | 88 |
| 4.7.5. Installation of FRP..... | 90 |
| 4.7.6. Installation of Anchorage. | 93 |
| 4.8. INSTRUMENTATION AND TESTING PROCEDURE | 95 |
| 4.8.1. Longitudinal Strain Gauges..... | 96 |
| 4.8.2. Strain Gauges on Novel Anchorage System. | 96 |
| 4.8.3. Load Cells on Novel Anchorage System. | 96 |
| 4.8.4. Test Setup. | 99 |
| 4.8.5. Testing Procedure..... | 101 |
| 5. EXPERIMENTAL RESULTS AND DISCUSSION..... | 102 |
| 5.1. GENERAL..... | 102 |
| 5.2. OVERALL BEHAVIOR OF REPAIRED COLUMNS | 102 |
| 5.2.1. Overall Behavior. | 102 |
| 5.2.2. Comparison to Original Column Behavior. | 110 |
| 5.3. PERFORMANCE OF ANCHORAGE SYSTEMS..... | 114 |
| 5.3.1. Novel Anchorage System..... | 114 |
| 5.3.1.1 Behavior of Novel Anchorage for Column #1..... | 115 |
| 5.3.1.2 Behavior of Novel Anchorage for Columns #2 and #3. | 122 |
| 5.3.1.3 Summary of Novel Anchorage Behavior..... | 130 |

- 5.3.2. U-Anchors. 131
- 5.3.3. Transverse Wrapping Anchorage. 131
- 5.4. DESIGN RECOMMENDATIONS 132
- 6. SUMMARY AND CONCLUSIONS..... 135
 - 6.1. SUMMARY OF RESEARCH PERFORMED 135
 - 6.2. CONCLUSIONS..... 136
 - 6.3. ONGOING STUDIES 137
 - 6.4. RECOMMENDATIONS FOR FUTURE RESEARCH..... 137
- APPENDICES
 - A. PHOTOS OF DAMAGED COLUMNS PRIOR TO REPAIR..... 139
 - B. DESIGN AND STRENGTH CALCULATIONS FOR NOVEL ANCHORAGE..... 146
 - C. DETERMINATION OF ANCHOR ROD FORCES FROM STRAIN GAUGE DATA 151
- BIBLIOGRAPHY 154
- VITA 159

LIST OF ILLUSTRATIONS

| Figure | Page |
|---|------|
| 1.1. FRP Debonding Failure Modes (Teng et al., 2002)..... | 5 |
| 2.1. Details of 90° Fiber Anchors Used by Piyong et al. (2003) | 11 |
| 2.2. Installation Pattern for 90° Anchor Spikes Used in Piyong et al. (2003) | 11 |
| 2.3. Comparison of 90° and 180° Anchor Spikes | 13 |
| 2.4. Potential Difficulties for Installation of 180° Anchor Spikes | 14 |
| 2.5. 180° Steel Anchor Spikes and GFRP Reinforcement From Prota et al. (2005) | 15 |
| 2.6. Details of 180° Anchor Spikes Studied in Sadone et al. (2010) | 15 |
| 2.7. Example of Transverse Wrapping Anchorage on T-Beam..... | 16 |
| 2.8. Transverse Wrapping Scheme from Antonopoulos and Triantafillou (2003) | 16 |
| 2.9. Transverse Wrapping Scheme from Khan and Ayub (2010)..... | 17 |
| 2.10. Prestressing Device for FRP Wraps Used in Zhuo et al. (2010) | 18 |
| 2.11. Schematic of Typical U-Anchor | 19 |
| 2.12. Types of U-Anchors..... | 19 |
| 2.13. Modified U-Anchor Used in Nagy-György et al. (2005) | 21 |
| 2.14. Longitudinal Chase Anchorage Used by Kalfat and Al-Mahaidi (2010) | 21 |
| 2.15. Example of FRP Strip Anchorage Systems | 22 |
| 2.16. Plated Anchorage Orientations in Ortega (2009)..... | 24 |
| 2.17. Plated Anchorage Details in Ortega (2009) | 24 |
| 2.18. Bolted Angle System Used by Foo et al. (2001) | 25 |
| 2.19. Bolted Angle System Used in Hwang et al. (2004)..... | 26 |
| 2.20. Steel Angle Anchorages Used in Antonopoulos and Triantafillou (2003)..... | 26 |
| 2.21. CHS Anchorage System from Hiotakis (2004) | 27 |
| 2.22. Ductile Anchorage System Used in Hall et al. (2002)..... | 28 |
| 2.23. Detailing Limitations When Extending an FRP Sheet Around a 90° Joint | 34 |
| 2.24. Debonding Due to Prying Action in Bolted Steel Angle Anchorage | 37 |
| 2.25. Optimized Anchor rod Reaction Forces for CHS Anchorage | 38 |
| 2.26. Single-Shear Anchorage Testing Setups..... | 45 |
| 2.27. Double-Shear Anchorage Testing Setups | 46 |

| | |
|---|----|
| 2.28. Pull-Out Type Anchorage Tests..... | 48 |
| 2.29. Bending Type Anchorage Test Used in Orton (2007) | 48 |
| 2.30. Bending Type Anchorage Test Used in Sami et al. (2010) | 49 |
| 3.1. Example of Type I Anchorage Device..... | 51 |
| 3.2. Comparison of Type II and Type III Anchorage (U-Anchor Example) | 52 |
| 3.3 Anchor Bend Force Transfer Mechanism Reported by Orton (2007) | 53 |
| 3.4. Force Transfer Mechanism of 180° Anchor in Type II Application | 54 |
| 3.5. Behavior of an After-Corner U-Anchor..... | 55 |
| 3.6. Type I Force Transfer Mechanism of FRP Strip Anchorage | 56 |
| 3.7. Type II Force Transfer Mechanism of Plate Anchors | 57 |
| 3.8. Process Leading to Field Implementation of New Anchorage Systems..... | 59 |
| 3.9. Summary of Anchorage Test Procedures and Categorization | 62 |
| 4.1. Original Column Elevations | 65 |
| 4.2. Cross-Sectional Arrangement of Reinforcement in Original Columns | 66 |
| 4.3. Definition of “Spalled Length” and “Core Crush Depth” | 67 |
| 4.4. Repair Design Drawing for Column #1 | 72 |
| 4.5. Repair Design Drawing for Column #2 | 73 |
| 4.6. Repair Design Drawing for Column #3 | 74 |
| 4.7. Embedment Locations of Anchor Rods in Footing | 77 |
| 4.8. Conceptual Diagram of Novel Anchorage System..... | 78 |
| 4.9. Assumed Behavior of Novel Anchorage System..... | 79 |
| 4.10. Final Details of Novel Anchorage System For Column #1 | 82 |
| 4.11. Final Details of Novel Anchorage System For Column #2 | 82 |
| 4.12. Final Details of Novel Anchorage System For Column #3 | 83 |
| 4.13. Restrictions Imposed on Anchorage Design For East and West Sides..... | 84 |
| 4.14. U-Anchors Used on East and West Faces of Columns #2 and #3 | 84 |
| 4.15. Column Straightening Setup For Columns #2 and #3 | 86 |
| 4.16. Columns After Removal of Loose Concrete..... | 87 |
| 4.17. Columns With Formwork Placed Around Exterior | 88 |
| 4.18. Concrete Surface Preparation | 89 |
| 4.19. Application of MBrace® Primer..... | 90 |

| | |
|--|-----|
| 4.20. Application of MBrace [®] Putty | 91 |
| 4.21. Installation of CF 130 Carbon Fiber Sheets..... | 92 |
| 4.22. Temporary Placement of Anchorage Over “Wet” Saturant..... | 93 |
| 4.23. Injecting Epoxy Into Anchor Rod Holes | 94 |
| 4.24. Installed Novel Anchorage System..... | 95 |
| 4.25. Longitudinal Strain Gauge Locations on Column #1 | 97 |
| 4.26. Longitudinal Strain Gauge Locations on Column #2 | 97 |
| 4.27. Longitudinal Strain Gauge Locations on Column #3 | 98 |
| 4.28. Strain Gauge Locations on Novel Anchorage System..... | 98 |
| 4.29. Load Cells Used on Novel Anchorage System for Column #1 | 99 |
| 4.30. Column Testing Setup..... | 100 |
| 4.31. Definitions of Positive and Negative Forces | 101 |
| 5.1. Shear Cracking in Footing Observed During Column #1 Testing..... | 103 |
| 5.2. Contact Between CFRP and Novel Anchorage in Column #1 Test | 104 |
| 5.3. Failure of Column #1 by Rupture of CFRP at Anchorage..... | 105 |
| 5.4. Pullout Failure of U-Anchors for Column #2 | 106 |
| 5.5. Rupture of Transverse CFRP at Base of Column #2 | 106 |
| 5.6. Rupture of CFRP on South Face of Column #2 | 107 |
| 5.7. Debonded Areas of CFRP on Column #2 After Testing | 108 |
| 5.8. Concrete Cracking Above CFRP on West Face of Column #3 | 109 |
| 5.9. Rupture of Transverse CFRP on Southwest Corner of Column #3 | 109 |
| 5.10. Column #3 During Final Cycle of Testing | 110 |
| 5.11. Bending Moment Versus Average Actuator Displacement for Column #1 | 111 |
| 5.12. Bending Moment Versus Average Actuator Displacement for Column #2 | 111 |
| 5.13. Bending Moment Versus Average Actuator Displacement for Column #3 | 112 |
| 5.14. Torsion Versus Twist for Column #2 | 112 |
| 5.15. Torsion Versus Twist for Column #3 | 113 |
| 5.16. Load Cell Readings and Bending Moment Versus Time for Column #1 | 116 |
| 5.17. Longitudinal Strain Measurement in North Face of Column #1 | 118 |
| 5.18. Longitudinal Strain Measurement in South Face of Column #1 | 118 |
| 5.19. Prediction of Strain in CFRP at Column-to-Footing Interface of Column #1 | 119 |

| | |
|---|-----|
| 5.20. Strains Measured in Anchorage Plate for Column #1 | 120 |
| 5.21. Possible Secondary Force Transfer of Novel Anchorage (Conceptual) | 122 |
| 5.22. Strains Measured on Anchorage Plates for Column #2 | 124 |
| 5.23. Strains Measured on North Anchorage Plate for Column #3 | 124 |
| 5.24. Strains Measured on South Anchorage Plate for Column #3 | 125 |
| 5.25. Prediction of Anchor Rod Loads From Strain Gauge Data for Column #1..... | 126 |
| 5.26. Prediction of Anchor Rod Loads From Strain Gauge Data for Column #2..... | 126 |
| 5.27. Prediction of Anchor Rod Loads From Strain Gauge Data for Column #3..... | 127 |
| 5.28. Longitudinal Strain Measurement in North Face of Column #2 | 128 |
| 5.29. Longitudinal Strain Measurement in South Face of Column #2 | 128 |
| 5.30. Longitudinal Strain Measurement in North Face of Column #3 | 129 |
| 5.31. Longitudinal Strain Measurement in South Face of Column #3 | 129 |
| 5.32. Free-Body Diagram of Anchor Rod Contribution to Moment Capacity | 130 |
| 5.33. Failed U-Anchor After Removal From Groove..... | 132 |
| 5.34. Possible Modifications to Assumed Behavioral Model for Novel Anchorage..... | 133 |
| 5.35. Design Recommendations Summary for Novel Anchorage | 134 |
| A-1. Damage Photos of Column #1 Prior to Repair | 140 |
| A-2. Damage Photos of Column #2 Prior to Repair | 141 |
| A-3. Damage Photos of Column #3 Prior to Repair | 142 |
| A-4. Damage Photos of Column #4 Prior to Repair | 143 |
| A-5. Damage Photos of Column #5 Prior to Repair | 144 |
| A-6. Damage Photos of Column #6 Prior to Repair | 145 |

LIST OF TABLES

| Table | Page |
|--|------|
| 2.1. Sizes of Anchor Spikes Used in Orton (2007)..... | 12 |
| 2.2. Experimental Results of Tests Involving Anchorage | 39 |
| 2.3. Notes on Anchorage Studies From Table 2.2 | 44 |
| 4.1. Column Number Designation | 64 |
| 4.2. Summary of Original Column Damage | 66 |
| 4.3. Properties of MBrace [®] Materials..... | 69 |
| 4.4. Properties of Concreasive [®] LPL Paste | 69 |
| 4.5. Bond Strength Test Results Per <i>ASTM C7234</i> | 70 |
| 4.6. Compressive Strengths of Original Column Concrete and Repair Mortar | 70 |
| 4.7. Functional Strain Gauges on Novel Anchorage System..... | 99 |

NOMENCLATURE

| Symbol | Description |
|-----------|--|
| d_H | Diameter of holes drilled in novel anchorage system |
| d_T | Outside diameter of cylindrical section on novel anchorage system |
| E_f | Elastic modulus of FRP |
| $F_{B,x}$ | Shear force induced in anchor rods by FRP loading |
| $F_{B,y}$ | Tensile force induced in anchor rods by FRP loading |
| F_F | Reaction of FRP onto novel anchorage system |
| $F_{F,x}$ | Horizontal component of reaction of FRP onto novel anchorage system |
| $F_{F,y}$ | Vertical component of reaction of FRP onto novel anchorage system |
| k | Constant used in Niu and Wu's (2000) effective bond length model |
| L_e | Effective bond length |
| l_{P1} | Distance from end of novel anchorage plate closest to column to centerline of anchor bolt holes |
| l_{P2} | Distance from end of novel anchorage plate farthest from column to centerline of anchor bolt holes |
| N_n | Tensile capacity of a single anchor rod |
| N_{ua} | Actual tensile force present in a single anchor rod |
| q_P | Distributed bearing reaction from novel anchorage system |
| t_f | FRP Thickness |
| t_{PL} | Novel anchorage plate thickness |
| V_n | Shear capacity of a single anchor rod |
| V_{ua} | Actual shear force present in a single anchor rod |

1. INTRODUCTION

1.1. GENERAL

Over the past several decades, fiber-reinforced polymer (FRP) composites have been used for the retrofit and repair of structurally deficient members. Their use in field applications has grown significantly since the late 1980s and early 1990s due in part to a decrease in their cost as well as a widespread necessity for the strengthening of improperly or insufficiently designed structural elements, especially in seismic areas (ACI Committee 440, 2008; Teng et. al, 2002). The growth in the use of composite materials in civil infrastructure, most specifically those used for the strengthening of reinforced concrete (RC) elements, has prompted a significant amount of published laboratory research studying the feasibility of these materials for repair and focusing on the establishment of design standards for their implementation.

Despite promising developments in the implementation of FRP for the repair and retrofit of RC structures, many challenges exist that have prevented additional growth of this market. Such challenges include: brittle failure of FRP-strengthened RC structures due to sudden failure modes such as FRP rupture or debonding (Galal and Mofidi, 2010); deterioration of the mechanical properties of FRP due to harsh environmental conditions such as wet-dry cycles and freeze-thaw conditions (Belarbi and Bae, 2007); a reduction in strength due to the effects of improper installation procedures (Orton, 2007); and lack of agreement among debonding behavior and bond length models (Ben Ouezdou et al., 2009). This thesis focuses on another of these challenges: the stated need for mechanical anchorage systems to improve FRP strength in situations where debonding or lack of development length is a problem (ACI Committee 440, 2008), and the lack of anchorage-related research data to support widespread implementation of FRP anchorage systems (Ceroni et al., 2008).

The topic of this thesis presented itself when searching for solutions to provide an emergency repair to severely damaged bridge columns in an experimental study that is discussed later in this chapter. During the review of existing literature for FRP anchorage systems capable of fulfilling the needs of this project, it became clear that existing FRP anchorage research and testing had remained in its beginning stages for the past several

decades. Thus, a significant amount of organization and additional research would be necessary in order to advance the popularity of both FRP strengthening systems for RC structures and the anchorage systems that could improve the performance of the FRP systems. Therefore, a categorization of existing FRP anchorage systems was proposed and a novel anchorage system was developed in order to meet the unique requirements of the experimental program.

This introductory chapter provides an overview of FRP usage for the strengthening of RC structures, as it relates to the experimental program, in addition to introduction to FRP anchorage systems in Section 1.2. In Section 1.3, the experimental program is briefly discussed, and the problems associated with selecting an appropriate anchorage system for this study are presented. The objectives and desired outcomes from this research are stated in Section 1.4, while the applicability of the contents of this thesis is discussed in Section 1.5. Finally, the organization and format of this thesis is presented in Section 1.6.

1.2. BACKGROUND

In this section, the background and history of externally bonded FRP usage as it relates to the experimental program and anchorage device categorization are discussed. First, an overview of FRP composites is given. A brief history of the use of externally bonded FRP as a construction material in civil engineering is then presented, followed by a list of common strengthening applications for FRP with regard to RC structures. Next, a description of rapid, or emergency, repair of RC structures with FRP is given. Finally, the concept of FRP anchorage systems is established along with its importance in the overall FRP strengthening scheme.

1.2.1. Overview of FRP Composite Systems. FRP composite systems are created by creating a resinous matrix into which continuous fibers are embedded. The fibers, which provide the strength and stiffness to the composite system, are typically carbon fibers, glass fibers, or aramid fibers. The type of fiber dictates the nomenclature of the composite system: glass fibers are used in glass fiber-reinforced polymer (GFRP) composites; carbon fibers are used in carbon fiber-reinforced polymer (CFRP) composites; and aramid fibers are used in aramid fiber-reinforced polymer (AFRP)

composites. The resinous matrix, which provides rigidity and protection to the embedded fibers, is typically made from epoxy, polyester, or vinylester resin (Teng et al., 2002).

CFRP composites are generally very durable, have excellent fatigue characteristics, and can withstand most environmental conditions. They are, however, extremely stiff and brittle and are susceptible to galvanic corrosion. GFRP composites provide exceptional thermal insulation and low cost, but are susceptible to moisture in high alkaline environments. AFRP composites exhibit excellent toughness, damage tolerance, and have good fatigue characteristics. Challenges related to AFRP composites include high costs, high moisture absorption, and poor compressive properties (Ortega 2009).

1.2.2. Externally Bonded FRP in Civil Engineering. Externally bonded FRP has been used to strengthen several types of structural members such as steel (Zhao and Zhang, 2007) and masonry (Hall et al., 2002; Holberg, 2000) members. The broadest application of externally bonded FRP in civil engineering, however, is the strengthening of RC members. The first application of externally bonded FRP was in 1984 when carbon fiber-reinforced polymer (CFRP) plates were used to strengthen RC beams. While FRP had been used in other industries for many years prior to 1984, the high cost of FRP composites prevented their widespread use in civil engineering. Over the past two decades, however, the cost of composites has dropped drastically, and their use has become more widespread (Teng et al., 2002).

Even before the recent decrease in cost, FRP had already established itself as an attractive material for retrofit and repair of RC structures due to its high strength-to-weight ratio, ability to form to the surfaces of RC members of nearly all shapes and sizes, and corrosion resistance. Because of its light weight and versatility, the installation of externally bonded FRP involves low labor costs and provides the ability to perform the strengthening procedure with minimal service interruption. Additionally, the corrosion resistance of the material ensures a durable performance (Teng et al., 2003).

Externally bonded FRP used to strengthen RC members has broad applications in civil and structural engineering. These applications include, but are not limited to, the following: flexural strengthening of RC beams and slabs; shear strengthening of RC beams; improving the shear and flexural resistance of RC shear walls; strengthening

axial- and eccentrically-loaded columns; and protecting against seismic failure modes of RC columns. Experimental examples of the aforementioned applications are presented in Chapters 2 and 3.

1.2.3. Rapid Repair of Earthquake Damaged Structures. As is discussed in Section 1.3, a portion of this thesis is dedicated to the design and evaluation of a novel anchorage system used in rapid repair of square RC bridge columns tested under combined loadings. In the context of this study, “rapid repair” refers to a repair period lasting no longer than 72 hours with the goal of restoring the column’s original design strength. The capability to perform such repairs is essential to the quick restoration of bridge service that may be needed for evacuations or emergency vehicle access in the case of a devastating earthquake, a need stated in current seismic design criteria documents (Applied Technology Council, 1997). While a limited number of studies (Vosooghi et al. 2008) have been performed that focus on the rapid repair of bridges with a timeline on the scale of a few days, the demonstration of such repair methods is invaluable to the populations who depend on these bridges for convenience and safety in their everyday lives.

1.2.4. FRP-to-Concrete Anchorage Systems. In nearly every application of externally bonded FRP used to strengthen RC members, the failure mode that results in the most efficient utilization of FRP, although not necessarily the most ideal, is the failure by rupture of the FRP sheet or plate (Orton, 2007). However, achieving failure by FRP rupture is often difficult due to the common debonding failure modes shown below in Figure 1.1. The debonding modes depicted in this figure are as follows: (a) concrete cover separation; (b) intermediate flexural crack-induced interfacial debonding; (c) plate-end interfacial debonding; (d) intermediate flexural shear crack-induced interfacial debonding; and (e) FRP debonding in a shear strengthening application. While the debonding failure modes depicted in Figure 1.1 are specifically related to FRP for RC beams, FRP for other strengthening applications exhibits similar debonding failure modes.

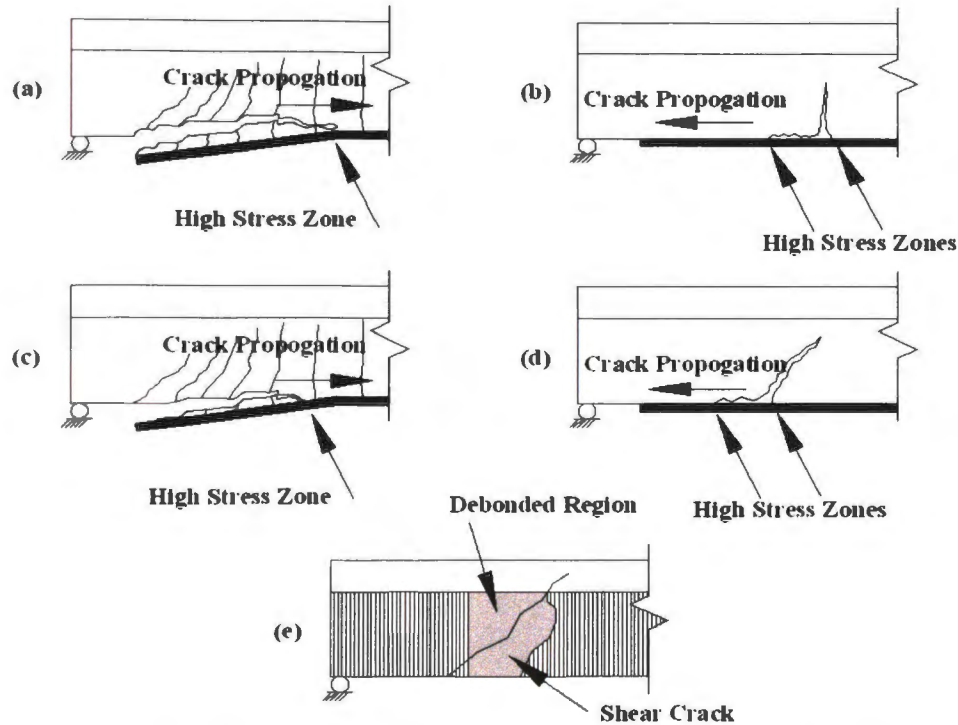


Figure 1.1. FRP Debonding Failure Modes (Teng et al., 2002)

Plate-end debonding and concrete cover separation are due to the same cause: high interfacial shear and normal stresses near the plate end due to the termination of the plate (Smith and Teng, 2002). While the interfacial shear and normal stresses can be reduced to an extent by extending the bonded length of FRP, there exists a certain length, frequently referred to as the effective bond length (L_e), over which the majority of the bond stress is transferred to the concrete substrate. Studies have shown that an increase in the bonded length in excess of the effective bond length does not increase the tensile capacity of the externally bonded FRP system or prevent against debonding failure (Orton, 2007). Therefore, methods other than extending the bonded length of FRP are needed to increase the strength of the FRP system.

The failure modes shown in Figure 1.1, especially concrete cover separation, have been frequently documented and have led to the creation of FRP anchorage systems. In general, FRP anchorage systems are used to allow the anchored FRP to reach a higher design strength. In some cases, as will be discussed in Chapter 3, anchorage systems provide a force transfer mechanism that is critical to the strength of the FRP system. To

date, published research focusing specifically on FRP anchorage systems has been limited, although studies have shown promising results regarding the functionality of various systems.

The performance of anchorage systems becomes critical in the design of FRP strengthening systems because the improved strength of the FRP system due to the anchorage may not be high enough to develop the full tensile strength of the FRP. Therefore, failure is often due to anchorage failure, FRP rupture due to local stress concentrations imposed by the anchorage, or FRP debonding. Because FRP debonding, anchorage failure, and FRP rupture can be sudden and brittle, a thorough understanding of the behavior of anchorage systems is essential for designing a safe and reliable FRP retrofit or repair.

1.3. PROBLEM DEFINITION

A thorough understanding of anchorage performance is essential for the advancement of FRP as an attractive construction material for structural retrofits and repairs. Since only a limited amount of the tensile force in the FRP system can be transferred to the concrete substrate regardless of the bonded length, FRP anchorage systems are necessary to improve the efficiency of externally bonded FRP systems. In fact, in certain cases discussed in Chapter 3, the strength of the anchorage systems dictates the strength of the overall FRP system.

This section defines the problems that currently exist in the implementation of anchorage systems for externally bonded FRP systems. Additionally, the need for a novel anchorage system resulting from the unique requirements of the experimental program is discussed.

1.3.1. General Challenges for Anchorage System Research. Chapter 2 of this thesis discusses the wide variety of anchorage systems that have been created, tested, and reported upon by various researchers. Despite the existence of such information, the process of selecting an anchorage system for a specific strengthening application is often difficult due to differences in their behavior and the subsequent lack of categorization. To date, all anchorage systems have been grouped together in the single category of

“FRP anchorage” or a similar term, although different systems are not necessarily interchangeable. Therefore, a clear system of categorization based on anchorage behavior will be useful for the advancement of anchorage research and for engineers who are only vaguely familiar with FRP anchorage systems.

Because of the critical nature of FRP anchorage performance, current design guidelines require that a proposed anchorage system be heavily scrutinized under representative physical testing (ACI Committee 440, 2008). Recent publications of test procedures, however, have limited applicability. Furthermore, while test data for a specific type of anchorage system may be available, those data may not be relevant to a different application of the same system. Thus, the aforementioned categorization system should also serve as an aid for designing the proper anchorage testing procedure.

1.3.2. Anchorage Systems for Repaired Bridge Columns. A requirement of the experimental program, which is discussed in detail in Chapter 4, was that an anchorage system should be developed to anchor longitudinally oriented FRP bonded to the surface of square bridge columns. This project, entitled “Rapid Repair of Severely Damaged Bridge Columns Under Combined Loading Effects” and funded by the University of Missouri Research Board, involved the repair of six half-scale square bridge columns tested under a constant axial load and varying torque-to-moment ratios. Of the six repaired columns, it was determined that an anchorage system was needed at the column-footing interface for three of the columns. For these three columns, since the applied lateral force would cause the column to bend as a cantilever, it was determined that the strength of the anchorage system would control the design of the longitudinal, or flexural, FRP reinforcement.

Due to the severely damaged state of the square bridge columns, a significant FRP force was required to be anchored at the base of the column in order to replace the strength of the damaged reinforcing bars. This presented an even greater challenge for the design of the anchorage systems, as the anchorage systems reported upon in literature were generally not designed to resist large forces of the magnitude required by the experimental program. Therefore, an extensive review of anchorage systems was required in order to properly design a system for the column repair program.

1.4. OBJECTIVES

The objectives of this thesis are as follows:

1. Conduct a comprehensive review of anchorage systems used for externally bonded FRP on RC members.
2. Categorize the existing anchorage systems according to their behavior and use.
3. Evaluate and suggest testing procedures to aid in anchorage and FRP strengthening system design.
4. Propose direction for future anchorage system research.
5. Design, create, and test suitable anchorage systems for rapid repair of the severely damaged bridge columns in the experimental program.
6. Evaluate the tested anchorage systems and make recommendations for future use.

1.5. SCOPE AND LIMITATIONS OF RESEARCH

This thesis investigates many types of anchorage systems for FRP bonded externally to RC elements. Some mention is made of anchorage systems for FRP bonded to masonry structures. While the anchorage system performance is very similar for RC and masonry elements, the bonded behavior of the FRP certainly varies between the two types of materials. Therefore, anchorage systems that relate to masonry structures are presented herein solely because they have the potential to be adapted for RC structure use. Their inclusion is not intended to suggest that FRP-strengthened masonry structures exhibit similar behavior to FRP-strengthened RC structures.

Additionally, references to “FRP systems” made within this thesis refer exclusively to sheets or plates externally bonded to RC structural elements. The topic of near-surface mounted (NSM) FRP bars, considered by some to be an externally bonded FRP system, is not discussed in this thesis. While other applications of FRP and fiber composites certainly exist in civil engineering, such as FRP reinforcing bars embedded in concrete, or fiber-reinforced concrete, references to FRP herein are made in regard to the use of externally bonded FRP sheets or plates. While externally bonded FRP sheets and plates can be used to strengthen many types of structural members, such as structural steel or masonry, the discussion of FRP within this thesis will focus solely on RC members unless noted otherwise.

1.6. THESIS ORGANIZATION

This thesis contains six chapters. Chapter 1 introduces the topic of FRP anchorage systems and defines the challenges inherent in anchorage system research. The experimental program is also briefly introduced along with the overall objectives of the research. Chapter 2 contains a thorough literature review of all types of FRP anchorage systems, as well as an overview of some common anchorage testing procedures. In Chapter 3, a categorization system for FRP anchorage is proposed in order to facilitate a better understanding of anchorage behavior and applicable testing procedures. Chapter 4 describes the experimental program, as well as the selection and creation of a novel anchorage device. Chapter 5 contains the experimental results. In this chapter, the performance of the anchorage systems designed and selected in Chapter 4 is evaluated and discussed. Finally, Chapter 6 summarizes the research reported upon in this thesis and presents conclusions based on the findings.

2. LITERATURE REVIEW

2.1. GENERAL

This literature review presents a thorough overview of past research regarding anchorage systems for FRP used for strengthening RC members. Most of the anchorage system research reported in this section falls into the following categories: experiments that focused on anchorage testing independent of its intended inclusion in an FRP strengthened RC member; experiments that tested FRP-strengthened RC members that included an anchorage system for the FRP; and studies that combined the two aforementioned types of experiments.

2.2. TYPES OF ANCHORAGE SYSTEMS

This section describes types of anchorage systems reported in literature. Studies utilizing each anchorage system are presented, along with general comments about the fabrication of the anchorage systems. Details about the performance of the anchorage systems mentioned in this section are presented in Section 2.4.

2.2.1. Anchor Spikes. Anchor spikes are strands of bundled fibers that have one end embedded in the composite matrix and the other end embedded in the concrete below or adjacent to the FRP sheet that is being anchored. Anchor spikes have been widely used as anchorage systems, and their physical geometry is dictated by their role in the strengthening application. The following subsections describe the types of anchor spikes that have been used for anchoring FRP strengthening systems to RC members.

2.2.1.1 90° Anchor Spikes. When the fibers used to fabricate an anchor spike are embedded into the concrete substrate through the FRP, with the embedded portion of the anchor orthogonal to the plane of the FRP, and the remaining fibers above the FRP fanned out on the FRP surface and incorporated into the FRP matrix, these anchors are termed as 90° anchor spikes.

Piyong et al. (2003) used 90° anchor spikes made from GFRP fibers to anchor prestressed CFRP sheets to the substrate in an attempt to strengthen concrete slabs. The anchor spikes were fabricated from plain GFRP fibers that were thoroughly pre-impregnated with low viscosity epoxy to about half their height, while the other half of

the fiber bundle was left “dry” so that it could be bonded to the CFRP sheet. The fibers were then passed through a hole in a steel plate to obtain the correct spike diameter. After this, the fibers were left to cure at ambient temperature. Details and dimensions of the fibers used in this study are displayed in Figure 2.1.

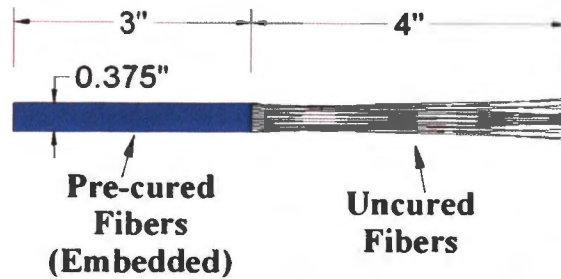


Figure 2.1. Details of 90° Fiber Anchors Used by Piyong et al. (2003)

The 90° fiber anchors were installed at the same time as the CFRP sheets. A hole was cut into the CFRP sheets to accommodate the anchor spike passing through into the concrete. Using the same low viscosity resin that was used to pre-impregnate half of the anchor spike, the cured end of the anchor spike was inserted into a hole drilled into the concrete and the uncured fibers bonded to the CFRP sheet on the concrete surface. The installation pattern is shown in Figure 2.2.

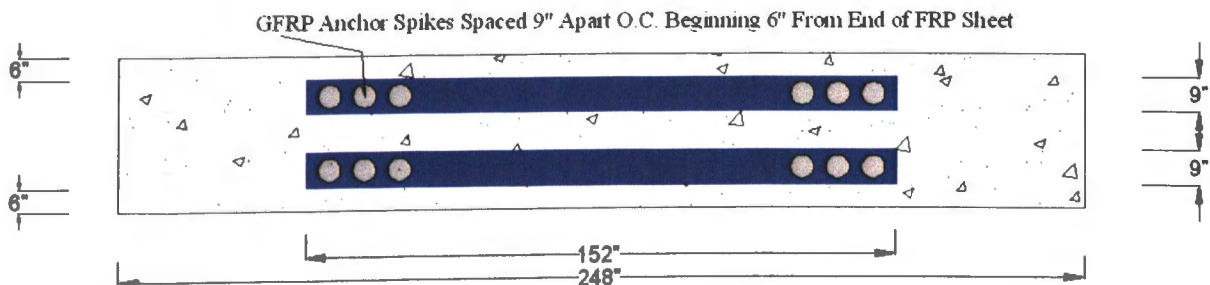


Figure 2.2. Installation Pattern for 90° Anchor Spikes Used in Piyong et al. (2003)

Eshwar et al. (2003) used nearly the same 90° anchor spikes that were used in Piyong et al. (2003) to anchor flexural CFRP sheet reinforcement to the soffit of beams with curved soffits. The fabrication process for these anchor spikes was identical; only the embedment depth was changed. Details and dimensions of the fibers used in this study are the same as those displayed in Figure 2.2. In addition to the fabrication of the anchor spikes used by Eshwar et al. (2003) being nearly identical to the anchor spikes used by Piyong et al. (2003), the installation procedures were also identical. The anchor spikes were installed at intervals of 20 in. throughout the entire length of the beams, with the first spike installed at 4 inches from the end of the FRP sheet.

Teng et al. (2000) used 90° fiber anchor spikes to anchor GFRP strips at the free end of a cantilever slab. The fibers were fabricated similarly to those used by Eshwar et al. and Piyong et al., except that the pre-cured portion was 2.0 to 2.4 inches long and 0.3 inches in diameter, while the total length of the anchor spikes was 4.7 inches. These spikes were inserted into 0.4 inch diameter holes and were installed 5.9 inches apart, with the first spike installed 5.9 inches from the end of the sheet nearest the free end of the cantilever.

In a study performed by Orton (2007), 90° anchor spikes were used to strengthen CFRP sheets being for flexural strengthening on beams with height transitions. Some beams without height transitions were also tested for control purposes. The anchor spikes in this study were fabricated using CFRP sheets cut into strips, which were wrapped around a piece of steel wire and inserted into a hole in the CFRP sheets and concrete substrate. Instead of pre-curing the ends of the fibers, the fibers were cured at the time of the lay-up of the CFRP sheets. All anchors were embedded 5 to 6 inches into the concrete to ensure they penetrated past the internal steel reinforcement into the “core” concrete. Various sizes of anchors were used in this study, all of which are presented in Table 2.1.

Table 2.1. Sizes of Anchor Spikes Used in Orton (2007)

| Diameter of Hole Drilled in Concrete (inches) | Width of CFRP Sheet Used to Make Anchor (inches) | Embedment Depth of Anchor Spikes (inches) |
|---|--|---|
| 5/8 | 6 | 5 to 6 |
| 9/16 | 4 | |
| 1/2 | 3 | |
| 3/8 | 2 | |

90° fiber anchors were also used in a study by Li and Chua (2009) to anchor both GFRP and CFRP sheets to repair eccentric and concentric beam-wide column joints and beam-wall joints. Specific details of the anchor geometry were not reported, including the materials used to make the anchors and the installation details. However, it was noted that the embedment depth was 2.0 in., and that the anchors were applied to the strengthened specimens at 11.8 in. intervals.

Sami et al. (2010) used fiber anchor spikes in evaluating bond between CFRP sheets and a structure junction such as a column-beam or column-slab junction. The study reported on several types of anchors, among which were 90° fiber anchors. The anchors produced were made from CFRP fibers having a length of 7.9 in. The embedment length of anchor spikes was not specified in this report.

2.2.1.2 180° Anchor Spikes. Another type of anchor spike that has shown potential for use is a 180° anchor spike. 180° anchor spikes are typically installed in-line with the anchored FRP so that the fibers in the anchors can be transfer the tensile force in the anchored FRP to the anchor embedment. While the fabrication of 180° anchor spikes is similar to that of 90° anchor spikes, they each have different applications for FRP system strengthening. While applications and mechanics are discussed in Sections 2.4.1.2 and 3.3.1.2, it is worth noting briefly that 180° anchor spikes are used to anchor FRP strengthening systems where geometric complexities in concrete members require that the FRP sheet or plate must be discontinued, whereas 90° anchor spikes are typically used for anchorage throughout the length of the FRP sheet or plate. Differences in the installed geometry between 180° and 90° anchor spikes can be seen in Figure 2.3.

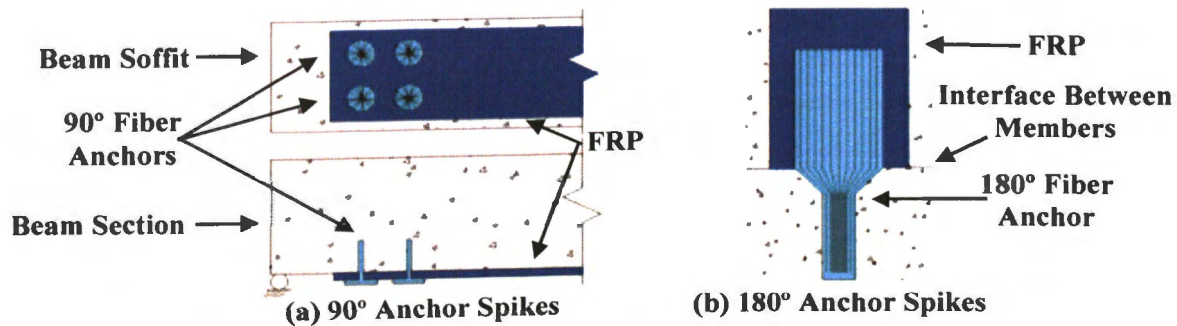


Figure 2.3. Comparison of 90° and 180° Anchor Spikes

Ideally, the angle between the embedded portion of the anchor spike and the FRP-bonded portion of the spike should be 180° ; however, practical installation procedures may prevent the anchor spike from being installed at 180° , leading to a slightly larger angle as shown in Figure 2.4 below. Despite the angle of installation being slightly larger than 180° , these anchors will still be referred to in this thesis as 180° anchor spikes due to the similarities in their usage.

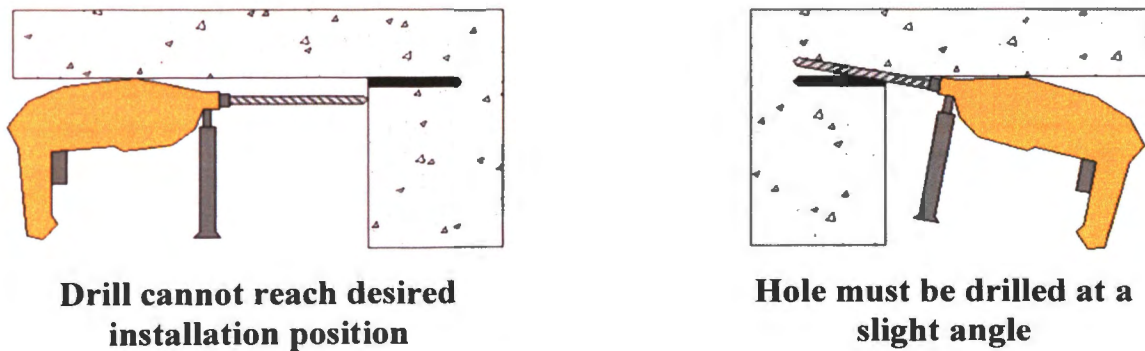


Figure 2.4. Potential Difficulties for Installation of 180° Anchor Spikes

Prota et al. (2005) used 180° anchor spikes made from steel fibers to anchor flexural (longitudinal) GFRP reinforcement on RC columns at the column-footing interface. The spikes were made from zinc-coated steel cords that were inserted into holes drilled into the footing on each side of the column. In each hole, a structural epoxy bonding agent was inserted along with the hand twisted steel cord strip. The remaining portion of the spike was then bonded to the concrete column surface, with the FRP placed over the top of the spikes. The strengthening system that was used in this study is depicted in Figure 2.5.

180° anchor spikes were also used in a study by Sadone et al. (2010) and were fabricated from CFRP plate. These anchor spikes were part of a study that focused on independent anchor testing, so they were not used as part of an FRP strengthening system for a structural member. The CFRP plate used to fabricate the spike was bundled on one end and formed into a cylinder with a diameter of $5/8$ in. The rest of the plate was allowed to remain flat so that it could be bonded to the surface of the FRP to be anchored. Details of these anchor spikes are depicted in Figure 2.6.

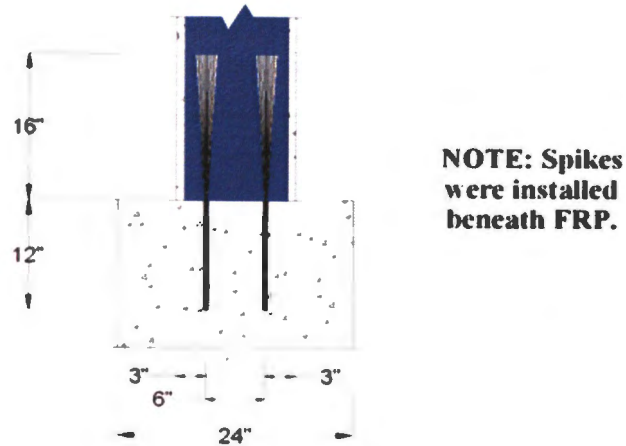


Figure 2.5. 180° Steel Anchor Spikes and GFRP Reinforcement From Prota et al. (2005)

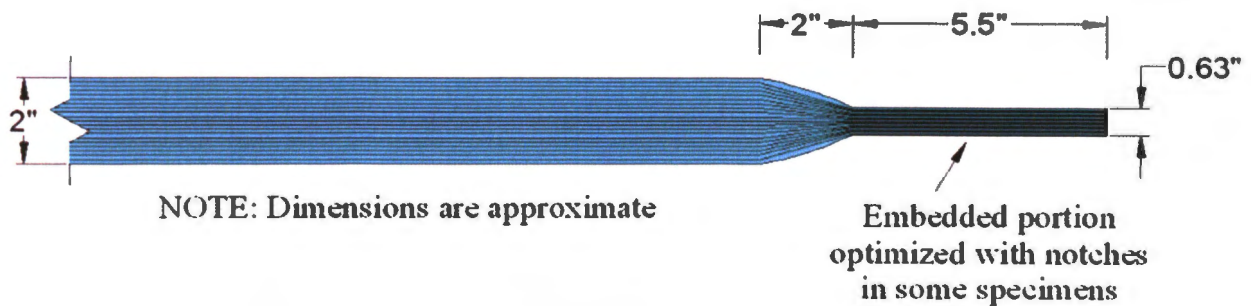


Figure 2.6. Details of 180° Anchor Spikes Studied in Sadone et al. (2010)

In the study reported by Sami et al. (2010) mentioned in Section 2.2.1.2, 180° anchor spikes were used for strengthening of the bond between CFRP and structure junctions. In this study, the geometric complexities of the strengthened member allowed for a minimum 195° angle between the embedded portion of the spike and the FRP-bonded portion of the spike. The spikes used in this study were fabricated from CFRP sheets having a width of 8 in. Embedment depth was not reported in this study.

2.2.2. Transverse Wrapping. In some situations of FRP strengthening of RC members, wrapping of a sheet of bonded FRP transversely with another sheet of FRP, sometime referred to as a “U-Wrap”, will provide a confining effect to the underneath FRP sheet, thus providing a form of anchorage. An example of transverse wrapping anchorage is shown in Figure 2.7.

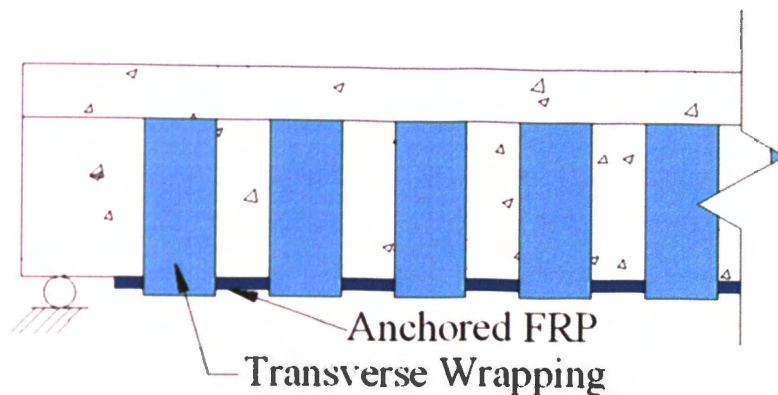


Figure 2.7. Example of Transverse Wrapping Anchorage on T-Beam

A study reported by Antonopoulos and Triantafillou (2003) used transverse wrapping anchorage to strengthen beam-column joints. Two layers of wrapping were applied over the top of the anchored FRP sheets. The details of this wrapping scheme are displayed in Figure 2.8.

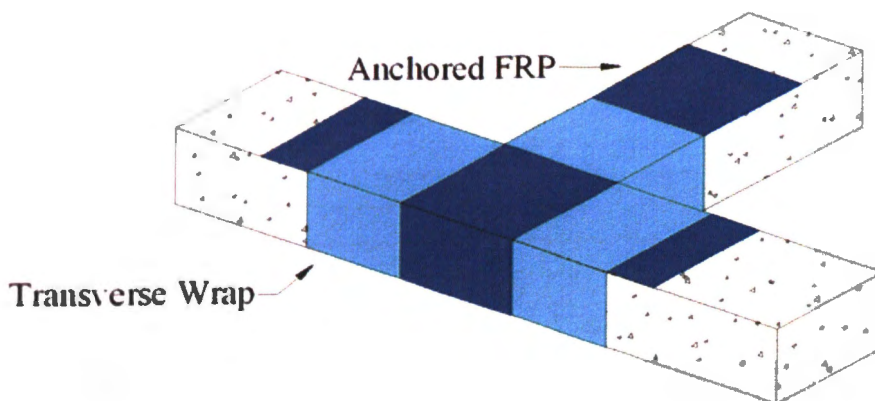


Figure 2.8. Transverse Wrapping Scheme from Antonopoulos and Triantafillou (2003)

The study mentioned in Section 2.2.1.1 by Orton (2007) also used transverse wrapping anchorage to strengthen CFRP sheets used as flexural reinforcement in beams with height transitions. The transverse wraps were 6 in. wide and applied as both single and double wraps, which were placed over the top of the flexural FRP reinforcement.

Khan and Ayub (2010) used transverse wrapping anchorage for CFRP sheets used as flexural reinforcement on RC beams. The transverse wraps were placed in

predominant flexure and shear regions, i.e., at midspan and near the supports. In addition to comparing the behavior of FRP strengthened beams with transverse wrap anchorages to control specimens with FRP strengthening and no anchorage, other variables in the test included the heights of the transverse wraps and the distance between the loading points in the four-point bending test. Figure 2.9. shows details of the wrapping scheme used in this study.

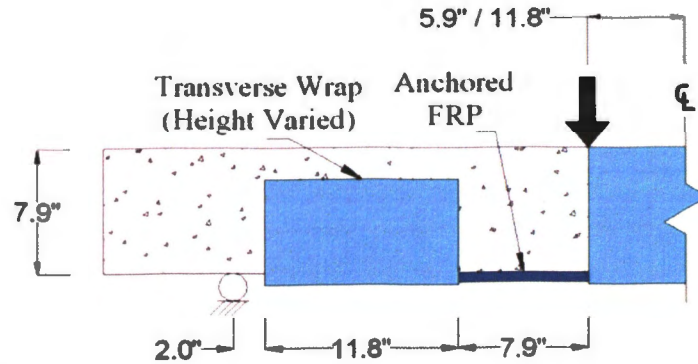


Figure 2.9. Transverse Wrapping Scheme from Khan and Ayub (2010)

A study by Pan et al. (2010) used transverse wrapping of flexural CFRP reinforcement on RC beams. The transverse wraps used in this study, however, were not the focus of the study. The study was concerned with debonding failures caused by flexural and shear crack opening along the beam. The flexural CFRP was designed to debond at a specified point along the length of the beam, which was constructed symmetrically and loaded symmetrically in four-point bending. In order to ensure that debonding would occur at the specified point, a transverse wrap was applied to the beam opposite the beam centerline from the specified debonding point. While the performance of the transverse wrap was certainly not the focus of this study, its ability to prevent or delay debonding at a specified location certainly validates its usefulness as an anchorage system.

Transverse wrapping of flexural FRP was also reported by Sadeghian et al (2010). The anchored FRP was flexural FRP on eccentrically loaded columns, and anchorage was provided by the confining effect of the transverse wraps, which were placed as the outermost layers of FRP. While these transverse wraps were not placed specifically as anchorage, they were shown to improve the bond between the flexural FRP and concrete.

It is important to note that transverse wrapping anchorage is not effective unless the transverse wraps are stressed in tension. The five aforementioned studies relied on transverse wraps that were stressed due to external loads applied to their respective structures. The external loads, however, may not provide the desired stress levels in the transverse wraps. In this case, it may be desirable to prestress the transverse wraps in order to generate a higher confining force. While prestressing of surface-bonded FRP has been rather unsuccessful in practice, a system tested by Zhuo et al. (2009) shows promise to create significant prestressing forces in FRP wraps that could be used for many applications, one of which being providing additional anchorage as a transverse wrap. This system involves clamping the FRP wraps between wave-shaped gear grips, causing a forced elongation in the FRP wrap that results in a pretension in the FRP wrap. A schematic showing the concept of the FRP wrap prestressing device is shown in Figure 2.10.

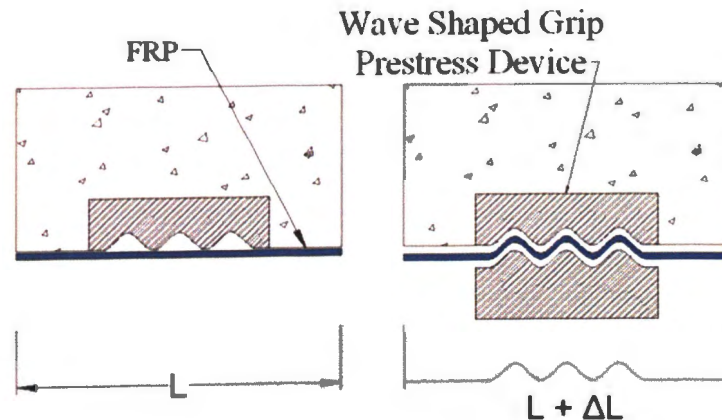


Figure 2.10. Prestressing Device for FRP Wraps Used in Zhuo et al. (2010)

2.2.3. U-Anchors. Several studies have focused on anchorage systems known as U-Anchors. A U-Anchor is created when a groove is made in the concrete surface onto which or adjacent to where the FRP sheets for strengthening are placed. The FRP sheets are then pressed into the grooves so that they line the groove walls, and the groove is then filled with a filler material, usually consisting of epoxy and sometimes in combination with an FRP bar. The U-Anchor system works by increasing the bonded area of FRP to concrete; the increase in bonded area is attributed to the FRP bond to concrete in the

walls of the groove. A schematic of a typical U-Anchor is shown in Figure 2.11 and various arrangements of U-Anchors are shown in Figure 2.12.

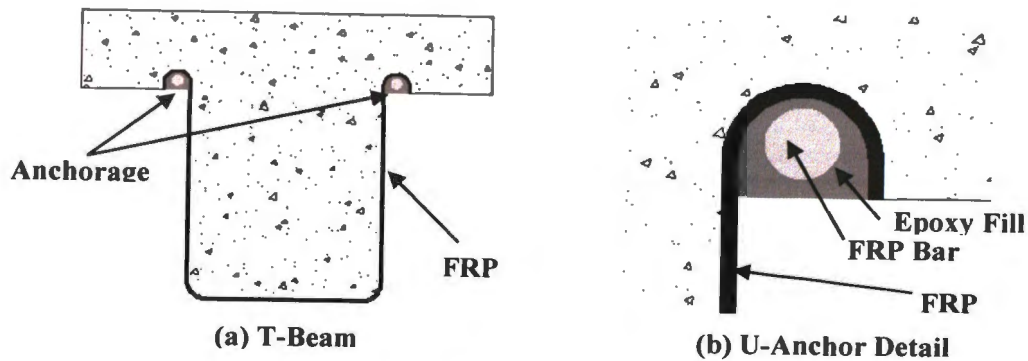


Figure 2.11. Schematic of Typical U-Anchor

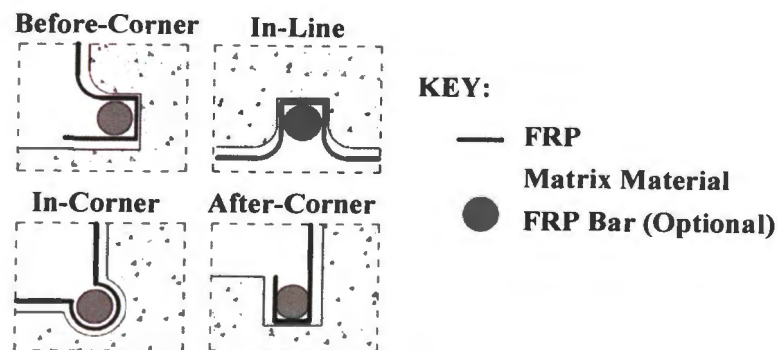


Figure 2.12. Types of U-Anchors

Khalifa et al. (1999) studied “after-corner” U-Anchors as a form of end anchorage for FRP sheets used for shear reinforcement for T-beams. The grooves for the U-Anchors were created by making two parallel saw cuts in the concrete surface at a predetermined depth and spacing. The concrete between the two cuts was then chipped out and the surface of the groove roughened and cleaned. The walls of the groove were prepared to the same specifications as the other concrete to which the FRP was bonded. After preparation, the FRP sheets were impregnated with epoxy saturant and pressed into the groove. Once the saturating epoxy had set, a high viscosity epoxy paste was set into the groove, followed by an FRP bar. While the presence of the FRP bar is optional and provides no structural purpose (Khalifa et al., 1999), its placement after the high viscosity epoxy forces the epoxy to flow around it and completely fill the voids in the groove.

Teng et al. (2001) used “after-corner” U-Anchors as an anchorage system for GFRP sheets bonded to RC cantilever slabs. Grooves were placed in the wall adjacent to the strengthened cantilever slab, and the GFRP sheets were pressed into the groove and filled with epoxy mortar.

Micelli et al. (2002) also used U-Anchors for end anchorage of FRP shear reinforcement of RC T-beams. The U-Anchors were prepared nearly identically to those in Khalifa et al. (1999), but in this study it was noted that a 0.5 in. diameter GFRP rod was used and that the grooves were cut 0.75 in. wide and 0.75 in. deep, or 1.5 times the the GFRP rod diameter. The U-Anchors used in this study were “after-corner” U-Anchors.

As part of an anchorage strength testing program, Ceroni et al. (2008) tested “in-plane” and “in-corner” U-Anchors. The anchorages were used in T-shaped specimens in order to simulate a common shape onto which FRP is typically applied. The “in-plane” anchor was cut to a depth of 0.8 in. and a width of 1.2 in.; however, neither the details of the bar placed in the groove nor the details of the “in-corner” U-Anchor were given.

Beigay et al. (2010) used “after-corner” U-Anchors for anchorage of FRP reinforcement on previously unreinforced concrete masonry walls. While many details of the U-Anchor were not reported, it was noted that a composite rod was placed into the groove in a similar fashion to other U-Anchor systems. In addition, epoxy was placed in the groove to fill the remainder of the voids.

A modified “after-corner” U-Anchor system was used by Nagy-György et al. (2005) to anchor CFRP sheets that were used to strengthen RC shear walls with staggered openings. A typical “after-corner” U-Anchor without a composite bar in the groove was created at the base of the shear wall, but a modification was made by adding a steel angle that was bolted through the U-Anchor into the foundation, as shown in Figure 2.13.

2.2.4. Longitudinal Chase. In a study reported by Kalfat and Al-Mahaidi (2010), a new form of anchorage termed as a “longitudinal chase” was used in an anchorage-specific test. The longitudinal chase was created by cutting a groove along the length of the concrete in the direction of the applied load. After the groove was filled in with epoxy and a steel bar, the FRP sheet was bonded to the concrete and over the top of the groove. The fiber direction of the FRP was placed parallel to the length of the groove.

Details of the longitudinal chase system used in Kalfat and Al-Mahaidi (2010) are displayed in Figure 2.14.

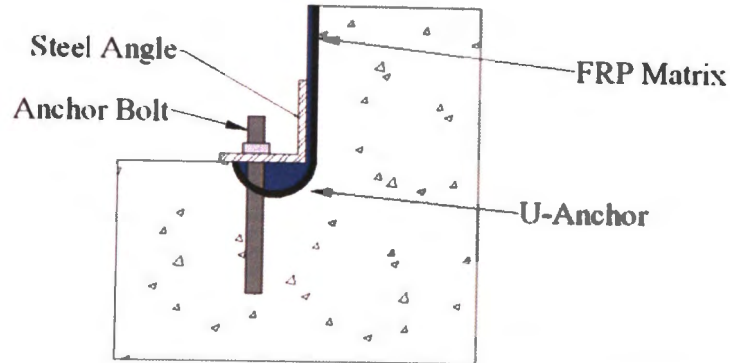


Figure 2.13. Modified U-Anchor Used in Nagy-György et al. (2005)

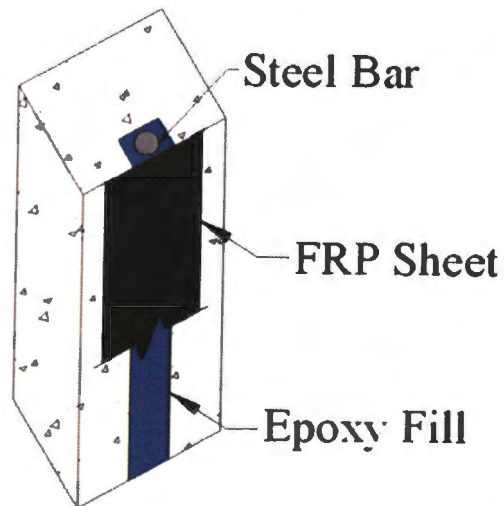


Figure 2.14. Longitudinal Chase Anchorage Used by Kalfat and Al-Mahaidi (2010)

The longitudinal chase anchorage system works by utilizing the exceptional mechanical properties of the bonding epoxy to distribute the shear stresses to a larger area of concrete. The additional bonded area for this system is equal to the width and twice the depth of the groove times the length of the groove. The concept was developed for use in combined shear and torsional strengthening of box girder bridge webs, but has wide applications for FRP strengthening. Additionally, while the original anchorage system included a 0.94 in. diameter steel reinforcing bar, the report notes that exclusion

of the reinforcing bar from the chase system should not affect the strength of the anchorage system.

2.2.5. FRP Strips. A very simple form of anchorage are FRP strips, which are installed on top of an FRP sheet used for strengthening. The FRP strip anchorages are typically installed perpendicular to the FRP strengthening sheets, although in some cases, the geometry of the RC members do not allow for a right angle between the strip and strengthening sheet. While anchorage using FRP strips may seem similar to transverse wrapping, which is described in Section 2.2.2, it can be distinguished because the strips do not provide a confining effect to the strengthening sheets. Because of this, the FRP strip anchorages must be loaded out-of-plane, or in other words, loaded in a direction that does not stress the fibers in pure tension, leading to an inefficient force transfer mechanism. Despite this limitation, a major advantage to using an FRP strip anchorage system is that the anchorage and strengthening materials are the same, which allows for easy construction and eliminates any potential corrosion hazards. An example of FRP strip anchorages are displayed in Figure 2.15.

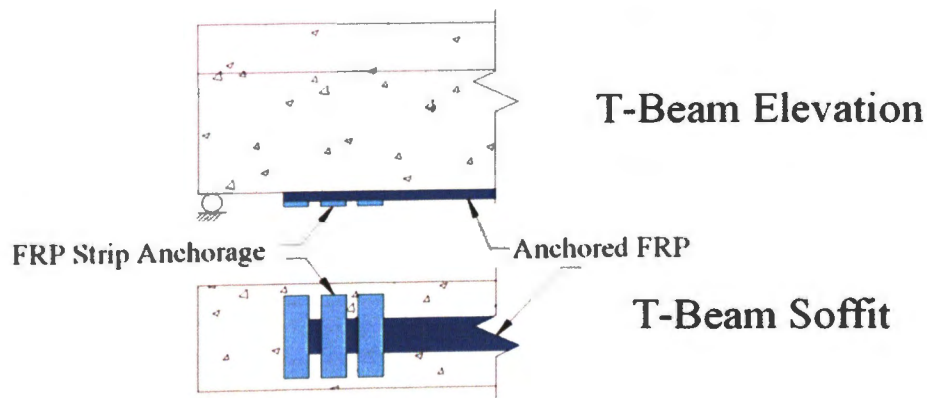


Figure 2.15. Example of FRP Strip Anchorage Systems

Antonopoulos and Triantafillou (2003) used FRP strip anchorages to anchor other FRP strips, which were used to reinforce shear-critical exterior RC beam-column joints. Ortega (2009) used FRP strips to anchor shear FRP reinforcement of RC and PC bridge girders. Additionally, Donchev and Nabi (2010) used various forms of FRP strips for end anchorage of FRP sheets used for flexural strengthening of RC slabs.

2.2.6. Plate Anchors. Metallic and composite plates have been used as a form of anchorage in several studies. Detailing of such plates varies between studies, but in general, the FRP sheets being anchored are bonded to the plates, which are either bolted or glued to the concrete substrate.

In a study involving comparative anchorage tests, Ceroni et al. (2008) tested several plated anchorage configurations. The plates used in this study were either steel plates or FRP plates, some of which were glued to the concrete substrate while others were bolted. Additionally, the plate configurations were varied such that plates were placed only before the 90° concrete joint, as well as before and after the 90° concrete joint.

Ortega (2009) studied FRP plates used to anchor shear FRP reinforcement on RC and PC bridge girders. The plates used in this study varied in several ways. First, the FRP plates were used to anchor externally bonded FRP “stirrups” that were inclined at 45° and 90° with respect to the longitudinal axis of the beam. Next, the plates were varied to be continuous and discontinuous along the length of the beam. Two variations of these anchorages are displayed in Figure 2.16.

In addition, two different styles of anchor plates were studied. The first anchorage was a typical plated anchorage device, created by bonding the overlaying FRP plate to the FRP sheet and bolting the plate to the concrete. After noting the performance of this system, a second type of anchor was created and referred to as a “sandwich plate”. The “sandwich plate” was created much like the original plate, except that the FRP sheet was bent over the first installed plate and “sandwiched” between that plate and another. Details of the original plated anchorage system, as well as the “sandwich plate” are shown in Figure 2.17.

2.2.7. Bolted Angles. Steel and aluminum angles have been used as FRP anchorage devices at 90° joints in several studies. Typically, the FRP is laid around the joint, the angle bonded to the FRP in the joint, and the angle bolted to the concrete either through or around the FRP sheet. Because steel angles are easy to obtain and require little fabrication for use as an anchorage device, they have been a popular choice for anchorage in literature. However, bolted angles have several limitations: first, because they are typically made from steel, they are subject to corrosion; second, the 90° corner in

the angle leads to stress concentrations in the FRP, causing premature failure due to restrictions imposed upon the FRP system by the anchorage.

Foo et al. (2001) used bolted angles to anchor CFRP sheets at the base of an RC shear wall. This system involved bolts that were embedded only through the bottom leg of the angle; in other words, there were no bolts passing through the leg of the angle that was parallel to the wall. The bolted angle used in this study is displayed in Figure 2.18

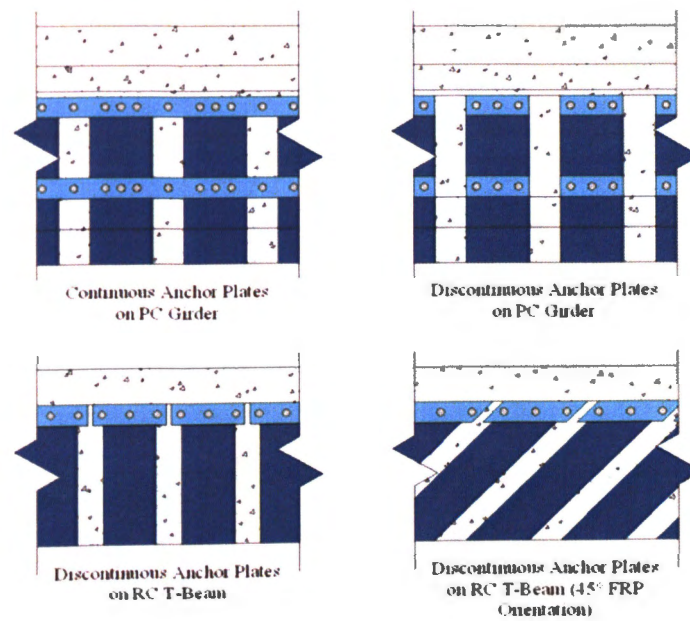


Figure 2.16. Plated Anchorage Orientations in Ortega (2009)

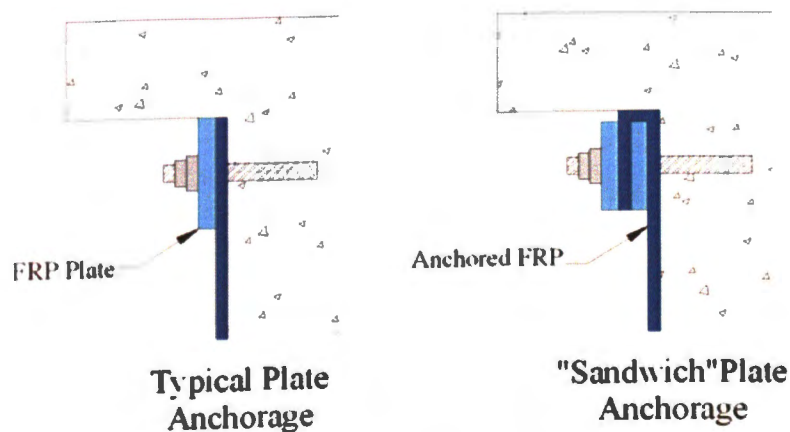


Figure 2.17. Plated Anchorage Details in Ortega (2009)

Bolted angles were also used by Hall et al. (2002) to anchor GFRP sheets to reinforce masonry shear walls. The angles in this study were placed at the same time as the GFRP layup to ensure that the GFRP was bonded to the angle. The bolts were placed around the GFRP sheets, and they were only placed in the bottom leg of the angle. Because the stress concentration in the 90° corner led to premature failure due to local stress concentrations, the angle system was modified to address this problem. The original bolted angle was nearly identical to the one shown in Figure 2.18 with the only difference being the dimensions of the angle and size of the anchor rod. The modified anchorage is discussed later in Section 2.2.9.

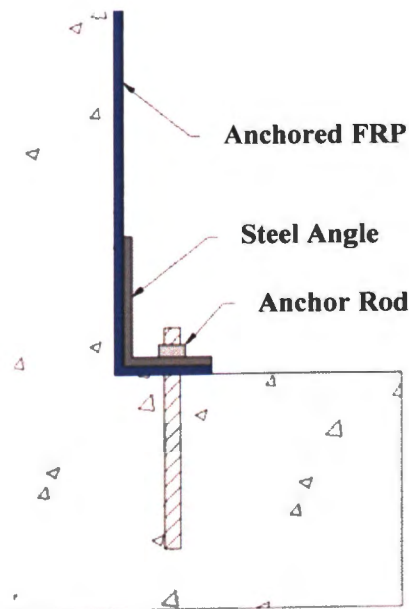


Figure 2.18. Bolted Angle System Used by Foo et al. (2001)

During the initial phase of a study, Hiotakis (2004) used bolted angles to anchor CFRP sheets at the base of RC shear walls. The angles were bolted through the CFRP sheets as the angle extended the entire length of the RC wall. Further information regarding detailing of the steel angle anchorage device was not reported; however, the steel angles led to numerous performance problems. To address these problems, a new anchorage device was created, which is discussed later in Section 2.2.8.

A study reported by Hwang et al. (2004) used bolted steel angles to anchor CFRP sheets to the top and bottom bases of RC shear walls. The angles extended continuously

along the length of the wall. Not only were the angles bolted to the bases, but also through the wall and were connected with the angle that was placed on the other side of the wall. The bolted steel angles used for anchorage in this study are shown in Figure 2.19.

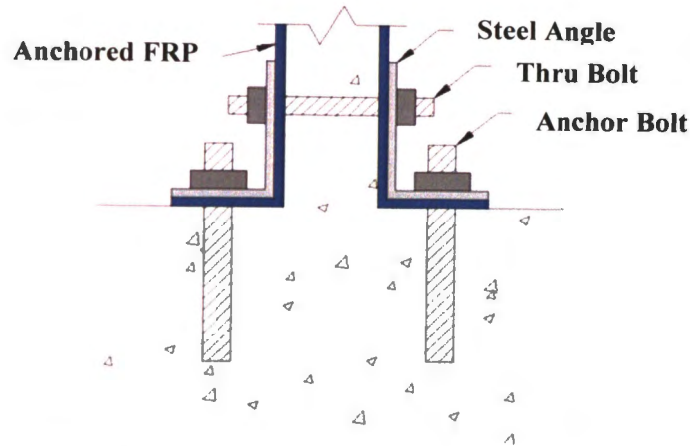


Figure 2.19. Bolted Angle System Used in Hwang et al. (2004)

A unique set of steel angle anchorage devices were used in Antonopoulos and Triantafillou (2003). Instead of the concrete surrounding the 270° section of the steel angle, the angle was used in an inverted corner so that the concrete substrate comprised the 90° section of the angle. These angles were used to anchor FRP sheets in combination with FRP strip anchorage to strengthen shear-critical RC beam-column joints. Details of these steel angle anchorage devices are shown in Figure 2.20.

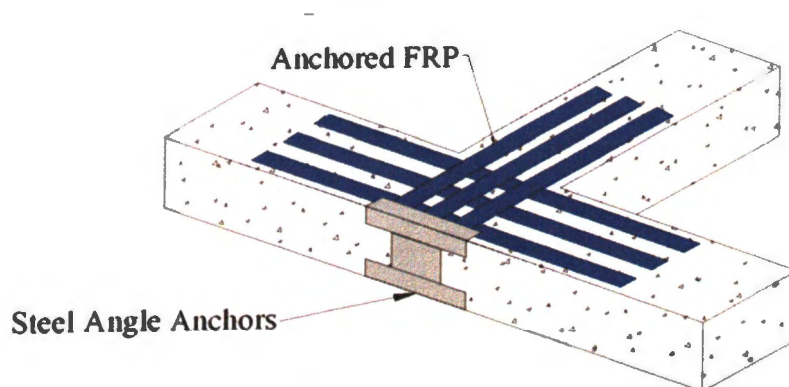


Figure 2.20. Steel Angle Anchorages Used in Antonopoulos and Triantafillou (2003)

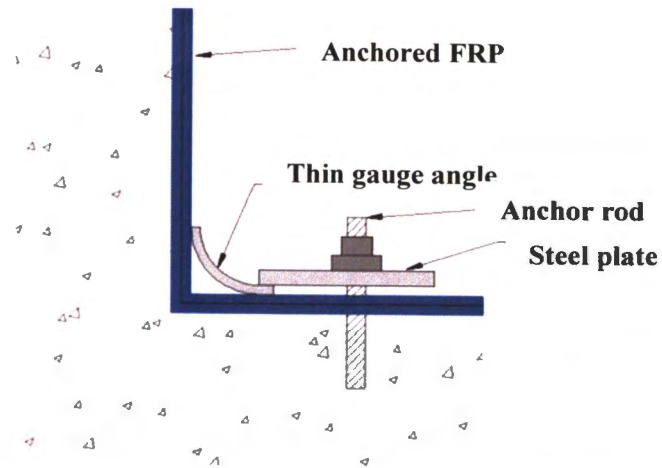


Figure 2.22. Ductile Anchorage System Used in Hall et al. (2002)

Using ductile, predictable steel allowed for the anchorage materials to be designed fairly simply. The capacity of the anchorage can be calculated by assuming cantilever bending about the centerline of the bolts, with the tip of the rounded steel angle being the free end of the cantilever.

2.3. APPLICATIONS FOR ANCHORAGE SYSTEMS

In general, the primary role of anchorage systems is to prevent or delay the process of debonding, which occurs when the externally bonded FRP detaches from the RC substrate because of the low strength of concrete in tension (Ceroni et al., 2008). Secondary roles of anchorage include providing a load transfer mechanism at critical locations on structural members and providing a ductile failure mode for the structural member instead of the typical sudden, brittle failure modes of FRP debonding and rupture. Overall, the role of anchorage depends on the FRP strengthening application. The following sections provide an overview of applications for anchorage systems with respect to the role of the overall FRP strengthening system. It is worthwhile to note that the applications listed in this section are not exhaustive; only the most common strengthening systems are presented.

A thorough understanding of the debonding process and other FRP failure modes is required to comprehend the necessity for anchorage in each situation. However, study of these processes is beyond the scope of this thesis. The reader is referred to Teng et al.

(2002) for a comprehensive description of debonding failure and other FRP failure modes.

2.3.1. Flexural Strengthening. Externally bonded FRP is frequently used for flexural strengthening of RC structural members. Flexural strengthening of RC beams is perhaps the most common application; however, flexural strengthening of RC columns, shear walls, and other members have been reported in literature.

In addition to the strengthening applications mentioned in this section, other more specialized applications exist. For example, Antonopoulos and Triantafillou (2003) studied FRP strengthening of RC beam-column joints, and Orton (2007) studied FRP strengthening of RC beams with height transitions. While FRP was used successfully to strengthen the structural members in both situations, the data obtained from the tests are very application-specific and cannot easily be used for comparative purposes.

2.3.1.1 Beams, Girders, and Slabs. RC beams, girders, and slabs are frequently strengthened using FRP bonded to their soffits. When these types of members are strengthened at midspan, anchorage is typically provided at the FRP sheet ends to prevent plate-end interfacial debonding and concrete cover separation. In many cases, anchorage is provided along the entire length of the FRP sheet to prevent intermediate flexural crack-induced interfacial debonding and intermediate flexural shear crack-induced debonding (collectively referred to as I.C. debonding). These debonding failure modes are presented in Figure 1.1 and are discussed in relation to FRP anchorage systems in Chapter 3.

In the case of a cantilever beam or slab, FRP reinforcement is bonded to the top side of the member assuming that the member is resisting gravity loads, which is typically the case. Because the point of maximum moment occurs at the fixed end, anchorage at this point is extremely critical. The FRP is unable to transfer any tensile forces from the beam or slab to the wall or column without anchorage, thus, the FRP system is only as strong as the anchorage. Additionally, anchorage may be placed at the FRP sheet end near the free end of the cantilever to prevent plate-end interfacial debonding and concrete cover separation. Anchorage may also be placed along the length of the FRP sheet to prevent I.C. debonding.

2.3.1.2 Columns. Flexural FRP reinforcement of RC columns has been studied minimally, although applications for its use certainly exist. As with cantilever beams and slabs, the crucial point for FRP anchorage in RC columns is often at the interface between the column base and the adjacent structural member. Anchorage used at these locations dictate the strength of the externally bonded FRP, as the FRP system is only as strong as its anchorage. While I.C. debonding, plate-end debonding, and concrete cover separation are legitimate concerns with flexural FRP strengthening of columns, any repaired or retrofitted column will more than likely be wrapped transversely with FRP to provide confinement, and these transverse wraps will provide anchorage along the length of the column. Therefore, anchorage for flexural FRP on RC columns away from the column joints generally need not be considered.

2.3.1.3 Shear Walls. RC (and masonry) shear walls are often repaired or retrofitted with externally bonded FRP to resist lateral loads. These lateral loads require that the walls resist both flexure and shear. In the case of flexure, FRP may be bonded to the wall surface along the height of the wall. Similar to cantilevers and columns, described in Sections 2.3.1.1 and 2.3.1.2, anchorage is placed at the wall base, and this anchorage dictates the strength of the flexural FRP. Base anchorage is the only type of anchorage that has been reported for flexural FRP reinforcement of columns; it does not appear that intermediate anchorage has been used for this purpose.

2.3.2. Shear Strengthening. FRP is frequently used for shear strengthening of RC beams, columns, and walls. Only in the case of RC beams, however, are anchorage systems typically used as a part of the FRP strengthening system. In the case of columns, a FRP sheet can be fully wrapped around the column, allowing for the FRP to be bonded to itself. To the author's knowledge, anchorage for horizontally-oriented FRP used as shear reinforcement on RC shear walls has not been reported upon in literature.

In the case of a rectangular beam, FRP used as shear reinforcement can be fully wrapped around the beam. This situation is ideal; however, it is rarely encountered in practice. Most RC beams support a slab, or have a flange that does not allow for the FRP shear reinforcement to be fully wrapped around the beam. Therefore, anchorage devices are typically needed at the discontinuities in the FRP sheets to prevent plate-end interfacial debonding. A few examples of typical installation locations for FRP

anchorage systems on RC T-beams and PC girders are shown in Figure 2.11 and Figure 2.16.

2.3.3. Other Strengthening Schemes. While shear, flexure, and confinement are the primary uses for FRP strengthening of RC structures, other strengthening schemes exist. The application of anchorage systems to these strengthening schemes, however, typically corresponds to one of the previously described flexure or shear applications. Torsional strengthening of RC beams, for example, with FRP would typically be installed in the same manner as FRP for shear strengthening and would therefore have the same type and location of anchorage. Additionally, FRP used for confinement of columns, a common FRP strengthening application, typically does not require anchorage since the FRP can be wrapped around the column as needed.

2.4. EXPERIMENTAL PERFORMANCE OF ANCHORAGE SYSTEMS

This section reviews anchorage test results from literature. The purpose is to provide a basic understanding of the performance of FRP-to-concrete anchorage systems as reported by other researchers. It will become apparent that test results often vary widely for a particular anchorage system, even within one particular study. This is due to the large number of variables affecting anchorage performance. Because reporting the intricacies of each testing program would require many additional pages of text that is not relevant to the remainder of this thesis, this information is not reported. Before using this information as a basis for design, it is recommended that the reader refer to the particular studies cited in this section for more detailed information. Test results in this section are reported briefly according to the anchorage type and are followed by Table 2.2, which summarizes the details of these results. The sections preceding the table are simply a supplement to the information in Table 2.2.

Much of the reported information about anchorage system performance may seem vague and incomplete; this is because the anchorage systems used are often not the focus of the reported study. Many of the referenced studies are focused on global behavior of an FRP-strengthened RC structure, and the behavior of the anchorage system is often an afterthought, or not reported at all. Additionally, in some studies, useful qualitative information is reported while quantitative data are not. These types of studies are not

included in the content of Table 2.2, although they are discussed in the text preceding Table 2.2.

2.4.1. Anchor Spikes. Because of the difference in performance between 90° and 180° anchor spikes, their observed behavior is separated into the two sections below.

2.4.1.1 90° Anchor Spikes. The GFRP anchor spikes used by Eshwar et al. (2003) to anchor flexural FRP to curved soffits of RC beams were observed to fail by anchor spike pullout. Additionally, the FRP on the curved beam soffit was observed to debond. However, it was noted that the beams strengthened with the 90° GFRP anchor spikes did reach a higher peak load than the beams with no anchorage. Piyong et al. (2003) used similar GFRP anchor spikes and noted their effectiveness in preventing debonding by the observation of a reduction in stress concentrations near the ends of the anchored FRP strips.

Orton (2007) noted that when anchoring flexural FRP to the surface of beams, a greater number of smaller and more closely spaced 90° anchor spikes are more effective than using a smaller number of larger 90° anchor spikes. However, using fewer of the larger anchor spikes allows for ease of installation, but sacrifices material efficiency. Orton's study also evaluated the effect of concrete surface preparation on FRP-reinforced beams. While poor surface preparation expectedly led to a decrease in the beam strength, when 90° anchor spikes were used, the negative effects of poor surface preparation were reduced. Additionally, Orton's study investigated the performance of flexural FRP on beams with height transitions; however, due to the unique nature of these specimens, the data have limited applicability and are not reported in this thesis.

2.4.1.2 180° Anchor Spikes. Sadone et al. (2010) tested 180° CFRP anchor spikes made from pultruded carbon fiber plates under both monotonic and low-cycle fatigue loading. These anchor spikes were tested independently of an overall FRP strengthening system. Two types of spikes were tested: normal spikes with a smooth embedded portion and optimized spikes with notches carved into the embedded portion of the spike. It was found that the optimized spike performed better by reaching a higher peak load, and that the low-cycle fatigue loading did not have a noticeable effect on the strength of anchor spikes.

Among the other studies mentioned in Section 2.2.1.2 that used 180° anchor spikes as an anchorage system for their respective FRP strengthening systems, none reported any significant information regarding their performance. However, 180° anchor spikes require little effort to fabricate and it is expected that future studies will embrace their usage.

2.4.2. Transverse Wrapping. Antonopoulos and Triantafillou (2003) used transverse wrapping of flexural and shear FRP used to reinforce RC beam-column joints, as mentioned in Section 2.2.2. While little description was given of the performance of the transverse wrapping anchorage behavior, it was noted that this system increased the effectiveness of FRP sheets in terms of strength and energy by 30% and 40%, respectively.

Khan and Ayub (2010) used transverse wrapping at the ends of FRP strips and at midspan to anchor flexural FRP on a simply-supported RC beam. These anchors provided an increase in strength and ductility when compared to the control specimen without anchorage. One of the variables in this test was the height of the transverse wraps on the vertical surface of the beams. It was noted that the height of the transverse wrap does not significantly affect the load carrying capacities in predominant flexural regions. In predominant shear regions, however, the wraps that extended the entire height of the vertical surfaces of the beams were the most effective.

Orton (2007) used transverse wrapping to anchor flexural FRP on beams. Orton noted that while the transverse wraps were nearly as effective as the anchor spikes used in the study, the wraps were an inefficient use of FRP. Because material efficiency is directly related to cost, Orton recommended that FRP anchor spikes should be used when cost is a concern.

Sadeghian et al. (2010) utilized transverse wrapping as a method to anchor flexural FRP on eccentrically loaded columns. The transversely wrapped FRP in this case served a dual purpose: to provide shear reinforcement for the strengthened column and to anchor the longitudinal, or flexural, FRP. A variable in this study was the number of layers of longitudinal FRP on the column, and the common failure mode was FRP rupture, regardless of the number of layers of longitudinal FRP. While the test data show that the FRP failed at strains lower than the rupture strain of the FRP, the difference can

be attributed to stresses that were not unidirectional along the length of the FRP sheets. It was also noted that the transverse wrapping could not provide confinement to the FRP on the compression face of the column, where the FRP had a tendency to debond away from the concrete surface at strain levels that were approaching the crushing strain of the concrete.

2.4.3. U-Anchors. The in-corner and in-plane U-Anchors used in Ceroni et al. (2008) were both subject to premature failure due to difficulties in detailing. In both cases, the FRP must abruptly change directions in order to enter the U-Anchor groove. This change of direction creates less than ideal bond conditions at the anchorage and may lead to an undesirable failure. Similarly, in the case of in-corner U-Anchors or any other form of anchorage at a 90° joint, Ceroni et al. recommended that the FRP sheet should not be extended around the corner. While the additional bond to the adjacent concrete would seemingly add strength to the FRP system, the difficulties in obtaining adequate bond to the concrete near the joint actually result in decreased strength of the FRP system. This condition is depicted in Figure 2.23.

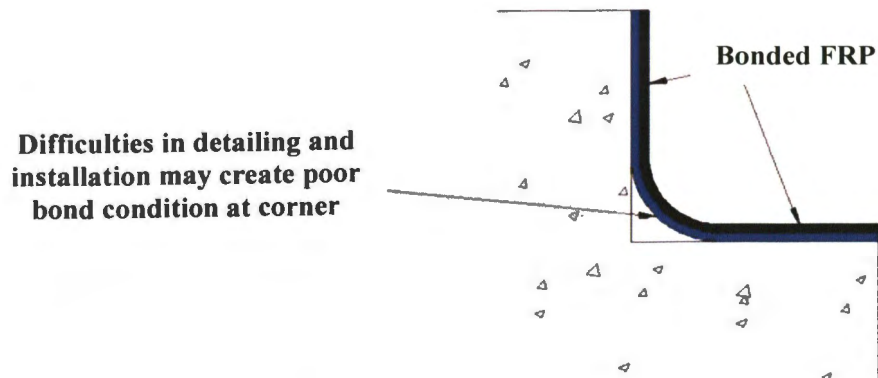


Figure 2.23. Detailing Limitations When Extending an FRP Sheet Around a 90° Joint

The after-corner U-Anchors used in Khalifa et al. (1999) allowed the shear FRP reinforcement on RC T-beams to contribute to a 30% increase in strength when compared to unanchored shear FRP reinforcement. In this study, the failure mode of the FRP system was not specified, but it was noted that in the design of these types of U-Anchors, the debonding failure mode should not be considered and that FRP rupture should control

the design. Other studies, however, have shown that FRP rupture will not control design for after-corner U-Anchors (Micelli et al., 2002; Huang and Chen, 2005).

Similarly, Micelli et al. (2002) studied after-corner U-Anchors used to anchor shear FRP reinforcement on RC T-beams. Despite the design recommendations given in Khalifa et al. (1999), Micelli et al. observed debonding behavior in both anchored and unanchored specimens. In fact, debonding failure at the anchorage was the controlling failure mode. Thus, when compared with the theoretical models given by Khalifa et al. (1999) and *ACI 440.2R-08: Externally Bonded FRP Systems for Strengthening Concrete Structures*, the experimental results were much lower.

Teng et al. (2001) used after-corner U-Anchors as anchorage for flexural FRP reinforcement of RC cantilever slabs. The FRP in these tests failed by complete debonding of the FRP attached to the slab. The debonding noted in this study may have initiated away from the U-Anchor, and since the U-Anchors were not discussed as contributors to the failure mode, it can be assumed that the debonding occurred with the U-Anchor intact.

2.4.4. Longitudinal Chase. The performance of the longitudinal chase anchorage used by Kalfat and Al-Mahaidi (2010) was not reported upon in detail; however, it was noted that the specimen containing anchorage showed significant improvement in both the maximum load and strain reached prior to failure.

2.4.5. FRP Strips. Donchev and Nabi (2010) used FRP plates to anchor other FRP plates being used for flexural reinforcement of RC slabs. The behavior of the anchorage strips were understood to behave by redistributing the stress at the end of the anchored FRP plate, thus reducing stress concentrations at the plate end. When one transverse strip was used to anchor the flexural FRP, very little effect was noted. Additional strips were added at the plate ends and oriented to be parallel to the flexural FRP; these were noted to have performed better than one transverse strip. The best performance was noted when two transverse strips were applied at the ends of the flexural FRP reinforcing plate.

Ortega (2009) used FRP strips to anchor shear FRP reinforcement to RC and PC girders. While the installation procedure was much simpler than some of the other bolted anchorage system used in the study, the anchorage did not perform as effectively as other

anchorage systems. In all of the specimens tested with FRP strip anchorage, the FRP system failed by debonding of both the anchor strip and the shear FRP reinforcement.

2.4.6. Plate Anchors. Bolted steel plates, glued steel plates, and glued FRP plates were used in two different configurations in the anchorage study by Ceroni et al. (2008). For the specimens in which the FRP was bent around the 90° joint of the anchorage test specimen and continued on the adjacent surface, two anchorage plates were used: one immediately before the corner and one immediately after the corner. For the specimens in which the FRP was terminated before the 90° joint, only one anchorage plate was used before the joint. The best overall performance was given by the single-plate system, with both the FRP and steel plates reaching very similar peak loads and failing by debonding with a slip of the FRP from the anchorage. The two-plate system using the glued FRP plates also performed well and failed by the detachment of the plates and rupture of the FRP at the 90° joint. The two-plate systems using glued steel plates and bolted steel plates performed worst; this was attributed to the detailing condition mentioned in Figure 2.23.

Ortega (2009) used three types of plated anchorage systems to anchor shear FRP reinforcement to RC bridge girders: continuous FRP plates, discontinuous FRP plates, and FRP “sandwich” plates, described in Section 2.2.6. The “sandwich” plates performed best, with no slipping of the FRP sheets with respect to the anchorage or anchor rod failure being observed. Failure due to debonding occurred in the discontinuous FRP plates along with some FRP slipping, and while this system performed effectively, it was not as effective as the “sandwich” plates. The worst performance was given by the continuous FRP plates, which buckled under high loads and forced the anchor rods to pull out from the concrete.

2.4.7. Bolted Angles. Hall et al. (2002) tested bolted angles made from steel in an independent anchorage test and compared them to other optimized anchorage systems. When testing a steel angle with a 90° corner, the FRP failed prematurely due to stress concentrations in the corner of the specimen, which included longitudinal, shear, and through-the-thickness stresses. Because of these stress concentrations, an angle with a rounded corner was fabricated from steel tube and used as the anchorage. By optimizing the geometry of the angle, noticeable improvements in strength and ductility were noted.

Hiotakis (2004) used observations from a previous study involving a bolted angle to create a new, optimized anchorage system discussed later in Section 2.4.8. The limitations of the bolted angle system in the previous study were due to prying action leading to debonding of the steel angle and FRP. A schematic of the prying action involving the steel angle is shown in Figure 2.24.

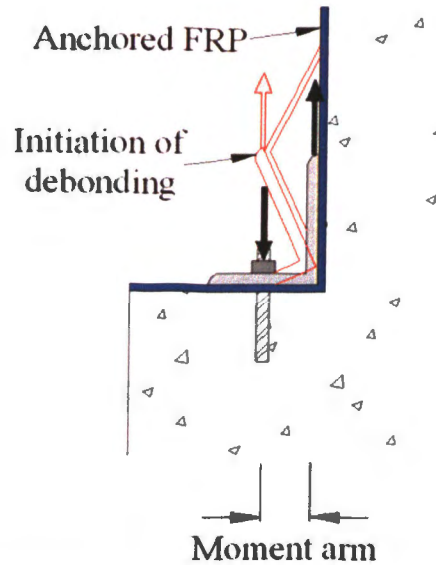


Figure 2.24. Debonding Due to Prying Action in Bolted Steel Angle Anchorage

Hwang et al. (2004) anchored flexural and shear FRP reinforcement for RC shear walls at the wall base using bolted steel angles. While little information was given involving anchorage performance, it was noted that the bolted angles performed “as expected” and were effective in anchoring the FRP strips to the base. Additionally, Hwang et al. reported that this anchorage resulted in increases in shear strengths of 88% and 126% when compared with the unanchored specimens.

2.4.8. Cylindrical Hollow Section (CHS) Anchorage. After noticing the limitations of a bolted angle anchorage system, Hiotakis (2004) developed an optimized anchorage device referred to as CHS anchorage. Hiotakis theorized that installing anchor rods in the manner shown in Figure 2.25 would provide for an optimized reaction forces from the anchorages. The CHS anchorage system performed “as expected”, transferring load from CFRP sheets to the footing and eliminating the prying action. No experimental data, however, were provided to confirm the behavioral assumptions.

2.4.9. Ductile Anchorage Systems. Hall et al. (2002) created an optimized plate-and-angle anchor system, described in Section 2.2.9, to better predict the failure strength of FRP used for flexural reinforcement of masonry shear walls, as well as to allow the anchored FRP to be stressed to a higher level. The plate-and-angle anchorage system failed in a ductile manner as expected, although the experimental values did not correlate well with the predicted values. Additionally, the authors noted that the load transfer mechanism of the system needed improvement since the FRP was only able to reach approximately half of its tensile strength.

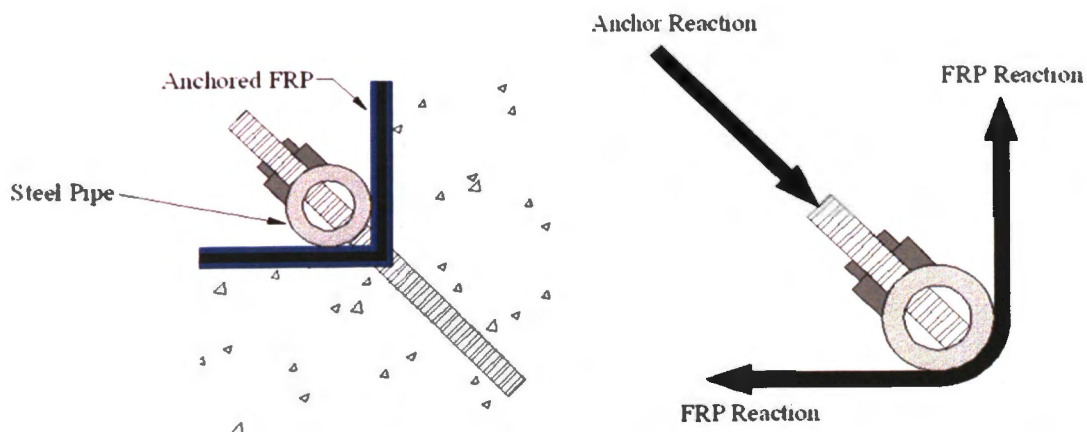


Figure 2.25. Optimized Anchor rod Reaction Forces for CHS Anchorage

2.4.10. Anchorage Summary. A summary of reviewed anchorage studies is presented in Table 2.2. It should be noted that not all of the anchorage systems mentioned in the preceding sections are included in the table since not all of the studies provided qualitative data related to anchorage performance. Additionally, some studies included in the table may not be discussed in the preceding sections. In this case, some quantitative data were reported in the studies, although little description of the anchorage system performance was noted. The superscript numbers in Table 2.2 reference the notes provided in Table 2.3. The failure mode abbreviations in Table 2.2 are as follows: anchorage failure (AF); debonding (DB); not specified (NS); other non-FRP failure (ON); other FRP failure (OF); FRP rupture at anchorage (RA); FRP rupture away from anchorage (RP); test instability (TI).

Table 2.2. Experimental Results of Tests Involving Anchorage

| Study | Anchorage System Type | Anchorage Application | Percent Increase in Strength of Anchored FRP System Compared to Unanchored FRP System | Maximum Strain Reached in Anchored FRP | Strain Measured or Calculated | Percent of Ultimate FRP Strength Reached | Failure Mode(s) of FRP System |
|-------------------------|---|--|---|--|-------------------------------|--|-------------------------------|
| Beigay et al. (2010) | U-Anchor (After Corner) | Retrofit of Masonry Wall (Shear/Flexure Test) | | 0.010 | M | 67% | OF |
| Beigay et al. (2010) | U-Anchor (After Corner) | Retrofit of Masonry Wall (Flexure Test) | | 0.012 | M | 80% | OF |
| Ceroni et al. (2008) | Glued Steel Plates (Before and After Corner) | Independent Anchorage Test | 39% | 0.006 | C | 41% | DB, AF |
| Ceroni et al. (2008) | Glued FRP Plates (Before and After Corner) | Independent Anchorage Test | 115% | 0.009 | C | 63% | RA, AF |
| Ceroni et al. (2008) | Bolted Steel Plates (Before and After Corner) | Independent Anchorage Test | 38% | 0.006 | C | 40% | DB, RA |
| Ceroni et al. (2008) | U-Anchor (In-Plane) | Independent Anchorage Test | 14.5% ¹ | 0.002 ¹ | C | 15% ¹ | RA |
| Ceroni et al. (2008) | Glued FRP Plate (Before Corner) | Independent Anchorage Test | 55% | 0.010 | C | 68% | DB |
| Ceroni et al. (2008) | Glued Steel Plate (Before Corner) | Independent Anchorage Test | 57% | 0.010 | C | 69% | DB |
| Ceroni et al. (2008) | U-Anchor (In-Corner) | Independent Anchorage Test | 84% ² | 0.008 ² | C | 57% ² | RA, RP |
| Eshwar et al. (2003) | 90° GFRP Anchor Spike | Anchorage of Flexural FRP to Curved Beam Soffit | 66% | 0.009 | M | 60% | AF, DB |
| Galal and Mofidi (2009) | Ductile Anchorage System | End Anchorage for Bonded Flexural FRP on Beam Soffit | 30% | 0.011 | M | 64% | RP |
| Galal and Mofidi (2009) | Ductile Anchorage System | End Anchorage for Unbonded Flexural FRP on Beam Soffit | 2% | 0.009 | M | 50% | AF, OF |
| Hall et al. (2002) | Steel Angle | Independent Anchorage Test | 350% | | | 16% | RA |
| Hall et al. (2002) | Steel Angle with Rounded Corner | Independent Anchorage Test | 688% | | | 27% | TI, AF |

Table 2.2. Experimental Results of Tests Involving Anchorage (Continued)

| Study | Anchorage System Type | Anchorage Application | Percent Increase in Strength of Anchored FRP System Compared to Unanchored FRP System | Maximum Strain Reached in Anchored FRP | Strain Measured or Calculated | Percent of Ultimate FRP Strength Reached | Failure Mode(s) of FRP System |
|------------------------------|--|--|---|--|-------------------------------|--|-------------------------------|
| Hall et al. (2002) | Plate and Angle Assembly (1 Ply FRP) | Independent Anchorage Test | 447% ³ | | | 19% ³ | TI, AF, DB |
| Hall et al. (2002) | Plate and Angle Assembly (2 Plies FRP) | Independent Anchorage Test | | | | 11% ⁴ | TI, AF |
| Kalfat and Al-Mahaidi (2010) | Longitudinal Chase | Independent Anchorage Test | 76% ⁵ | 0.005 ⁵ | M | 33% ⁵ | DB |
| Khalifa et al. (1999) | U-Anchor (After Corner) | End Anchorage for Shear FRP on T-Beams | 30% | 0.006 | C | 35% | NS |
| Micelli et al. (2002) | U-Anchor (After Corner, 1 Ply FRP) | End Anchorage for Shear FRP on T-Beams | 226% | | | | AF |
| Nagy-György et al. (2005) | U-Anchor (After Corner) and Bolted Angle (Specimen RW1) | Anchorage of Vertical FRP for In-Plane Bending of Shear Wall | | 0.005 | M | 32% | DB, OF |
| Nagy-György et al. (2005) | U-Anchor (After Corner) and Bolted Angle (Specimen RW23) | Anchorage of Vertical FRP for In-Plane Bending of Shear Wall | | 0.006 | M | 37% | DB, OF |
| Nagy-György et al. (2005) | U-Anchor (After Corner) and Bolted Angle (Specimen RW45) | Anchorage of Vertical FRP for In-Plane Bending of Shear Wall | | 0.008 | M | 46% | DB, OF |
| Nagy-György et al. (2005) | U-Anchor (After Corner) and Bolted Angle (Specimen RW67) | Anchorage of Vertical FRP for In-Plane Bending of Shear Wall | | 0.006 | M | 34% | DB, OF |
| Nagy-György et al. (2005) | U-Anchor (After Corner) and Bolted Angle (Specimen RW8) | Anchorage of Vertical FRP for In-Plane Bending of Shear Wall | | 0.008 | M | 49% | DB, OF |
| Ortega (2009) | Bolted FRP Plate (Continuous) | Anchorage for Shear FRP (90° orient.) on AASHTO T4 Beam | | 0.001 | M | 8% | DB, FA |
| Ortega (2009) | Bolted FRP Plate (Discontinuous) | Anchorage for Shear FRP (90° orient.) on AASHTO T4 Beam | | <0.001 | M | 4% | FA, ON |
| Ortega (2009) | Bolted FRP Plate (Discontinuous) | Anchorage for Shear FRP (45° orient.) on AASHTO T4 Beam | | <0.001 | M | 4% | DB, FA, ON |
| Ortega (2009) | Bolted FRP "Sandwich" Plate (Discontinuous) | Anchorage for Shear FRP (90° orient.) on AASHTO T4 Beam | | 0.001 | M | 6% | ON |

Table 2.2. Experimental Results of Tests Involving Anchorage (Continued)

| Study | Anchorage System Type | Anchorage Application | Percent Increase in Strength of Anchored FRP System Compared to Unanchored FRP System | Maximum Strain Reached in Anchored FRP | Strain Measured or Calculated | Percent of Ultimate FRP Strength Reached | Failure Mode(s) of FRP System |
|---------------|---|---|---|--|-------------------------------|--|-------------------------------|
| Ortega (2009) | Bolted FRP Plate (Discontinuous) | Anchorage for Shear FRP (90° orient.) on AASHTO T3 Beam | | <0.001 | M | 2% | ON |
| Ortega (2009) | Horizontal FRP Strip | Anchorage for Shear FRP (90° orient.) on AASHTO T3 Beam | | 0.004 | M | 21% | AF, DB |
| Ortega (2009) | Bolted FRP "Sandwich" Plate (Discontinuous) | Anchorage for Shear FRP (90° orient.) on AASHTO T3 Beam | | 0.002 | M | 9% | AF, RA, DB |
| Ortega (2009) | Bolted FRP Plate (Discontinuous) | Anchorage for Shear FRP (90° orient.) on RC T-Beam | | 0.002 ⁶ | M | 11% ⁶ | DB, OF, RP |
| Ortega (2009) | Bolted FRP "Sandwich" Plate (Discontinuous) | Anchorage for Shear FRP (90° orient.) on RC T-Beam | | 0.001 | M | 7% | DB, RP |
| Ortega (2009) | Horizontal FRP Strip | Anchorage for Shear FRP (90° orient.) on RC T-Beam | | 0.001 | M | 6% | DB |
| Ortega (2009) | Horizontal FRP Strip | Anchorage for Shear FRP (45° orient.) on RC T-Beam | | <0.001 | M | 5% | AF, DB |
| Ortega (2009) | Bolted FRP "Sandwich" Plate (Discontinuous) | Anchorage for Shear FRP (45° orient.) on RC T-Beam | | <0.001 | M | 3% | DB, RP |
| Orton (2007) | Transverse Wrap (Single Layer) | Anchorage of Flexural FRP to Beam | 112% | 0.009 | M | 64% | AF, DB |
| Orton (2007) | Transverse Wrap (Double Layer) | Anchorage of Flexural FRP to Beam | 180% | 0.011 | M | 83% | RP |
| Orton (2007) | 90° CFRP Anchor Spike (Orientation 2s1) | Anchorage of Flexural FRP to Beam | 11% | 0.004 | M | 34% | DB, OF |
| Orton (2007) | 90° CFRP Anchor Spike (Orientation 2s2) | Anchorage of Flexural FRP to Beam | 103% | 0.008 | M | 62% | AF, DB |
| Orton (2007) | 90° CFRP Anchor Spike (Orientation 4g1) | Anchorage of Flexural FRP to Beam | 70% | 0.008 | M | 58% | OF |
| Orton (2007) | 90° CFRP Anchor Spike (Orientation 4s1) | Anchorage of Flexural FRP to Beam | 100% | 0.008 | M | 61% | DB, RP |

Table 2.2. Experimental Results of Tests Involving Anchorage (Continued)

| Study | Anchorage System Type | Anchorage Application | Percent Increase in Strength of Anchored FRP System Compared to Unanchored FRP System | Maximum Strain Reached in Anchored FRP | Strain Measured or Calculated | Percent of Ultimate FRP Strength Reached | Failure Mode(s) of FRP System |
|-------------------------|--|--|---|--|-------------------------------|--|-------------------------------|
| Orton (2007) | 90° CFRP Anchor Spike (Orientation 4s2) | Anchorage of Flexural FRP to Beam | 138% | 0.010 | M | 72% | RP |
| Orton (2007) | 90° CFRP Anchor Spike (Orientation 4s3) | Anchorage of Flexural FRP to Beam | 197% | 0.012 | M | 91% | RP |
| Orton (2007) | 90° CFRP Anchor Spike (Orientation 6s1) | Anchorage of Flexural FRP to Beam | 202% | 0.012 | M | 92% | RP |
| Pan et al. (2010) | Transverse Wrap (Steel Cut) | Intermediate Anchorage for Flexural FRP on Rect. Beam | XXXXXX | 0.007 ⁷ | M | 38% ⁷ | DB, OF |
| Pan et al. (2010) | Transverse Wrap (Steel Not Cut) | Intermediate Anchorage for Flexural FRP on Rect. Beam | XXXXXX | 0.010 ⁸ | M | 56% ⁸ | DB, OF |
| Piyong et al. (2003) | 90° GFRP Anchor Spike | Anchorage of Flexural FRP to Slab Soffit | XXXXXX | 0.010 | M | 59% | RP |
| Sadeghian et al. (2010) | Transverse Wrap (2 Layers Long. FRP, Series 200) | Anchorage for Flexural FRP on Eccentrically Loaded Columns | XXXXXX | 0.007 | M | 64% | RP |
| Sadeghian et al. (2010) | Transverse Wrap (4 Layers Long. FRP, Series 200) | Anchorage for Flexural FRP on Eccentrically Loaded Columns | XXXXXX | 0.004 | M | 53% | OF |
| Sadeghian et al. (2010) | Transverse Wrap (2 Layers Long. FRP, Series 300) | Anchorage for Flexural FRP on Eccentrically Loaded Columns | XXXXXX | 0.007 | M | 84% | RP |
| Sadeghian et al. (2010) | Transverse Wrap (4 Layers Long. FRP, Series 300) | Anchorage for Flexural FRP on Eccentrically Loaded Columns | XXXXXX | 0.005 | M | 64% | RP |
| Sadone et al. (2010) | 180° Anchor Spike (Un-notched, monotonic) | Independent Anchorage Test | 63% ⁹ | 0.004 ⁹ | C | XXXXXX | AF, DB |
| Sadone et al. (2010) | 180° Anchor Spike (Un-notched, cyclic) | Independent Anchorage Test | 66% ¹⁰ | 0.004 ¹⁰ | C | XXXXXX | AF, RA |
| Sadone et al. (2010) | 180° Anchor Spike (Notched, monotonic) | Independent Anchorage Test | 69% ¹¹ | 0.004 ¹¹ | C | XXXXXX | DB, RP |
| Sadone et al. (2010) | 180° Anchor Spike (Notched, cyclic) | Independent Anchorage Test | 33% ¹² | 0.003 ¹² | C | XXXXXX | AF, OF |

Table 2.2. Experimental Results of Tests Involving Anchorage (Continued)

| Study | Anchorage System Type | Anchorage Application | Percent Increase in Strength of Anchored FRP System Compared to Unanchored FRP System | Maximum Strain Reached in Anchored FRP | Strain Measured or Calculated | Percent of Ultimate FRP Strength Reached | Failure Mode(s) of FRP System |
|--------------------|--------------------------------------|--|---|--|-------------------------------|--|-------------------------------|
| Teng et al. (2001) | U-Anchor (After Corner, Specimen A2) | Anchorage for Flexural FRP on RC Cantilever Column | | 0.013 ¹³ | M | 100% ¹³ | RP |
| Teng et al. (2001) | U-Anchor (After Corner, Specimen A3) | Anchorage for Flexural FRP on RC Cantilever Column | | 0.008 ¹³ | M | 58% ¹³ | DB |
| Teng et al. (2001) | U-Anchor (After Corner, Specimen A4) | Anchorage for Flexural FRP on RC Cantilever Column | | 0.008 ¹³ | M | 58% ¹³ | DB |
| Teng et al. (2001) | U-Anchor (After Corner, Specimen B2) | Anchorage for Flexural FRP on RC Cantilever Column | | 0.015 ¹³ | M | 115% ¹³ | DB, RP |
| Teng et al. (2001) | U-Anchor (After Corner, Specimen B3) | Anchorage for Flexural FRP on RC Cantilever Column | | 0.008 ¹³ | M | 60% ¹³ | DB |
| Teng et al. (2001) | U-Anchor (After Corner, Specimen C2) | Anchorage for Flexural FRP on RC Cantilever Column | | 0.017 | M | 126% | DB, RP |
| Teng et al. (2001) | U-Anchor (After Corner, Specimen C3) | Anchorage for Flexural FRP on RC Cantilever Column | | 0.012 ¹³ | M | 88% ¹³ | DB |

NOTE: Refer to Table 2.3 for footnote designations.

Table 2.3. Notes on Anchorage Studies From Table 2.2

| Reference Number | Number of Specimens Tested | Standard Dev. of % of Ultimate FRP Strength | Notes |
|------------------|----------------------------|---|--|
| 1 | 2 | 47.4 | |
| 2 | 2 | 60.1 | |
| 3 | 8 | 4.5 | Detailing of anchorage differed slightly between specimens |
| 4 | 2 | 0.4 | Detailing of anchorage differed slightly between specimens |
| 5 | 2 | 1.4 | |
| 6 | 2 | 1.7 | |
| 7 | 4 | 2.5 | |
| 8 | 4 | 2.6 | |
| 9 | 4 | 0.0007 | Standard deviation is of strain values |
| 10 | 2 | 0.0000 | Standard deviation is of strain values |
| 11 | 4 | 0.0005 | Standard deviation is of strain values |
| 12 | 2 | 0.0009 | Standard deviation is of strain values |
| 13 | | | Value is average of two anchored FRP strips on same specimen |

2.5. ANCHORAGE TEST PROCEDURES

A limited number of tests have been reported upon in the literature in which anchorage systems are evaluated independently. Data obtained from these tests were critical to the understanding of anchorage system performance, as independent anchorage tests generally include only the variables necessary to understand the basic behavior of the anchorage system. Data from other tests that use anchorage devices as a part of a larger FRP strengthening scheme, while still very useful, may have limited applicability to the general state of knowledge of a particular anchorage system. This section will review several sets of testing procedures reported by various independent anchorage studies.

2.5.1. Shear Type Anchorage Tests. A popular type of anchorage test is the “shear” test setup, in which FRP is bonded to a fixed concrete block and a tensile force is applied to the FRP. Variations of this test include single-shear and double-shear tests, as well as some slight variations in test setup and specimen geometry. An advantage to shear-type tests is that the bonded area of FRP-to-concrete may be included, whereas pull-out tests generally do not include the bonded FRP area. For certain anchorage applications, as discussed in Chapter 3, including this bonded area more closely simulates anchorage performance since the FRP-to-concrete bond is responsible for transferring much of the tensile force in the FRP to the concrete. Shear type anchorage test specimens can also be customized to simulate unique anchorage conditions, such as the

90° joint at a beam-column interface, a beam-footing interface, or the interface between a T-beam web and flange.

Single-shear tests are the most simple test setup in this category. As shown in Figure 2.26, a concrete block is restrained in a way that prevents all movement, and a force is applied to the FRP bonded to the block. A major advantage to this test is its simplicity; because the force is applied directly to the FRP, an actual force measurement in the FRP may be taken rather than having to calculate the force based on a local strain measurement or an assumed specimen behavior. Despite the simplicity of the system, constructing a method to fix the concrete block may provide challenges. Some creativity is also needed to devise a system that applies load directly and uniformly to the FRP while eliminating or minimizing the effects of an eccentric load. Single-shear tests have been used by Kalfat and Al-Mahaidi (2010), depicted in Figure 2.26 (a), and Sadone et al. (2010), depicted in Figure 2.26 (b).

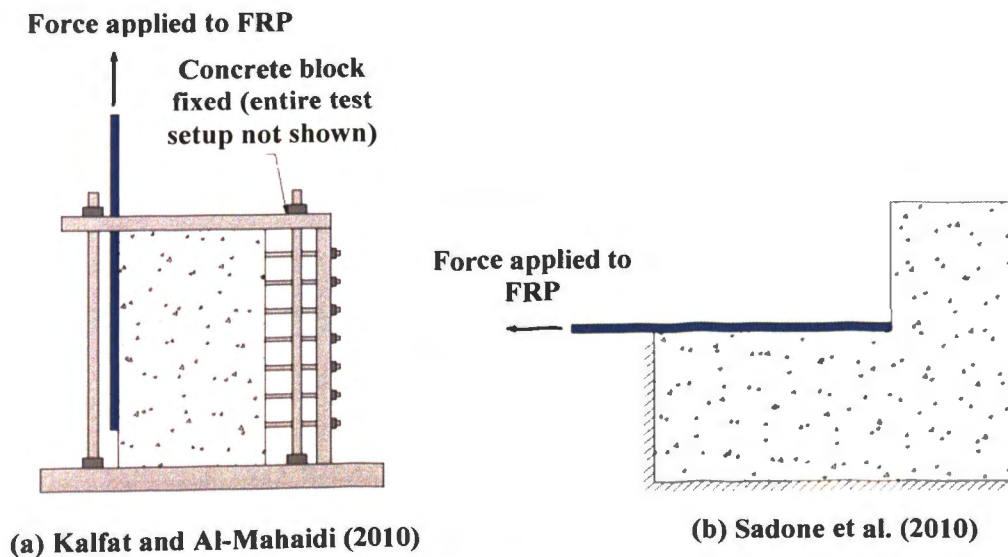


Figure 2.26. Single-Shear Anchorage Testing Setups

Double-shear tests utilize a symmetrical system so that load application presents fewer challenges than a single-shear test. Because of the specimen's symmetry, a load can be applied to the fixed concrete block, which is generally simpler than devising a system to apply load directly and evenly to the FRP. Limitations of this system include

its demand for system stability. Since debonding of FRP is a progressive failure, the initiation of debonding does not necessarily correspond with the ultimate strength of the FRP and anchorage system. However, debonding on one side of a double-shear test leads to system instability, and further testing would produce unequal loads in each side of the anchorage specimen. In general, this would suggest that double-shear anchorage tests tend to underestimate the strength of an anchorage system. Further, double-shear tests require two sets of anchorage systems and FRP to obtain one result or data point. While strain measurements may be taken on each side of the specimen for comparative purposes, they cannot be considered statistically independent since their performances are dependent on each other. Therefore, double-shear tests are not as materially efficient as other anchorage testing systems. The double-shear tests performed by Sami et al. (2010) and Kalfat and Al-Mahaidi (2010) are depicted in Figure 2.27 (a) and (b), respectively. Hall et al. (2002) used a system nearly identical to the Kalfat and Al-Mahaidi system, except that a hydraulic jack was placed between the two blocks to apply the load.

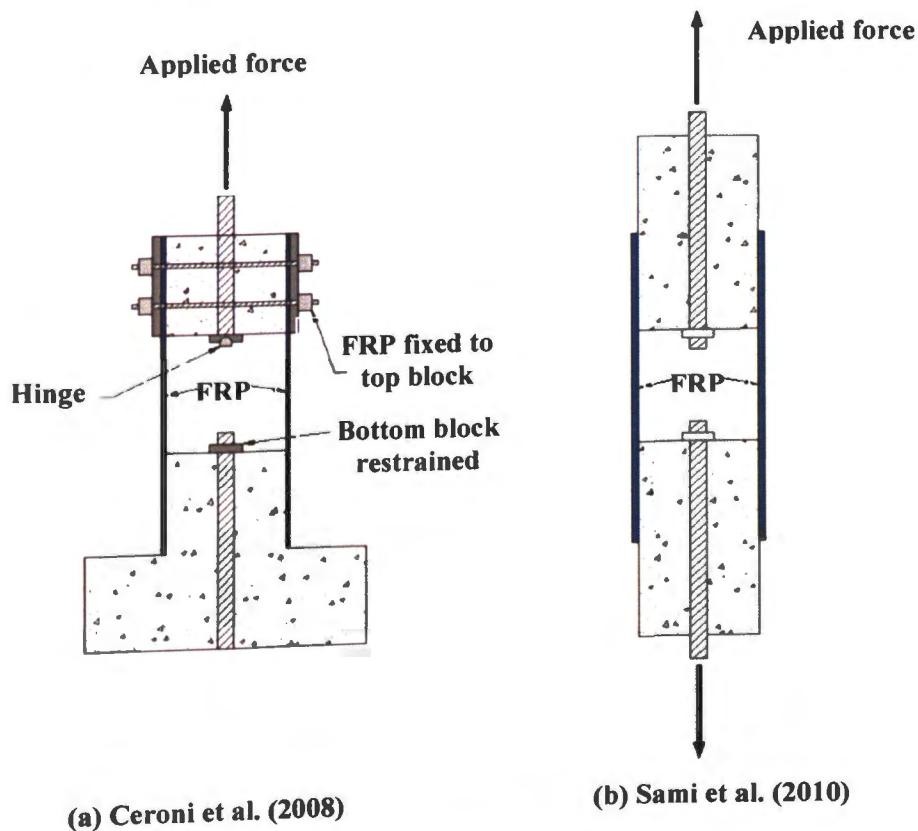


Figure 2.27. Double-Shear Anchorage Testing Setups

2.5.2. Pull-Out Type Anchorage Tests. Pull-out anchorage testing is the most basic form of anchorage testing. Rather than including a bonded area ahead of the anchorage system as in a shear type test (Section 2.5.1), a pull-out anchorage test simply evaluates the anchorage's ability to transfer the force in the FRP sheet or plate to the concrete in the absence of any shear load transfer between FRP and concrete. Pull-out anchorage tests have the fewest number of variables among any form of anchorage test. The test, however, is useful only for certain anchorage applications, which are discussed later in Chapter 3 of this thesis.

Sami et al. (2010) used two types of pull-out tests in their anchorage study. First was the basic pullout test depicted in Figure 2.28 (a). The anchorage system was simply attached to the concrete and loaded perpendicular to the concrete surface. Because of the few variables involved with this type of pull-out test, measurement of the lateral displacement between the FRP anchorage and the surface to which it is attached is simple. Simple pull-out tests were also used in studies by Eshwar et al. (2003), Piyong et al (2003), and Huang and Chen (2005). The tests performed by Eshwar et al. and Piyong et al., however, seem to have been performed in order to optimize the dimensions of the anchorage device rather than to determine the strength of the anchorage system. Sami et al. also used a double-sided pull-out test specimen. This system is similar to the double-shear anchorage test setup in that it relies on loading symmetry to evaluate anchorage strength. Despite that limitation, the system's major advantage is that the load can be applied to a fixture that is easily attached to the FRP rather than to FRP itself. The double-sided pull-out test is shown in Figure 2.28 (b).

2.5.3. Bending Type Anchorage Tests. Because FRP is stressed in tension when it is bonded to the "tension face" of an RC member in flexure, anchors that are properly placed on a bending specimen can be stressed in tension while experiencing the crack development associated with RC bending. In Orton's (2007) study of RC beams with and without height transitions, bending type anchorage tests were used to evaluate anchorage placed near the end of FRP sheets. Orton's anchorage testing setup included two RC blocks of equal length and equal or varying height that were placed end-to-end and bridged together with an FRP sheet. The outside ends of the blocks were fixed and a load was applied at midspan, or at the joint between the two blocks. This allowed for a

bending condition that simulated I.C. crack debonding to be induced in the FRP system. The force in the FRP at midspan was estimated by calculating the moment at midspan and determining the FRP force required for equilibrium of the section. Orton's test setup is shown in Figure 2.29.

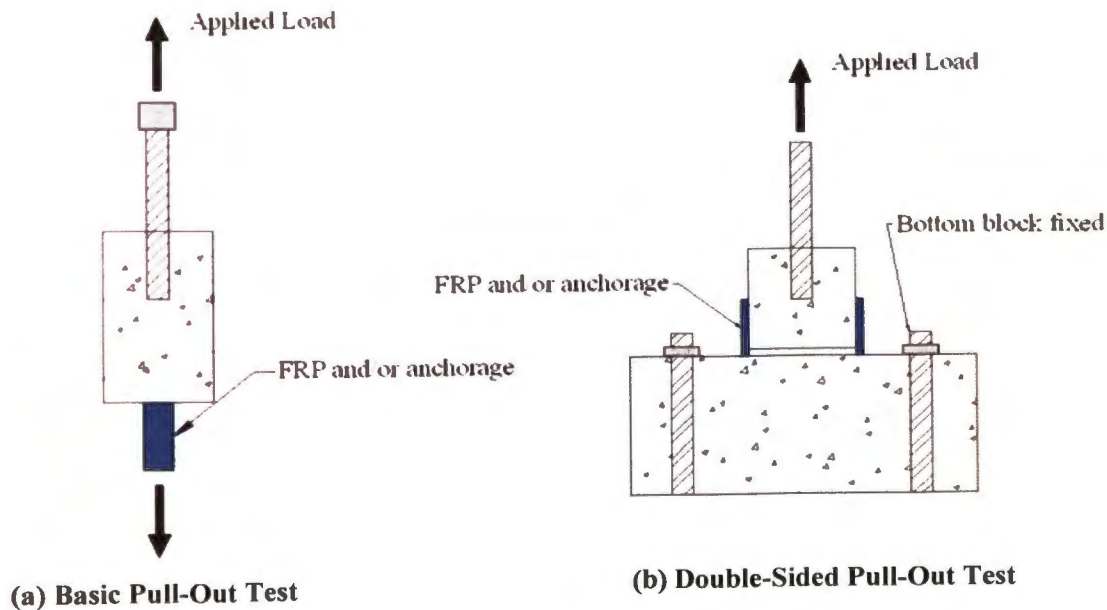


Figure 2.28. Pull-Out Type Anchorage Tests

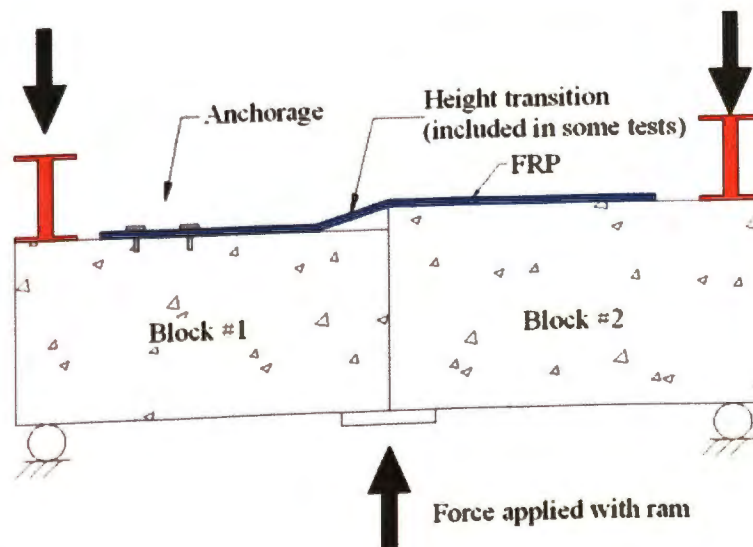


Figure 2.29. Bending Type Anchorage Test Used in Orton (2007)

Sami et al. (2010) utilized a bending type anchorage test setup that involved a beam with cross sections of varying height in three-point bending. The height change occurred at midspan so that the anchorage system could be installed into the taller half of the beam and bonded to the soffit of the shorter half, as depicted below in Figure 2.30. This setup allows for either horizontal or inclined anchorage installation and simulates the real condition of an anchor subjected to both a bending moment and a pull-out force.

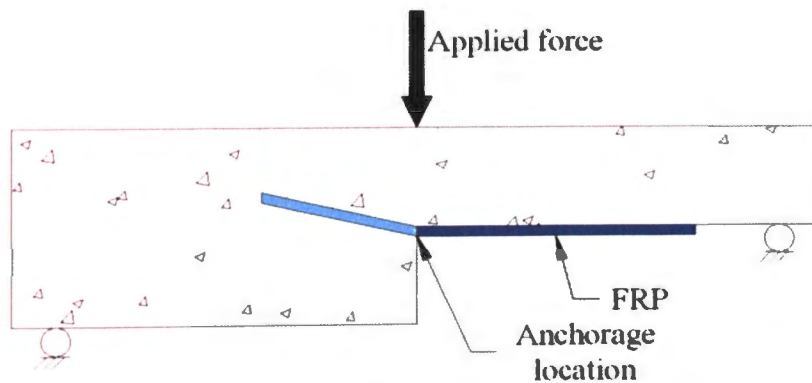


Figure 2.30. Bending Type Anchorage Test Used in Sami et al. (2010)

2.6. CONCLUDING REMARKS

Selection of an anchorage system is certainly application driven and depends on the unique circumstances of the overall FRP strengthening system being applied to the RC structure. It can be seen, however, that testing procedures for anchorage devices have been poorly defined despite the lack of extensive knowledge about their behavior and the critical role they play in an FRP strengthening scheme. Additionally, an insufficient amount of test data exists to substantiate claims that any particular anchorage device is effective in delaying debonding to a specified strength level, or, as some researchers have suggested, preventing the debonding failure mode completely. Therefore, in addition to the development of a new anchorage device, this thesis will also focus on the gaps and inconsistencies in the aforementioned FRP anchorage system research, as well as propose classifications and new directions for anchorage system research.

3. ANCHORAGE SYSTEM CATEGORIZATION

3.1. GENERAL

Chapter 3 of this thesis proposes a method for categorizing of the anchorage systems presented in Chapter 2 on the basis of anchorage behavior or intended application. The proposed anchorage categories will be useful to the expansion of knowledge of the subject of FRP anchorage systems for several reasons. First, no system currently exists to categorize anchorage systems, which makes the selection of an appropriate system difficult, especially for those who are only slightly familiar with the subject. Additionally, categorization aids in the discussion of anchorage testing applicability, which is crucial to the successful implementation of FRP as a method for strengthening RC structures.

Section 3.2 describes the proposed anchorage categories in terms of the purpose and behavior of the anchorage system, the FRP, and the RC substrate. In Section 3.3, the anchorage systems discussed in Chapter 2 are revisited and assigned to an anchorage category. The applicability of anchorage testing procedures is discussed in Section 3.4 with respect to the newly proposed categorization system. Additionally, recommendations for test procedures are given. Finally, concluding remarks on this chapter are presented in Section 3.5.

3.2. DEFINITION OF ANCHORAGE SYSTEM CATEGORIES

Anchorage systems for externally bonded FRP typically serve one or more of the following purposes: (I) to prevent or delay a premature debonding failure by resisting the tensile normal forces associated with certain debonding failure modes; (II) to reduce the in-plane development length required to achieve a specified design strength by transferring load from the FRP to the anchorage system via shear; or (III) transferring the force in the FRP laminate to another structural component where no development length is available. As will be discussed in the following subsections, anchorage devices serving these purposes will be categorized as Type I, Type II, and Type III anchorage systems for the remainder of this thesis.

3.2.1. Type I Anchorage Definition. Type I anchorage systems are most commonly used at the termination of FRP sheets or plates, and sometimes throughout their entire length, to resist tensile normal forces that occur due to the onset of debonding or failure of the concrete substrate. When debonding initiates at the sheet or plate end, as is the case with plate-end interfacial debonding or concrete cover separation failure, a Type I anchorage device can be used to prevent or delay these processes. An example of a Type I anchorage device is shown in Figure 3.1, in which the flexural FRP on a RC beam soffit is anchored at the sheet or plate end in order to prevent plate-end debonding.

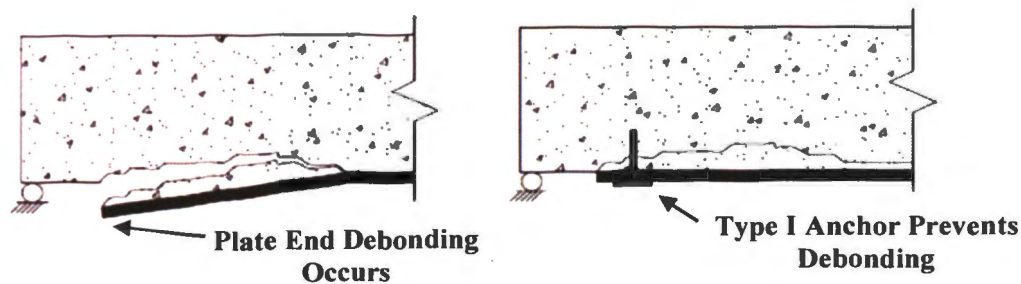


Figure 3.1. Example of Type I Anchorage Device

3.2.2. Type II Anchorage Definition. Type II anchorages are often used where insufficient space exists to develop the desired design strength of the FRP, usually due to the geometric conditions of the structural member, or simply to reduce the amount of FRP being used. The characteristic that distinguishes a Type II anchorage system from a Type I system is that it does not include a mechanism to resist the tensile normal forces associated with debonding. Instead, the force in the FRP is transferred via shear to the anchorage system, which in turn distributes the load to an area of the concrete substrate that is not directly in contact with the FRP sheet or plate. Several examples of Type II anchorage systems are discussed in Section 3.3.

3.2.3. Type III Anchorage Definition. A Type III anchorage system is used in locations where the point of maximum FRP stress lies at a sheet or plate end, or near a change in direction of the fibers, such as at the location of an interface between two structural members. The Type III anchorage system serves the crucial role of transferring the stress in the FRP at the point of maximum stress to another structural member without

transferring any load over a “bonded length” of FRP to concrete. Thus, Type III anchors do not benefit from a “bonded length” as Type I and Type II anchors do. Examples of Type III anchorage applications are when FRP strips are used as flexural reinforcement for a RC or masonry shear wall, or when FRP is used as flexural reinforcement on a cantilever beam.

While Type III anchorages certainly include many characteristics of Type I and Type II anchorage systems, Type III anchorages present a very special and difficult challenge in that the FRP strengthening system can be considered to have no strength before their inclusion. While some Type III anchorages may have debonding-preventing characteristics, they differ from Type I anchorages in that they must transfer the entire force in the FRP to another structural element instead of simply resisting the tensile normal debonding force. Additionally, Type III anchorage systems are different from Type II systems in that the demand on a Type II anchorage is less since some of the force is transferred along a “bonded length”. In Figure 3.2, the example of a U-Anchor is used to illustrate the difference in behavior of the same anchorage system being used in Type II and Type III applications.

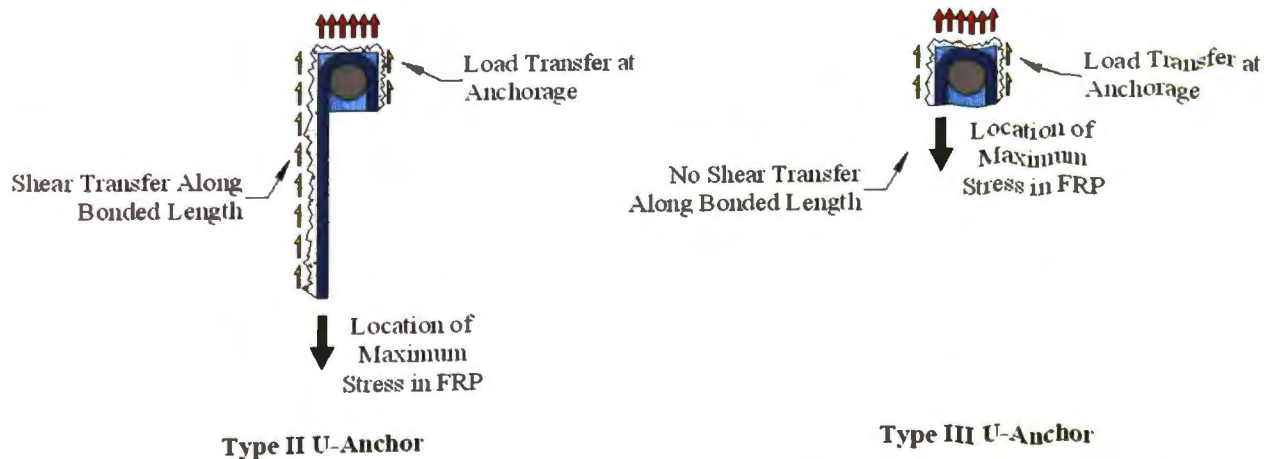


Figure 3.2. Comparison of Type II and Type III Anchorage (U-Anchor Example)

3.3. CATEGORIZATION OF EXISTING ANCHORAGE SYSTEMS

In this section, the anchorage systems reviewed in Chapter 2 are revisited and classified according to the anchorage categories defined in Section 3.2. In doing so, it

becomes apparent that certain anchorage devices fall into multiple categories, depending on their use. Additionally, certain anchorage devices by their nature incorporate both Type I and Type II behaviors.

3.3.1. Anchor Spikes. Anchor spikes, both the 90° and 180° varieties, are perhaps the most versatile form of FRP anchorage that exist. Because they can be seamlessly integrated with the matrix of the FRP being anchored, they can be fabricated to overcome nearly any geometric complexity that exists. However, their categorization depends on both their intended application and the type of anchor spike being used.

3.3.1.1 90° Anchor Spikes. 90° anchor spikes fall exclusively into the Type I anchorage category since their means of force transfer is exclusively through resisting the tensile normal forces associated with debonding. While some studies, such as Orton (2007), have relied on a force transfer model similar to that shown in Figure 3.3, it is not likely that typical 90° anchors transfer force in that manner due to their limited shear capacity. Instead, it is more likely that the 90° anchor spikes resist the normal debonding force, similar to the mechanism shown in Figure 3.1. Because 90° anchor spikes only transfer anchoring forces to the underlying concrete and do not have the capability of transferring force to another structural member, they cannot be used in a Type III anchorage application.

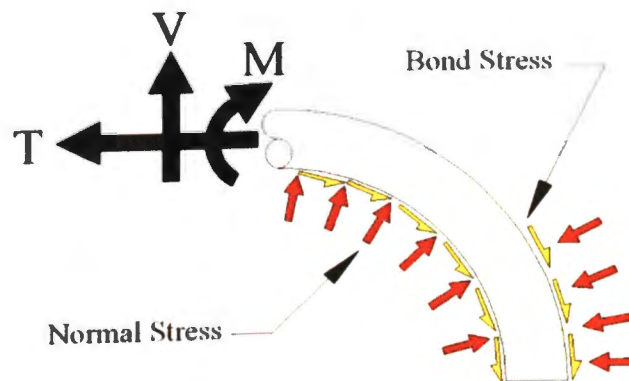


Figure 3.3 Anchor Bend Force Transfer Mechanism Reported by Orton (2007)

3.3.1.2 180° Anchor Spikes. 180° anchor spikes, whether fabricated from FRP or a metallic material, can be used as a Type II or Type III anchorage system. In a Type II

application, such as when shear FRP reinforcement on an RC or precast concrete T-beam is anchored to the beam flange, the force in the FRP sheet resulting from the opening of shear cracks along the face of the beam web is transferred in shear to the bonded concrete surface underneath the FRP, and the remaining force at the end of the FRP sheet is transferred through the 180° anchor spike to the embedded portion of the anchor, as shown in Figure 3.4.

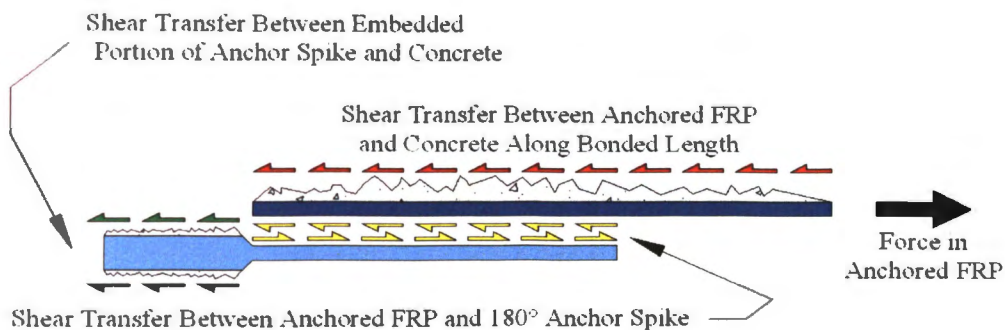


Figure 3.4. Force Transfer Mechanism of 180° Anchor in Type II Application

As previously mentioned, 180° anchor spikes can also be used as an anchorage system in a Type III application. For example, in the case of a cantilever RC member where FRP reinforcement is bonded to the tension side of the member, a Type III 180° anchor spike may be used at the fixed end to transfer the entire tensile force developed in the FRP to the adjacent concrete member.

It should be noted that Figure 3.4 is an idealized schematic of a 180° anchor spike. Actual applications of these anchors may be subject to the installation difficulties discussed in Section 2.2.1.2 of this thesis and depicted in Figure 2.4.

3.3.2. Transverse Wrapping. Because it can restrain FRP from debonding either by resisting the tensile normal forces by providing confinement to the FRP and concrete beneath it, transverse wrapping anchorage falls into the category of Type I anchorage. While it is possible that a small amount of shear force is transferred from the anchored FRP to the transverse wrap, and subsequently to the concrete under the transverse wrap, the vast majority of transverse wrapping anchorage strength comes from the FRP wrap's ability to confine and restrain the anchored FRP. The unlikelihood of significant force

transfer in shear between the transverse wrapping FRP and the anchored FRP is discussed in Section 3.3.4. Since transverse wrapping anchorage can only prevent debonding and cannot effectively transfer the shear forces in the FRP, it can only be used as a Type I anchorage system.

3.3.3. U-Anchors and Longitudinal Chases. The U-Anchor and longitudinal chase anchorage systems perform similarly as Type II anchorage devices. Regardless of the orientation of the U-Anchor, the extension of the FRP into the groove allows for the epoxy in the groove to transfer the force in the FRP to the surrounding concrete via shear and tension. No part of this anchorage system acts to prevent debonding, therefore U-Anchors do not exhibit Type I behavior. Additionally, while U-Anchors can certainly be used in Type III applications, they generally are not strong enough to resist the large anchoring forces typically required in Type III applications as will be discussed in Chapter 5 of this thesis. The basic behavior of an after-corner U-Anchor is shown in Figure 3.5

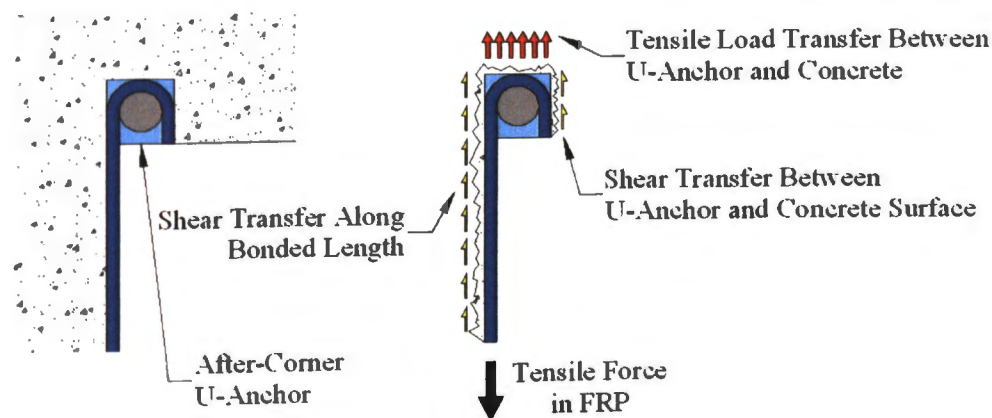


Figure 3.5. Behavior of an After-Corner U-Anchor

Longitudinal chase anchorage behaves in a similar manner to U-Anchors, except that since the chase typically extends in the direction of the applied load, all of the anchorage forces are transferred in shear along the walls of the chase groove. The anchorage forces in this case are the additional shear resistances provided by the walls of the chase perpendicular to the plane of the FRP sheet. Because of its unique nature and

its inability to transfer load to another member, the longitudinal chase cannot be used as a Type III anchorage system.

3.3.4. FRP Strips. Classification of FRP strip anchorage systems is difficult since their ineffectiveness compared to other anchorage devices has limited the number of studies in which they are used. Because of this, the behavior of FRP strip anchorage has not been widely reported. However, two force transfer mechanisms are possible for FRP strips. The first mechanism would anchor FRP by resisting the debonding tensile force normal to the surface. This would be accomplished by a mechanism similar to the one depicted in Figure 3.6, which can be categorized as a Type I system.

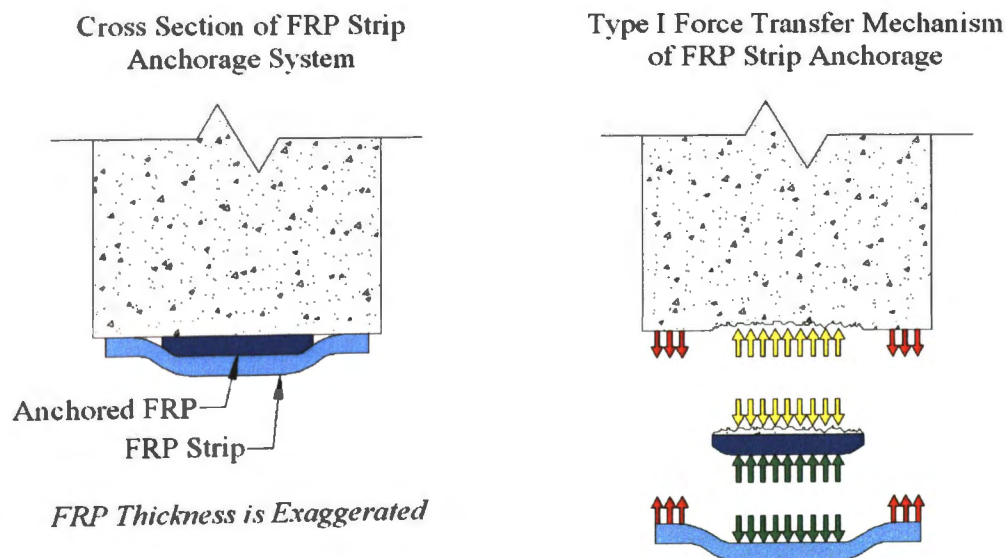


Figure 3.6. Type I Force Transfer Mechanism of FRP Strip Anchorage

The second force transfer mechanism of FRP strip anchorages is via shear between the anchored FRP and the FRP strip anchorage. This type of behavior can allow FRP strips to be classified as a Type II system.

As previously mentioned in Section 2.2.5, this anchorage system is inefficient due to the use of FRP strips to carry loads that cause the fibers in the strips to be stressed in a manner other than in pure tension. Since surface-bonded FRP is not intended to transfer load in this manner, it is advisable that other anchorage systems be considered before FRP strips are used.

3.3.5. Plate Anchors. Type I and Type II behavior is likely exhibited simultaneously by plate anchors depending on their construction (Ortega 2009). Because the FRP is typically bonded to the surface of the plate, force is transferred in shear between the FRP and plate. The plate then transfers that shear load to the concrete via its connection, which could be bolts through the plate into the concrete substrate, or areas of the plate outside of the FRP that are glued to the concrete. This mechanism of force transfer is shown in Figure 3.7.

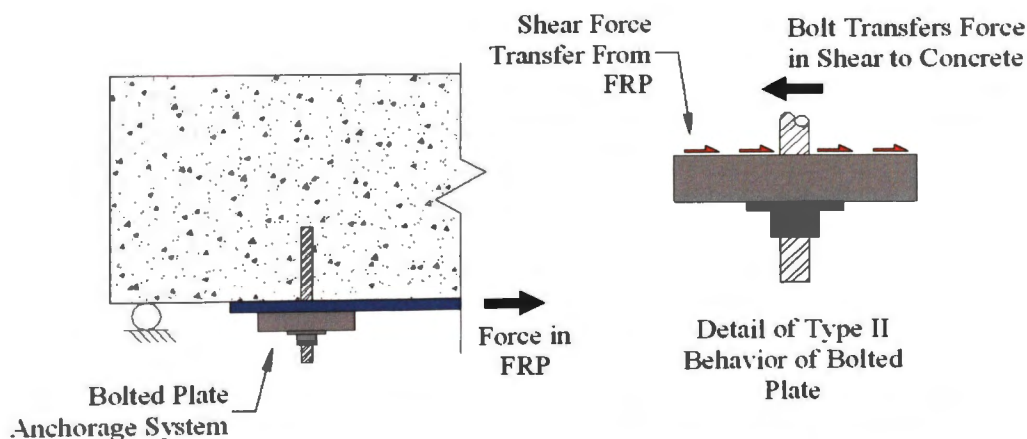


Figure 3.7. Type II Force Transfer Mechanism of Plate Anchors

In the case of bolted plate systems, the embedded bolts provide Type I resistance to forces normal to the concrete surface. This method of force transfer is essentially the same as is depicted in Figure 3.1. Glued plate anchorage systems do not provide significant strength as a Type I anchorage since their only means of force transfer is by shear to the concrete surface. The area over which the concrete is bonded to the FRP would likely not remain intact during the debonding process.

3.3.6. Bolted Angles. Because they are typically bonded to the FRP, there is usually Type II anchorage behavior present in a bolted angle anchorage system. The shear force transferred from the FRP to the angle is subsequently transferred to the anchor rods and the concrete into which they are embedded. In the case of a bolted angle system that contains anchor rods through the angle that are perpendicular to the plane of the anchored FRP such as in the system depicted in Figure 2.19, there likely is some Type I anchorage behavior present as well. Because these bolts extend into the concrete

beneath the anchored FRP, they are able to resist the debonding force that initiates in the anchorage zone. While a bolted angle system that contains bolts only in the direction parallel to the tensile force applied to the fibers, such as the system in Figure 2.18, may exhibit Type I behavior, the contribution of the Type I behavior to the overall strength of the system is likely to be much smaller when compared to the system with bolts in both directions, such as the system depicted in Figure 2.19. Based on the discussion of the performance of bolted angle anchorage systems in Chapter 2, it is clear that bolted angles can be used as Type III anchorage as well.

3.3.7. CHS Anchorage and Ductile Anchorage Systems. Based on the behavior of the CHS anchorage and ductile anchorage systems presented in Section 2.2.8 and 2.2.9, it is apparent that these systems were designed specifically for Type III applications. While elements of Type I and Type II anchorage behavior can certainly be observed in the CHS and ductile anchorage systems, a detailed discussion of Type I and Type II behavior with respect to the CHS and ductile system is not warranted since the CHS anchorage system was designed specifically for installation in a Type III application where a significant force must be transferred at a 90° joint.

3.4. APPLICABILITY OF ANCHORAGE TESTING PROCEDURES

In this section, each of the anchorage testing procedures reviewed in Section 2.5 are revisited and their applicability discussed in relation to the anchorage categories defined in Section 3.2. The importance of proper anchorage testing methods is significant due to the critical role they play in determining the design strength of the FRP system. Additionally, improper selection of an anchorage test method could lead to an overestimation of the strength of the anchorage system.

Because so few studies have reported results of independent anchorage tests, or tests that specifically evaluate the strength of an anchorage system in the absence of a global FRP strengthening system, it is crucial that future research selects and executes these types of tests correctly. It is important to note that the simplified methods of testing anchorage systems independently are certainly not a substitute for representative tests involving full FRP strengthening systems. However, these simplified tests include only the most basic variables needed to evaluate the fundamental mechanics of anchorage

behavior. This allows for a comparison between representative testing, or tests that evaluate an FRP-strengthened structural member containing an anchorage system, and independent testing. This comparison is crucial for industry acceptance of a new anchorage system as a viable method to increase the design strength of FRP strengthening system. The need for such testing is also substantiated by the requirements in *ACI 440.2R-08* that a proposed form of FRP anchorage should be “heavily scrutinized” and should undergo “representative physical testing”. A diagram of the research process necessary for industry acceptance of anchorage systems is shown below in Figure 3.8.

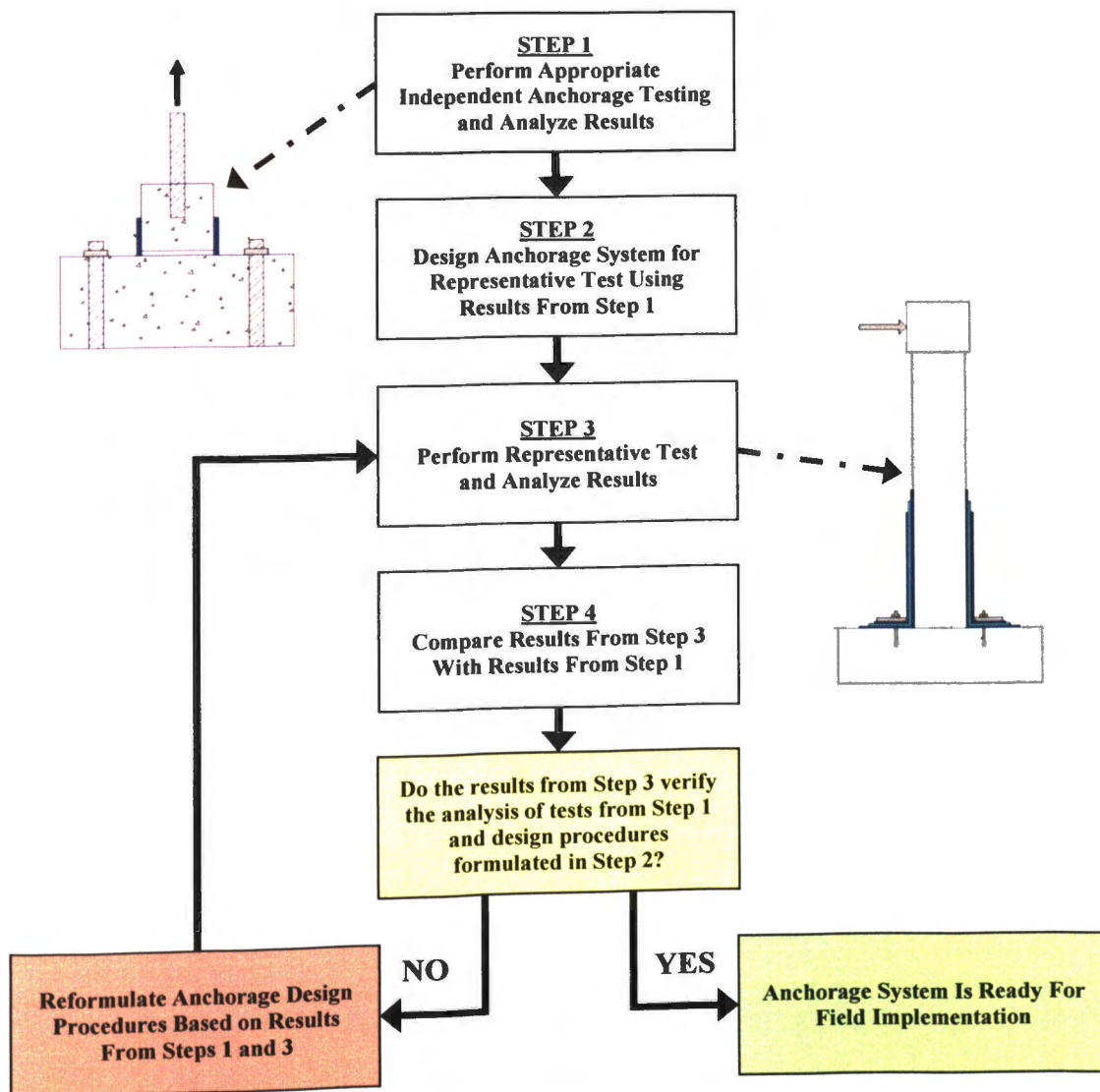


Figure 3.8. Process Leading to Field Implementation of New Anchorage Systems

3.4.1. Type I and Type II Testing Procedures. Type I and Type II anchorage systems should have similar testing procedures. The shear type anchorage tests discussed in Section 2.5.1 and depicted in Figures 2.26 and 2.27 are directly applicable to Type I and Type II anchorage tests. The bending-type anchorage tests presented in Section 2.5.3 and depicted in Figures 2.29 and 2.30 could also be used to evaluate Type I and Type II anchorage systems. If the Sami et al. (2010) system from Figure 2.30 is used for a Type I or Type II anchorage test, a superior, or stronger, form of anchorage should be used at the midspan location, with the anchorage system in question being used on the end of the anchored FRP nearer to the support. Due to the larger number of variables that are included in the bending-type tests, however, the baseline of anchorage performance should be established with simpler tests such as single- and double-shear tests. After enough testing has been performed to analyze the basic behavior of each anchorage system, the data obtained from these tests can be used to design more complicated tests, such as those that examine the effects of crack spacing (Kobayashi et al., 2001) or those that simulate the effects of more complicated variables on the anchorage system, such as the bending-type anchorage tests.

Important variables for Type I and Type II anchorage tests include the following: the geometry of the bonded composite laminate; the mechanical properties of the concrete, fibers, and the bonding resins; the loads and loading rates; and other anchorage-specific parameters that will vary among the many different types of anchorage systems. These variables should be clearly reported so that compatibility among various test results can be verified.

3.4.2. Type III Testing Procedures. Since Type III anchorage systems do not benefit from a FRP-to-concrete bond between the applied load in the anchorage zone, their testing procedures must reflect this. Therefore, the pull-out tests presented in Figure 2.28 should provide the basis for preliminary anchorage design before more complicated tests are performed. While many other variables certainly affect the anchorage performance, such as the effects of detailing, field implementation of new Type III anchorage systems will not occur unless large-scale representative testing can verify the results of small, independent anchorage tests, and vice versa. In addition to the simple pull-out tests applying to Type III anchorage testing, the bending-type anchorage test

from Sami et al. (2010) depicted in Figure 2.30 should also apply to Type III systems, given that the anchorage location is at midspan, which based upon test setup and specimen design should be the location of maximum FRP stress.

The important variables for a pull-out test of Type III anchorage systems are similar to those for Type I and Type II system testing. They include: FRP geometry; details about the connection between FRP and anchorage, if applicable; mechanical properties of FRP sheets, concrete, and bonding resins; the loads and loading rates; and other anchorage-specific parameters. Once again, these variables should be clearly reported.

3.5. CONCLUDING REMARKS

Based upon the review of anchorage systems and the data that exist to document their performance, it is safe to conclude that an insufficient amount of testing has been performed to warrant the inclusion of anchorage behavior to current design guidelines and practices. This is confirmed by the minimal mention of anchorage systems in current design guidelines such as *ACI 440.2R-08* despite the critical role they play in FRP strengthening of RC members. The proposed anchorage system categories should facilitate an easier and more comprehensive understanding of anchorage system behavior and applicability. More importantly, categorization can help standardize anchorage testing procedures, which is essential to creating well-documented design guidelines.

Summarized in Figure 3.9 is the categorization of anchorage devices from this chapter along with the applicability of testing procedures.

| | TYPE I | TYPE II | TYPE III |
|---------------------------------------|------------------|------------------|------------------|
| Anchorage System | | | |
| 180° Anchor Spikes | | PRIMARY | PRIMARY |
| 90° Anchor Spikes | PRIMARY | | |
| Bolted Angles | SECONDARY | PRIMARY | PRIMARY |
| CHS Anchors | SECONDARY | SECONDARY | PRIMARY |
| Ductile Plate Anchorage | SECONDARY | SECONDARY | PRIMARY |
| FRP Strips | SECONDARY | SECONDARY | |
| Longitudinal Chases | | PRIMARY | |
| Plate Anchors | SECONDARY | PRIMARY | SECONDARY |
| Transverse Wrapping | PRIMARY | | |
| U-Anchors | | PRIMARY | PRIMARY |
| Anchorage Test Procedures | | | |
| Bending-Type Test (Orton, 2007) | SECONDARY | SECONDARY | |
| Bending-Type Test (Sami et al., 2010) | SECONDARY | SECONDARY | SECONDARY |
| Double-Shear Test | PRIMARY | PRIMARY | |
| Double-Sided Pull-Out Test | | | PRIMARY |
| Simple Pull-Out Test | | | PRIMARY |
| Single-Shear Test | PRIMARY | PRIMARY | |

Figure 3.9. Summary of Anchorage Test Procedures and Categorization

4. EXPERIMENTAL PROGRAM

4.1. GENERAL

In this chapter, a description of the experimental program involving the Type III anchorage devices (defined in Section 3.2.3) used to anchor longitudinal, or flexural, FRP at the base of repaired square columns is presented. First, Section 4.2 provides a background of the unrepaired, damaged columns along with some preliminary test results from the original column testing program. Next, Section 4.3 discusses in detail the goals for the “rapid repair” strengthening program. Section 4.4 presents descriptions and details of the materials used to repair and strengthen the damaged columns. The design and construction of the anchorage devices are documented in Section 4.6. Next, the entire repair process of the damaged columns is presented in Section 4.7. Finally, the instrumentation relevant to the analysis of the novel anchorage system and the overall testing procedure are presented in Section 4.8. The results of the testing described in this chapter are presented in Chapter 5 of this thesis.

The evaluation of the anchorage systems presented in this thesis was performed as a part of a larger study involving the repair of severely damaged square bridge columns. These bridge columns were originally constructed and tested by Qian Li and Dr. Abdeldjelil Belarbi under loading programs described in Section 4.2. After surveying the damage to the columns and researching repair design recommendations published in technical reports, journals, and other literature, the design of the complete FRP strengthening system was completed by a committee consisting of Dr. Lesley Sneed, Ruili He, Yang Yang, and the author. The repaired columns were tested under loading programs similar to those used in the original testing, each of which involved loading with a different torque-to-moment ratio, described in Section 4.2. While the primary purpose of the study was to understand the behavior of the externally bonded FRP used in a “rapid repair” scenario for severely damaged bridge columns tested under combined loadings, the data obtained from the column instrumentation are certainly valuable in evaluating the performance of the anchorage systems.

4.2. BACKGROUND OF DAMAGED COLUMNS

4.2.1. Testing Program. The original, undamaged square columns were tested to failure under a combined loading of shear, bending moment, and torsion by Qian Li and Dr. Abdeldjelil Belarbi at Missouri S&T as part of a separate project, *NEESR-SG: Seismic Simulation and Design of Bridge Columns Under Combined Actions, and Implications on System Response* (Award Number 0530737). The purpose of the original testing program was to study the interaction of the combined loads. Therefore, the primary variable that differed between these tests was the torque-to-moment (T/M) ratio. A constant axial load of approximately 150 kips was also applied to the column. A total of six columns were tested under varying T/M ratios. The T/M ratios for the columns were zero, which corresponds to pure bending and shear, 0.2, 0.4, 0.6, and infinity, which corresponds to pure torsion. Two of the columns were tested with a T/M ratio equal to 0.4, but with slightly different loading protocols. Three of the specimens with T/M ratios of 0.2, 0.4, and 0.6 were loaded by incrementally increasing a set of different forces in each hydraulic actuator that maintained the specified T/M ratio during loading within each cycle. The second specimen with T/M ratio equal to 0.4 was loaded in each cycle by first applying the full torque and then incrementally increasing the moment and shear. This is referred to as a “sequential” loading program. In this loading program, the magnitude of torsion was equal to the torsion capacity of the other column with T/M ratio of 0.4. Table 4.1 shows the column number designations along with the T/M ratio and loading program type for each.

Table 4.1. Column Number Designation

| Column ID Number | T/M | Loading Program Type |
|------------------|----------|----------------------|
| 1 | 0 | Normal Cyclic |
| 2 | 0.2 | Normal Cyclic |
| 3 | 0.4 | Normal Cyclic |
| 4 | 0.6 | Normal Cyclic |
| 5 | ∞ | Normal Cyclic |
| 6 | 0.4 | Sequential Cyclic |

4.2.2. Original Column Design. The undamaged columns were designed with the same reinforcement and cross-sectional dimensions regardless of the loading protocol. The longitudinal and transverse reinforcement ratios were 2.13% and 1.32%, respectively. Elevation drawings of the original columns are shown in Figure 4.1.

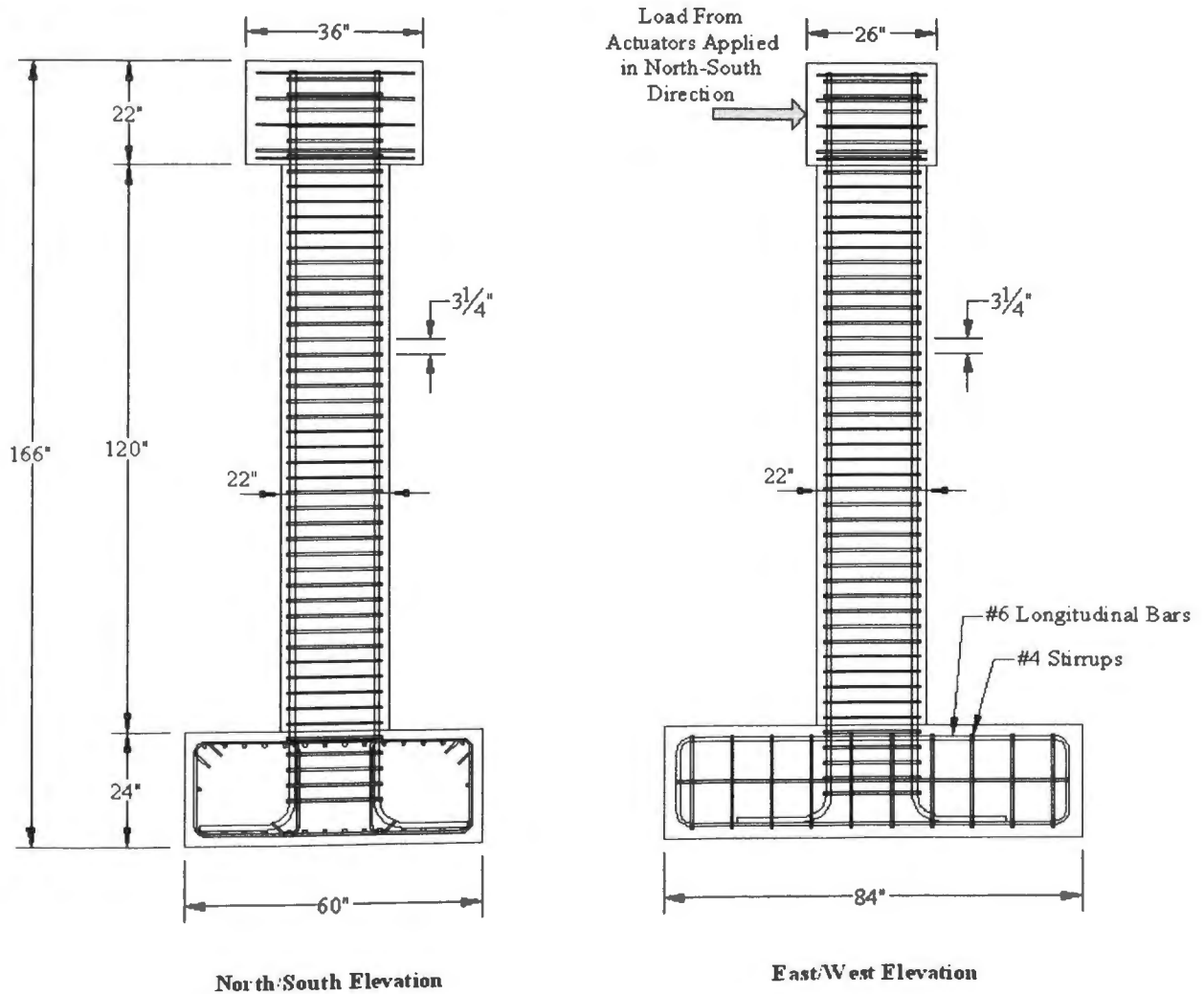
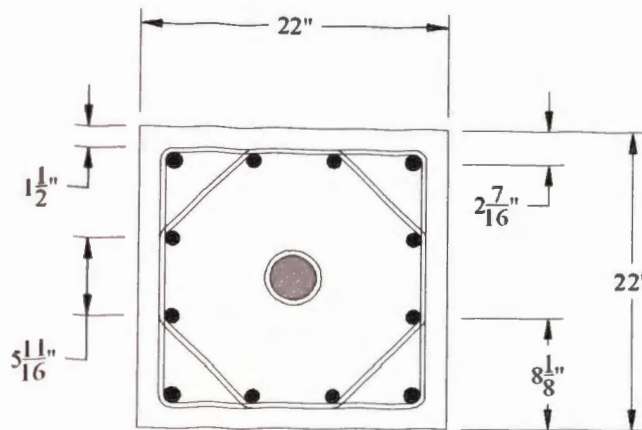


Figure 4.1. Original Column Elevations

The cross-sectional arrangement of longitudinal bars and ties in the original columns is depicted in Figure 4.2. Note that a PVC pipe was placed longitudinally in the column to facilitate the application of an axial load. The axial load was applied using seven steel prestressing strands that were placed through this PVC pipe and were fixed at the bottom and top of the column. Loading occurred when the strands were stressed in tension using a hydraulic jack placed on the top of the column.



Longitudinal Reinforcement:
 4#9 Bars (In Corners) & 8#8 Bars
Ties:
 Square & Octagonal #3 Bars
 PVC Pipe Placed in Center for Axial Load

Figure 4.2. Cross-Sectional Arrangement of Reinforcement in Original Columns

4.2.3. Damage Review of Original Columns. In the original testing program, each column was tested to failure under the specified torque-to-moment ratio, resulting in a severe degree of damage. For the purpose of designing a repair for these columns, it was necessary to review the extent of the damage for each column. The damage to the original columns is summarized in Table 4.2.

Table 4.2. Summary of Original Column Damage

| Column ID Number | T/M | CONCRETE DAMAGE | | REINFORCING BAR DAMAGE | | | |
|------------------|----------|-----------------|------------------|------------------------|--------------------|------------------|------------------|
| | | Spalled Length | Core Crush Depth | No. Buckled Bars | No. Fractured Bars | No. Damaged Ties | Height To Buckle |
| 1 | 0 | 25 in. | >7 in. | 11/12 | 2/12 | 4 | 6 in. |
| 2 | 0.2 | 51 in. | >7 in. | 10/12 | 0/12 | 3 | 12 in. |
| 3 | 0.4 | 60 in. | >6 in. | 10/12 | 0/12 | 1 | 12 in. |
| 4 | 0.6 | Entire | Entire | 4/12 | 0/12 | 0 | 43 in. |
| 5 | ∞ | 94 in. | Entire | 0/12 | 0/12 | 0 | 52 in. |
| 6 | 0.4 | Entire | Entire | 12/12 | 0/12 | 9 | 60 in. |

The “Spalled Length” and “Core Crush Depth” are measured as shown in Figure 4.3. Their measurement is included to provide insight to the damage locations of the column. The “Height to Buckle” is measured as the average height to the buckled point in the longitudinal reinforcing bar(s), measured from the top of the footing. All damaged

ties failed by yielding and straightening of the end hooks. Detailed photos of the damaged columns are shown in Appendix A.

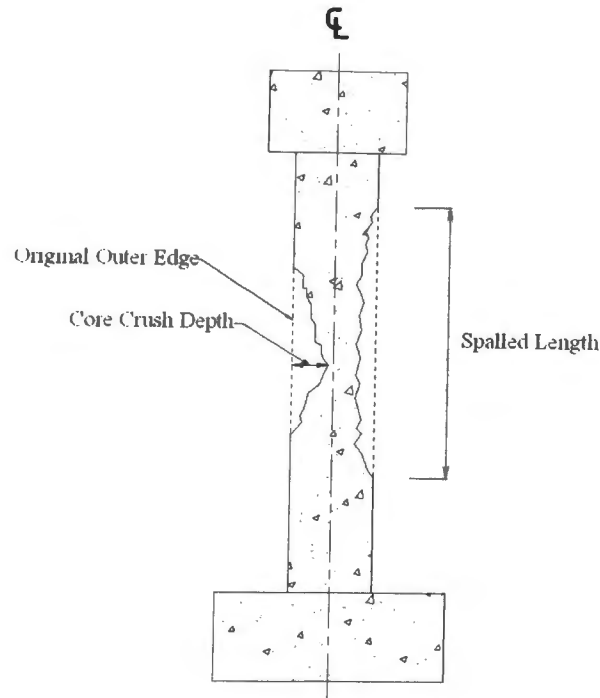


Figure 4.3. Definition of “Spalled Length” and “Core Crush Depth”

4.3. REPAIR GOALS

The goals of the overall square column repair project were as follows:

1. To show that the materials used for repair were compatible and capable of achieving their required strengths given a “rapid repair” period of 72 hours;
2. To restore the bending moment and torsion capacities of the damaged columns to their original levels in a “rapid repair” timeframe while maintaining as much ductility as possible and restoring the overall column stiffness;
3. To evaluate the behavior of the CFRP composite strengthening system under the combined loading effects;
4. To evaluate the contribution of the CFRP composite strengthening system to the restored capacity of the repaired column; and
5. To use the data to improve column repair design procedures by more accurately predicting the failure modes of columns repaired with FRP strengthening systems.

4.4. MATERIAL PROPERTIES

In this section, the materials used for the repair of the columns are presented along with their engineering properties. The materials used for repair include the epoxies used in the composite CFRP matrix, the carbon fiber sheets, the repair mortar used to replace the lost concrete, and the materials used to fabricate and install the anchorage system. Additionally, test results from the standard tests performed on the repair materials are presented.

4.4.1. Composite Repair Materials. The materials that comprised the CFRP strengthening system were the MBrace[®] composite strengthening system, which is manufactured by the BASF Company. The MBrace[®] system consists of three types of two-part epoxies: MBrace[®] Primer, MBrace[®] Putty, and MBrace[®] Saturant. MBrace[®] Primer is a low-viscosity epoxy that is applied directly to the prepared concrete surface to enhance the bond between the CFRP and concrete surface. MBrace[®] Putty is a high-viscosity epoxy paste used to level the concrete surface and fill in any voids or defects in the concrete. MBrace[®] Saturant is a low-viscosity epoxy that is used to impregnate and encapsulate fiber sheets on the surface of the reinforced concrete member. The combination of Primer, Putty, and Saturant is used to bond the carbon fiber sheets to the concrete substrate. The carbon fiber sheets were MBrace[®] tow sheets, a unidirectional fabric that was readily available and has been used by other researchers at Missouri S&T. Listed in Table 4.3 are properties of the MBrace[®] epoxy materials given by the manufacturer.

In addition to the MBrace[®] materials used for repair, Concrevisive[®] Paste LPL manufactured by the BASF Company was used in lieu of the MBrace[®] Putty for Column #1. The reasons for substituting this product are discussed in Section 4.7.5. The properties of Concrevisive[®] Paste LPL are shown in Table 4.4.

The carbon fiber tow sheets used for column strengthening had the following properties as reported by the manufacturer: an ultimate tensile strength of 550 ksi; a tensile modulus of 33,000 ksi; an ultimate rupture strain of 0.0167; and a nominal thickness of 0.0065 inches per ply.

Table 4.3. Properties of MBrace® Materials

| | MBrace® Primer | MBrace® Putty | MBrace® Saturant |
|---|---------------------|---------------------|---------------------|
| <i>Tensile Properties Determined Using ASTM D 638</i> | | | |
| Yield Strength (psi) | 2,100 | 1,800 | 7,900 |
| Strain at Yield | 0.020 | 0.015 | 0.025 |
| Elastic Modulus (psi) | 105,000 | 260,000 | 440,000 |
| Ultimate Strength (psi) | 2,500 | 2,200 | 8,000 |
| Rupture Strain | 0.40 | 0.07 | 0.035 |
| Poisson's Ratio | 0.48 | 0.48 | 0.40 |
| <i>Compressive Properties Determined Using ASTM D 695</i> | | | |
| Yield Strength (psi) | 3,800 | 3,300 | 12,500 |
| Strain at Yield | 0.040 | 0.040 | 0.050 |
| Elastic Modulus (psi) | 97,000 | 155,000 | 380,000 |
| Ultimate Strength (psi) | 4,100 | 3,300 | 12,500 |
| Rupture Strain (psi) | 0.10 | 0.10 | 0.05 |
| <i>Flexural Properties Determined Using ASTM D 790</i> | | | |
| Yield Strength (psi) | 3,500 | 3,800 | 20,000 |
| Strain at Yield | 0.040 | 0.040 | 0.038 |
| Elastic Modulus (psi) | 86,300 | 130,000 | 540,000 |
| Ultimate Strength (psi) | 3,500 | 4,000 | 20,000 |
| Rupture Strain | No Rupture | 0.07 | 0.05 |
| <i>Other Useful Properties</i> | | | |
| Coefficient of Thermal Expansion (°F ⁻¹) | 20x10 ⁻⁶ | 20x10 ⁻⁶ | 20x10 ⁻⁶ |
| Density (lb/ft ³) | 68.8 | 75.8 | 61.3 |

Table 4.4. Properties of Concessive® LPL Paste

| Concessive® LPL Paste | |
|---|---------|
| <i>Tensile Properties Determined Using ASTM D 638</i> | |
| Tensile Strength (psi) | 2,000 |
| Strain at Yield | 0.04 |
| <i>Compressive Properties Determined Using ASTM D 695</i> | |
| Compressive Yield Strength (psi) | 8,000 |
| Compressive Modulus (psi) | 400,000 |

Bond strength testing of the CFRP-to-concrete bond was performed in accordance with *ASTM D7234*. A representative sample of CFRP was bonded to a concrete surface, which was prepared using the same techniques and at the same time as the procedures described in Sections 4.7.4 and 4.7.5. A Proceq DYNA Pull-Off Testing Machine was used to perform the tests. The tests were performed at the time of testing of the repaired columns. All bond strength test results met the CFRP system manufacturer's and *ACI 440.2R-08* minimum specified bond strength of 200 psi. Bond strength test results are presented in Table 4.5, where the "Average Bond Strength" column lists the average of the three pull-off tests performed. "Test Location" refers to the location that the pull-off test specimens were bonded to the concrete. Specimens located "above FRP" were

placed on the column face above the highest layer of transverse or longitudinal CFRP. Specimens placed “on footing” were bonded to an CFRP sheet on the side of the footing. Finally, the “cast repair mortar specimens” were special blocks cast independently from the column at the time of mortar placement during column repair.

Table 4.5. Bond Strength Test Results Per *ASTM C7234*

| Column ID No. | Test Location | Average Bond Strength | Pass or Fail? |
|---------------|-------------------------------|-----------------------|---------------|
| 1 | Original Concrete, Above FRP | 378 psi * | Pass |
| 2 | Original Concrete, Above FRP | 225 psi | Pass |
| 3 | Original Concrete, On Footing | 583 psi | Pass |
| 4 | No Test Performed | N/A | N/A |
| 5 | Cast Repair Mortar Specimen | 310 psi | Pass |
| 6 | Cast Repair Mortar Specimen | 646 psi | Pass |

*Bond Strength is Average of Only Two Pull-Off Specimens For Column #1

4.4.2. Concrete Properties. The mortar used during the repair of the columns was LA40 Repair Mortar, a pre-extended micro concrete manufactured by the BASF Company. This mortar was chosen for several reasons. First, the strength of the mortar two to three days after placement would be similar to that of the original concrete. Next, the surface moisture present on the exposed concrete surfaces would be minimal when using this material. This was crucially important because the presence of moisture on the surface of the concrete could be detrimental to the interfacial bond between the FRP and underlying concrete. Finally, the fluidity of the repair mortar ensured that voids due to poor consolidation would not be present after pouring the repair mortar into the forms. The compressive strengths of the repair mortar used for the first three column repairs can be found in Table 4.6. These strengths were determined using 2 in. mortar cube specimens constructed and tested in accordance with *ASTM C109*.

Table 4.6. Compressive Strengths of Original Column Concrete and Repair Mortar

| Column ID Number | T/M | Original Concrete (<i>ASTM C39</i>) | | Repair Mortar (<i>ASTM C109</i>) |
|------------------|-----|---------------------------------------|-------------------------|------------------------------------|
| | | 28-Day Strength (psi) | Test Day Strength (psi) | Repair Test Day Strength (psi) |
| 1 | 0 | 5290 | 5260 | 5410 |
| 2 | 0.2 | 5870 | 5880 | 5860 |
| 3 | 0.4 | 6420 | 5860 | 5460 |
| 4 | 0.6 | 5570 | 5870 | 4670 |
| 5 | ∞ | 4760 | 4730 | 6260 |
| 6 | 0.4 | 4260 | 5890 | 4300 |

4.4.3. Anchorage Materials. The novel anchorage system used for the repairs of Columns #1, #2, and #3 consisted of a steel plate welded to a quarter-section of steel pipe reinforced with stiffeners and fastened to the concrete with threaded steel anchor rods that were embedded using a chemical adhesive. The plate steel, threaded anchor rods, and chemical adhesive were of particular interest when designing and predicting the behavior of the anchorage system.

The plate steel was the standard *ASTM A36* steel alloy, which has a specified minimum yield strength of 36 ksi and a Young's Modulus of 29,000 ksi. The threaded anchor rods were 1 in. diameter fully threaded *ASTM A193* Grade B7 anchor rods, which has a specified minimum yield strength of 105 ksi and an ultimate strength of 125 ksi. Finally, the chemical adhesive used for embedding the anchor rods was HIT-RE 500 Epoxy Adhesive manufactured by Hilti, Inc. The relevant material properties of HIT-RE 500 are discussed in the anchorage design section calculations, located in Appendix B.

4.5. REPAIR DESIGN

The repair design procedure and methodology for the damaged square columns is the subject of a future doctoral dissertation and is therefore beyond the scope of the work presented in this thesis. However, because it was determined that a Type III anchorage system was needed at the column-to-footing interface for Columns #1, #2, and #3, it is necessary to present the repair designs for these columns. Type III anchorage was not included at the column-to-footing interface of Columns #4, #5, and #6 because the damage to the original column was located away from the footing. Repair designs for Columns #4, #5, and #6 are not presented because they are not relevant to the content of this thesis.

4.5.1. Column #1 Design. Column #1 was designed with three layers of longitudinal (vertically oriented) CFRP on the North and South faces of the columns. No longitudinal CFRP was placed on the East and West faces. A varying number of layers of transverse (horizontally oriented) CFRP wraps were placed around the column to a height of 60 in. from the footing. No longitudinal or transverse CFRP was placed above the height of 60 in. from the footing because the concrete and steel remained undamaged above that height. The novel anchorage system described in Section 4.6 was used at the

column-to-footing interfaces on the North and South sides of the column. All longitudinal CFRP sheets were placed first on the column, followed by the transverse wraps. Every sheet of CFRP placed on the column was 20 in. wide. A drawing of the repair design for Column #1 is shown in Figure 4.4.

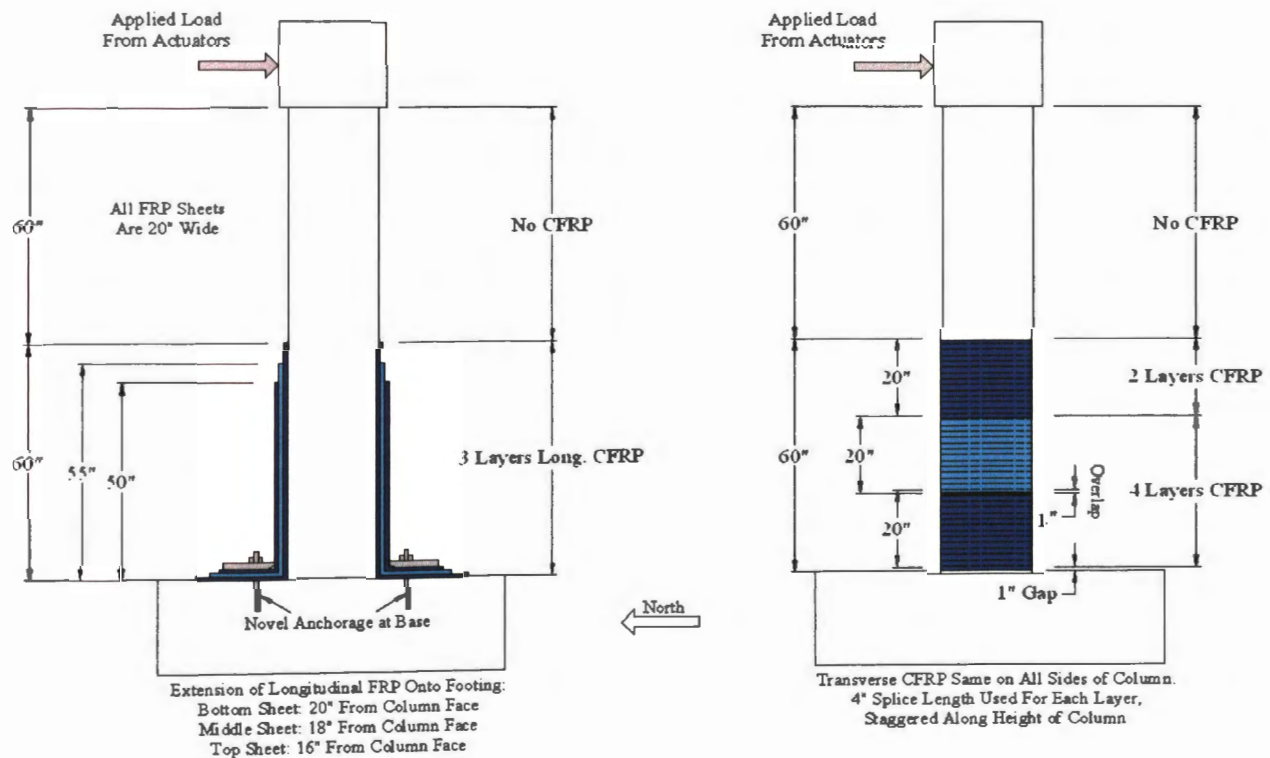


Figure 4.4. Repair Design Drawing for Column #1

4.5.2. Column #2 Design. Column #2 was designed with three layers of longitudinal FRP on its North and South faces, and with one layer of longitudinal FRP on its East and West faces. Longitudinal CFRP was present on the East and West faces for Column #2 to help restore the torsion capacity of the column. A varying number of layers of transverse CFRP were placed around the column to a height of 60 in. from the footing. As with Column #1, no longitudinal or transverse CFRP was placed above 60 in. from the footing. Anchorage systems for this column, described in Section 4.6, included the novel anchorage system placed on the North and South sides, and U-Anchors placed on the East and West sides. All longitudinal CFRP sheets were placed first, followed by

the transverse CFRP wraps. Every sheet of CFRP placed on the column was 20 in. wide. A drawing of the repair design for Column #2 is shown in Figure 4.5.

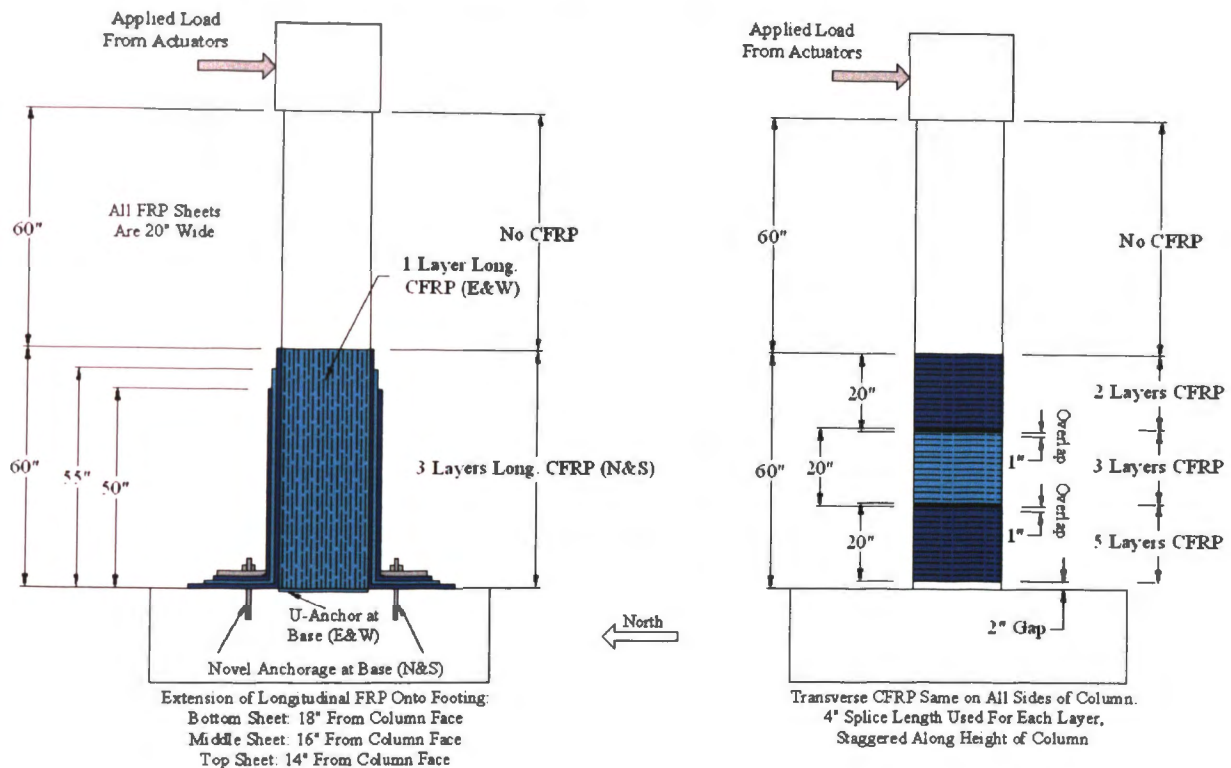


Figure 4.5. Repair Design Drawing for Column #2

4.5.3. Column #3 Design. Column #3 was designed with two layers of longitudinal FRP on the North and South column faces, and one layer of CFRP on the East and West column faces. As with Column #2, longitudinal CFRP was present on the East and West column faces primarily to help restore the torsion capacity. A varying number of transverse CFRP wraps were placed around the column to a height of 56 in. No longitudinal or transverse CFRP was placed above the height of 56 in. The anchorage systems for this column, described in Section 4.6, included the novel anchorage system at the column-to-footing interface on the North and South sides, as well U-Anchors at the interface on the East and West sides. All longitudinal CFRP sheets were placed first, followed by transverse CFRP wraps. Every sheet of CFRP placed on the column was 20 in. wide. The repair design for Column #3 is shown in Figure 4.6.

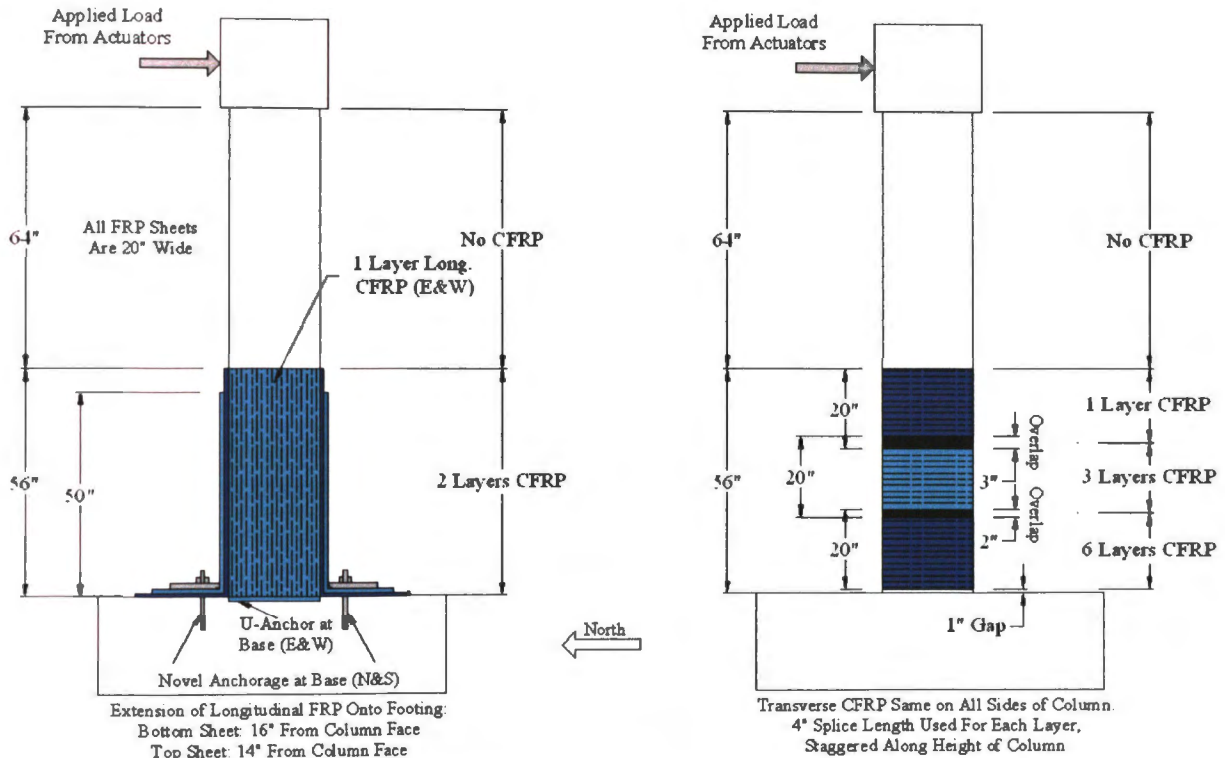


Figure 4.6. Repair Design Drawing for Column #3

4.6. ANCHORAGE DESIGN AND CONSTRUCTION

After it was determined that longitudinal CFRP was needed to restore the flexural strength of Columns #1, #2, and #3, it was also determined that an anchorage system would be necessary at the interface between the column and the footing. Since these columns would be experiencing cantilever bending, albeit with a constant axial load and in some cases torsion, a Type III anchorage system was needed. The determination of the necessity of the Type III anchorage system was based upon several factors. First, since the first column contained at least two ruptured longitudinal reinforcing bars, longitudinal CFRP was needed to replace their strength. Because the bars were ruptured near the interface between the column and footing, the longitudinal CFRP should be expected to develop its highest stresses in this region. Also, the necessity of longitudinal CFRP for flexural strengthening was based upon the location of damage with respect to the height of the column. For Columns #1, #2, and #3, the damage region was restricted to the first few feet above the interface between the column and footing. Because it was expected that the first flexural concrete cracking would occur at this interface, the CFRP stresses

again would be the highest in this region. These reasons led the design team to concur that a Type III anchorage system would be needed at the interface between the column and the footing, especially on the North and South faces of the column, where the bending stresses are at a maximum.

4.6.1. Design Philosophies. Initial design calculations resulted in a significant force that was required to be developed in the longitudinal CFRP at the interface between the column and the footing. Since this force would theoretically be developed at this interface, a Type III anchorage system was necessary, meaning that the anchorage must be capable of transferring the entire force developed in the CFRP to the footing. After the anchorage review performed in Chapter 2 was completed, it was determined that few, if any, of the Type III anchorage devices were capable of anchoring the significant forces required by the initial column repair design. A brief investigation of available anchoring materials, which included expansion anchors, chemical adhesive anchors, and other innovative anchoring techniques that were compatible with Type III anchorage systems, revealed that the required anchoring forces may have been in excess of the strengths of the anchoring materials. Therefore, it was determined that the CFRP design should be dependent upon the design of the base anchorage system.

Since the CFRP design was dependent upon the anchorage system strength, the goal of the anchorage system design was to design a system in which the vertical force developed in the CFRP could be maximized. From the perspective of anchoring a generalized force to concrete using post-installed anchors, it was determined that high-strength steel anchor rods anchored with an epoxy adhesive would provide the highest anchoring force given an optimized reaction. Because the forces developed in these anchors would likely control the strength of the anchorage system and thus the CFRP system, the anchorage system was designed by first attempting to maximize the strength of the post-installed concrete anchors, followed by the design of the other anchorage materials.

However, in order to determine the possible arrangement of anchor rods, it was necessary to gain a general understanding of the setup and geometry of the anchorage system. After careful review of the Type III anchorage systems presented in Chapter 3, it was determined that the “CHS Anchorage” would best fit the needs of this project. Since

the CHS Anchorage was designed to optimize the reaction shown in Figure 2.25, the load transferred from the CFRP system to the anchor rods could be maximized. Additionally, the large size of the anchor rods that could be accommodated by the CHS system would further maximize the anchorage potential.

When evaluating the possibility for installation of the CHS anchorage system onto the square columns, their potential for use was diminished by two factors. First, the high congestion of steel at the column-to-footing interface would make anchor rod placement and installation very difficult. Embedding the anchor rods at a 45° angle at this interface would require that the anchors be installed while trying to avoid potentially four layers of steel: the longitudinal column bars, the transverse column ties, the longitudinal footing bars, and the transverse footing stirrups. The placement of these bars is shown in Figure 4.1. Unfortunately, as-built locations of the reinforcing bars in the footings were not available. Thus, bar location with regard to vertical depth and horizontal placement was relatively unknown. While use of a Profometer, or rebar locator, was attempted to determine the locations of the footing bars, the high congestion of steel near the footing caused the Profometer to function poorly. Second, installing the anchor rods at a 45° angle at the column-to-footing interface would mean that a small section of the embedded bolts would be embedded above the footing and in the column. In all three columns that required Type III anchorage, a significant amount of damage corresponding to the development of a plastic hinge was noted at or near this column-to-footing interface. Since the provisions of *ACI 355.2-07: Qualification of Post-Installed Mechanical Anchors in Concrete* and Appendix D of *ACI 318-08* do not anticipate the large crack widths developed in plastic hinge regions, the installation of anchors in these regions should be avoided. For both of these reasons, it was determined necessary to install the anchors at a distance away from the face of the column.

4.6.2. Anchor Rod Arrangement. Because of the foreseeable challenges in constructing an anchorage system, it was desirable to design an anchorage system capable of being reused for multiple column tests. Therefore, the arrangement of the anchor rods should be designed such that their embedment would not interfere with any of the longitudinal bars or transverse stirrups in the footing. Cutting through these bars may have resulted in a deterioration of strength at the column-to-footing interface and

was therefore undesirable. To ensure that it was possible to embed the anchor rods without damaging the bars in the footing, the longitudinal bars and transverse stirrups were located in the footing using a Profometer. Because of the close spacing of these bars in the footing, possible arrangements of these bars were limited. After some consideration, it was determined that an arrangement of four one-inch diameter anchor rods, which required an embedment diameter of 1-1/8 in., could be arranged as shown in Figure 4.7, where the green solid shapes represent the area in which the rods could be embedded and the gray hatched areas represent the measured locations of embedded rebar in the footing.

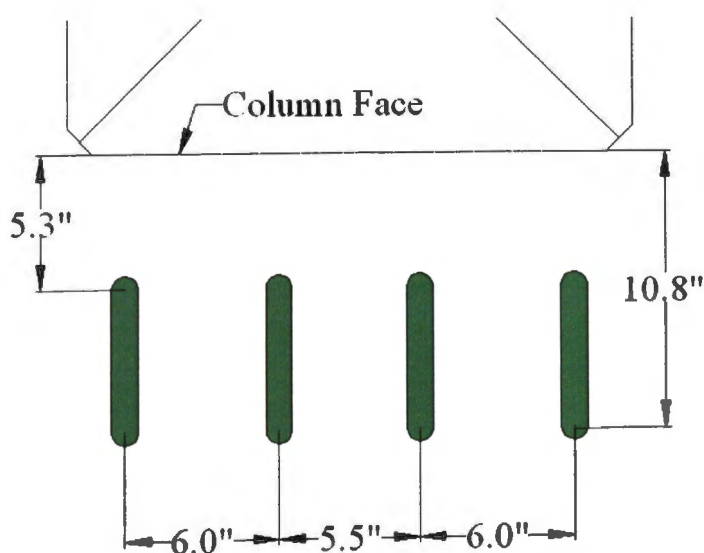


Figure 4.7. Embedment Locations of Anchor Rods in Footing

4.6.3. Anchorage System Concept and Design. Since the desired CHS Anchorage system was determined to be unfeasible for installation and use as described in Sections 4.6.1 and 4.6.2, modifications to the system were necessary. Using a pipe section in the 90° joint at the column-to-footing interface would still be advantageous since it would limit the local stress concentrations placed on the CFRP at the joint. Additionally, the system needed to be capable of transferring the bearing reaction of the CFRP associated with debonding at the joint to the anchor rods, which would be placed a distance away from the column as shown in Figure 4.7. Therefore, a modification of the

“ductile plate” anchorage system used by Hall et al. (2002) and discussed in Chapter 2 was a possible solution. However, the ductile plate system used by Hall et al. (2002) was fabricated with light gauge steel and was not capable of anchoring the large reaction required by this particular application.

In order to create a similar system with a higher strength, the novel anchorage system design involved cutting a heavy-gauge structural steel pipe into quarters about its cross section. This pipe section would be welded to a steel plate with the plate anchored to the footing by the embedded steel anchor rods. To ensure that no deformation of the steel pipe or failure of the weld occurred, stiffeners would be placed at intermediate locations along the length of the pipe. A conceptual diagram of the novel anchorage system is shown in Figure 4.8.

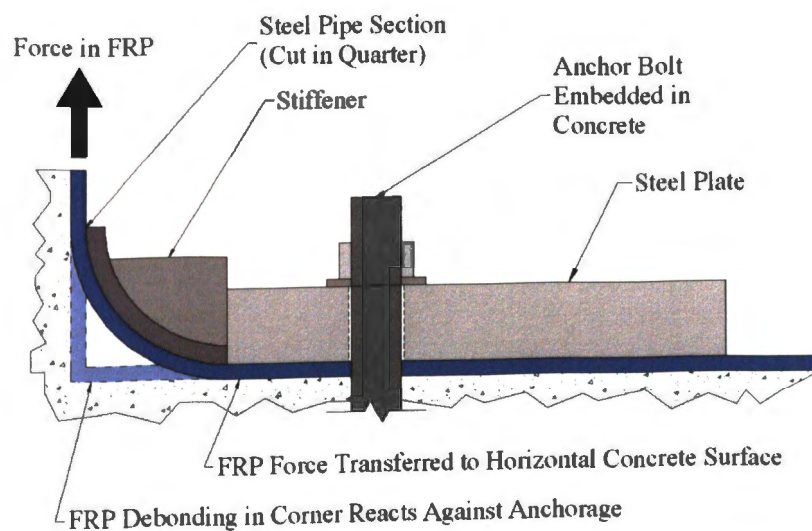


Figure 4.8. Conceptual Diagram of Novel Anchorage System

To facilitate the design of the plate thickness, a model of the anchorage system’s mechanical behavior was created. This model, shown in Figure 4.9, was based upon the assumption that the reaction of the CFRP onto the plate would cause the anchorage system to undergo cantilever bending about the line of the bolts, the same assumption made by Hall et al. (2002) when evaluating the behavior of their ductile plate system. The plate would then be extended a distance behind the anchor rods away from the column to provide a reaction that would counteract the moment present at the line of

anchor rods. The assumed behavior of the novel anchorage system is depicted in Figure 4.9.

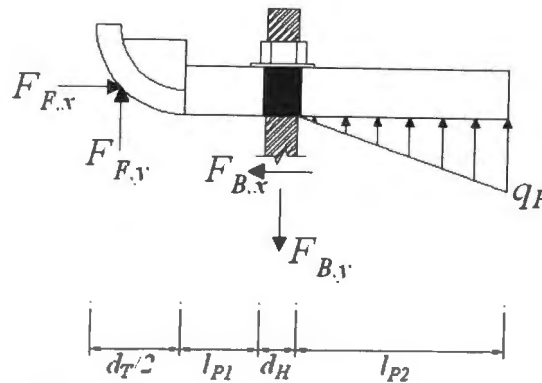
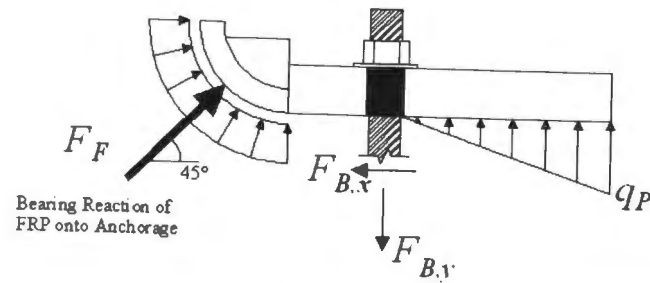


Figure 4.9. Assumed Behavior of Novel Anchorage System

Just as Hiotakis (2004) assumed that the bearing reaction of the FRP onto the steel pipe is acted at a 45° angle, the resultant force F_F for the novel anchorage system is also assumed to act at 45° about a line normal to the radius of the pipe section. The x - and y -components of F_F are then equal since it is assumed that F_F acts at 45° . The bearing reaction of the plate onto the concrete, q_P , is assumed to vary linearly from zero force at the anchor rod holes to q_P at the edge of the plate furthest from the column face. Two horizontal reactions exist in this model: the shear force in the anchor rods, $F_{B,x}$, and the horizontal component of the bearing reaction from the FRP, $F_{F,x}$. Static equilibrium of the above forces results in Equations [4.1], [4.2], and [4.3].

$$q_P = \frac{2F_{B,y} \left(\frac{d_T}{2} \times 0.707 + l_{P1} + \frac{d_H}{2} \right)}{l_{P2} \left(\frac{d_T}{2} \times 0.707 + l_{P1} + d_H + \frac{2l_{P2}}{3} \right)} \quad \text{Eq. [4.1]}$$

$$F_{F,y} = F_{B,y} - \frac{1}{2} (q_P)(l_{P2}) \quad \text{Eq. [4.2]}$$

$$F_{F,x} = F_{B,x} \quad \text{Eq. [4.3]}$$

Since reuse of the anchorage plate was desired, it was necessary to design the anchorage such that failure would occur in the anchor rods before the plate. Therefore, $F_{B,y}$ was taken to be the ultimate tensile capacity of the anchor rods after spacing effects and the interaction between shear and tensile forces on the bolts were considered. Since $F_{F,y}$ can be calculated given $F_{B,y}$, the moment about the anchor rods could be determined and used to calculate the required plate thickness. However, as shown in the design calculations in Appendix B, the calculated required anchorage plate thickness was deemed unreasonably large and a thinner plate was chosen. The selected anchorage plate thickness of 1-1/2 in. would result in the following forces as the anchorage plate yields about the line of the anchor rods: a tensile force in the anchor rods ($F_{B,y}$) of 61.47 kips; a shear force transferred to the anchor rods ($F_{F,x}$) of 40.83 kips; a vertical reaction of the CFRP onto the novel anchorage ($F_{F,y}$) of 40.83 kips; and a horizontal reaction of the CFRP onto the novel anchorage ($F_{F,x}$) of 40.83 kips.

In addition to designing the thickness of the plate used in the novel anchorage system, it was also necessary to determine the lengths from the base of the column that the CFRP sheets would be extended onto the footing. In order to determine these lengths, it was assumed that the FRP would debond from the concrete on the surface of the footing over a length extending from the base of the column to the centerline of the anchor rods. This was assumed since the cantilever bending action of the plate would result in small upward displacements from the quarter-pipe end of the plate to the anchor rods. These displacements, although very small, could allow for the CFRP to debond from the footing surface. The FRP should then be extended a distance greater than its

effective bond length (L_e) past the centerline of the anchor rods onto the surface of the footing.

Because so much discord exists among effective bond length models for FRP (Ortega, 2009), a conservative model created by Niu and Wu (2000) was used to determine L_e . This model is defined in Equation [4-4], where L_e is the effective bond length in millimeters, E_f is the tensile modulus of FRP in megapascals, t_f is the nominal thickness of FRP in millimeters, and k is a constant recommended by the authors to be 0.94.

$$L_e = k\sqrt{E_f t_f} \quad \text{Eq. [4-4]}$$

Using this equation to calculate the effective bond length of the MBrace[®] carbon fiber tow sheets results in effective bond lengths of 7.2 in., 10.1 in., and 12.4 in. for one, two, and three layers of carbon fiber sheets, respectively. For Columns #1 and #2, which utilized three layers of longitudinally-oriented carbon fiber sheets, the distance to extend the sheets onto the footing was determined to be the distance from the column to the anchor rods, 5.8 in., plus the effective bond length of 12.4 in, resulting in a distance of 18.2 in. from the face of the column. For Column #3, which utilized two layers of longitudinally oriented carbon fiber sheets, the distance to extend the sheets onto the footing was determined to be the distance from the column face to the anchor rods, 5.8 in., plus the effective bond length of 10.1 in., resulting in a distance of 15.9 in. from the face of the column.

For ease of construction, a distance of 18 in. was selected for the middle layer sheet on Column #1, and the upper and lower layers were tapered at 16 in. and 20 in. from the face of the column to avoid peeling failure at the plate end. Since no debonding failure was noted near the CFRP sheet ends on the footing of Column #1, these distances were reduced to 18 in., 16 in., and 14 in. on Column #2 for the bottom, middle, and top layers of CFRP sheets, respectively. The distances to extend the CFRP sheets on the footing of Column #3 were 16 in. and 14 in. for the bottom and top layers of CFRP sheets, respectively.

Figures 4.10, 4.11, and 4.12 show the final details of the novel anchorage systems for Columns #1, #2, and #3, respectively. Reasons for including the gap between the

edge of the quarter-pipe and the column face on Columns #2 and #3 are discussed in Section 4.7.6, as well as in Chapter 5.

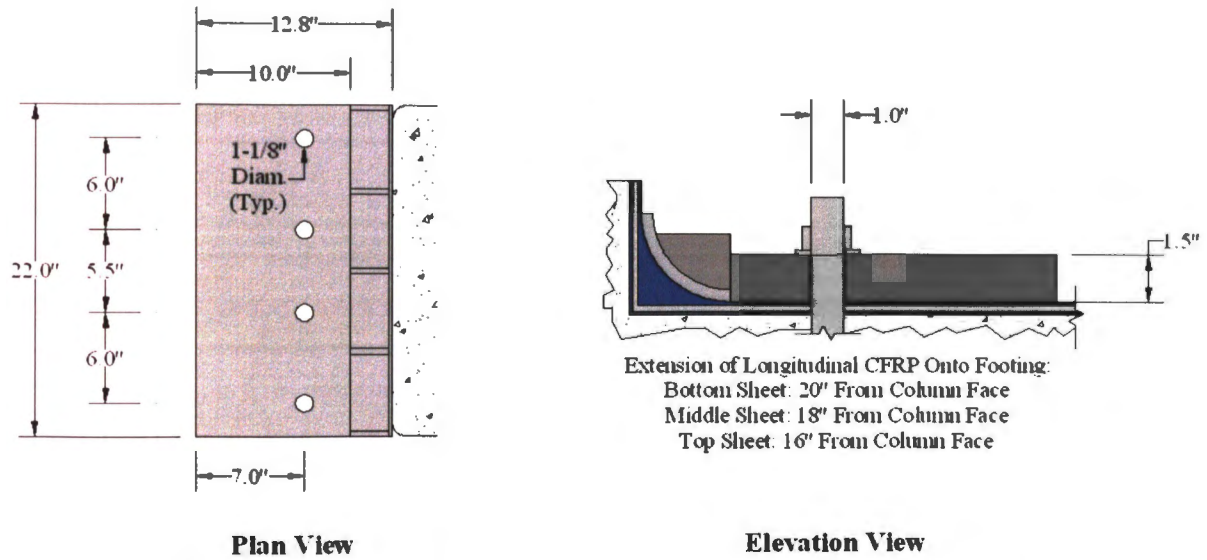


Figure 4.10. Final Details of Novel Anchorage System For Column #1

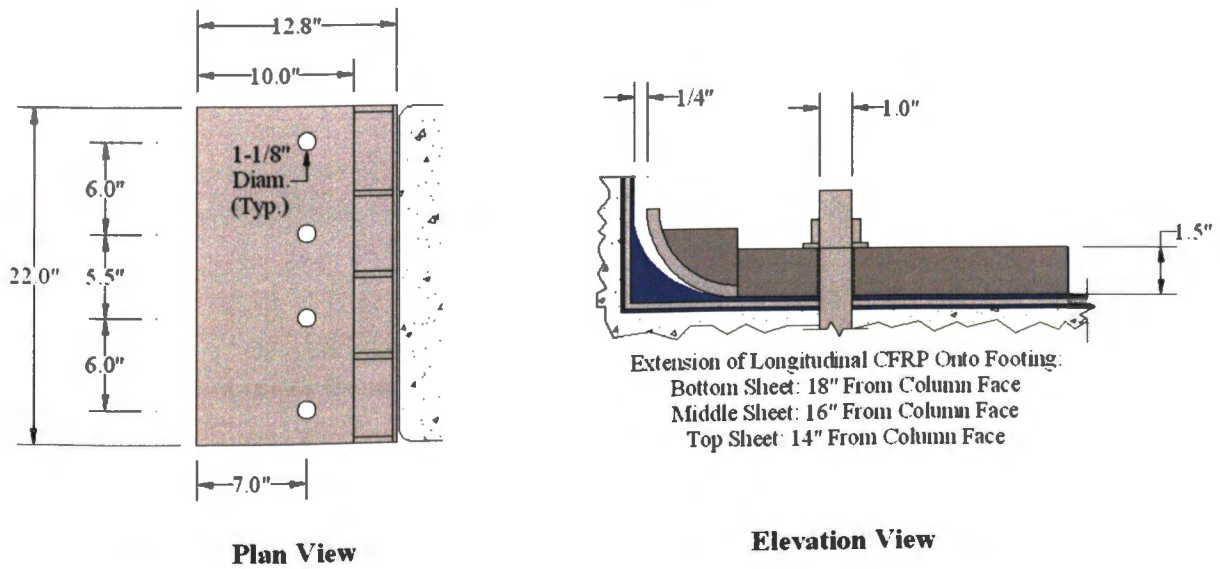


Figure 4.11. Final Details of Novel Anchorage System For Column #2

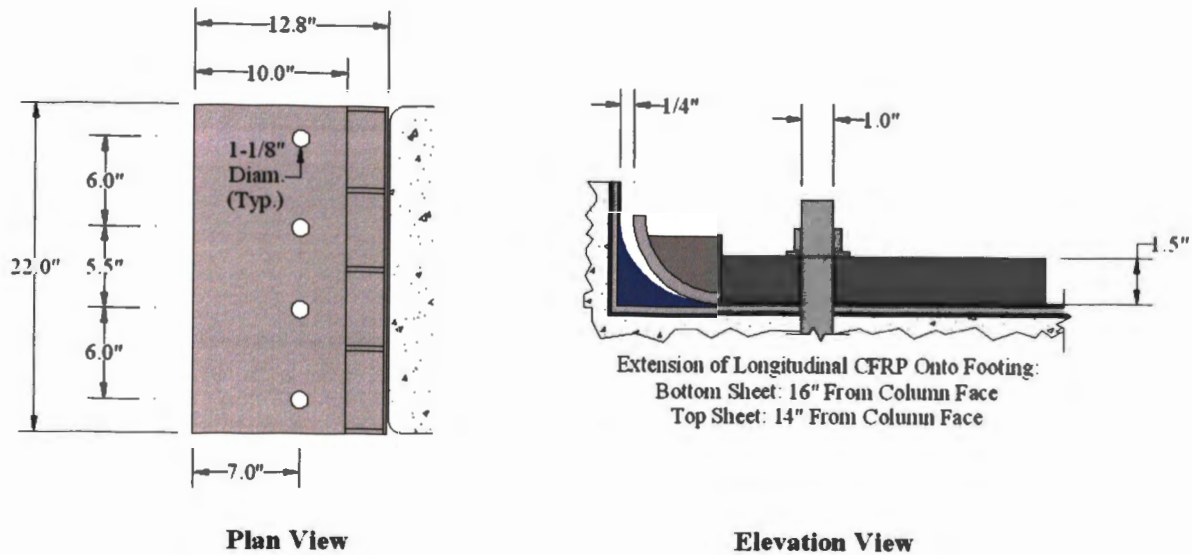


Figure 4.12. Final Details of Novel Anchorage System For Column #3

4.6.4. Other Anchorage. Two other forms of anchorage were used in the repair design of Columns #1, #2, and #3. Transverse Wrapping anchorage was provided along the entire length of longitudinal (vertically oriented) FRP sheets by the confining effects of the transverse (horizontally oriented) FRP sheets. This ensured that no debonding would occur at the ends of the longitudinal FRP on the column face. Additionally, since Columns #2 and #3 contained longitudinal FRP all four sides of the column, it was determined that Type III anchorage was needed at the bases of all four sides. However, the column test setup did not allow sufficient space for the novel anchorage system to be installed on the footing on the East and West sides of the column. The restrictions imposed by the column test setup on the East and West sides are shown in Figure 4.13. The test setup is described in more detail in Section 4.8.4.

Additionally, reinforcing bars were present in the footing directly beneath the East and West column faces which prevented any anchor embedment directly adjacent to the column face. This made installation of an embedded anchorage system, such as the 180° anchor spikes discussed in Section 2.2.1.2, impossible since imposing damage to the footing reinforcement was undesirable. Therefore, it was determined that a U-Anchor system was the only suitable option for anchorage of the longitudinal FRP at the column-to-footing interface on the East and West sides of the column. The U-Anchor systems were not explicitly designed, but rather constructed given the constraints of the column

test setup and rebar locations in the footing. These constraints allowed for U-Anchors to be constructed as shown in Figure 4.14.

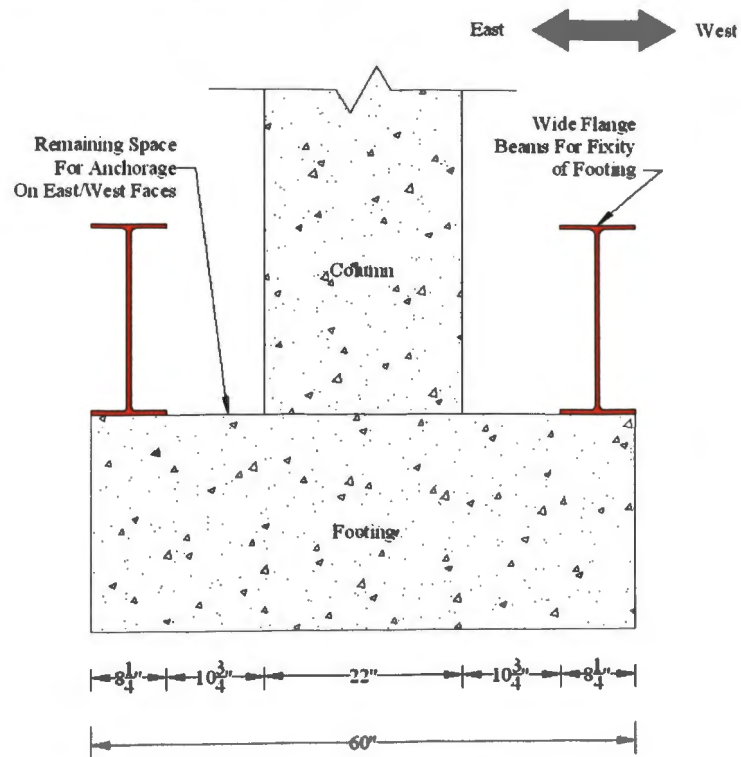


Figure 4.13. Restrictions Imposed on Anchorage Design For East and West Sides

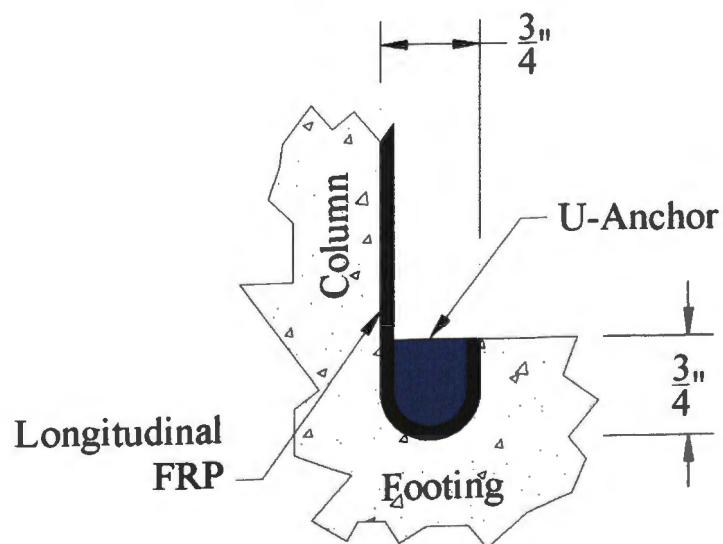


Figure 4.14. U-Anchors Used on East and West Faces of Columns #2 and #3

4.7. REPAIR PROCEDURE

This section describes the “rapid repair” procedure used to repair the square column specimens and achieve the goals discussed in Section 4.3. Since Columns #1, #2, and #3 were the only columns that required anchorage systems at the column-to-footing interface, the repairs of Columns #4, #5, and #6 are not discussed in this thesis. Sections 4.7.1 through 4.7.6 describe the generalized procedure that was used for the column repairs. Because some variations from the generalized procedure were inevitable, any deviation from the generalized procedure is described at the end of the section corresponding to the step in which it occurred.

4.7.1. Pre-Repair Work. Before the 72-hour “rapid repair” period began, several steps were taken to ensure that the column was capable of being repaired and retested. The first step was to attempt to straighten the column back to its original vertical position. Straightening of the column in the direction of the applied load (North/South direction) was not a difficult task, as the column could be attached to the hydraulic actuators used to test the columns, and the actuators used to push or pull the column back to its original position. However, straightening the column in the direction perpendicular to the applied load (East/West direction) proved difficult. In these situations, a jacking force was applied between the column cap and the reaction wall. The direction of the jacking force was dependent upon the direction of the displacement required to move the column back into its straightened position. The straightness of the columns was only determined visually, as measuring the verticality of the column was nearly impossible given their severe damage states.

Column #1 was straightened in the North/South and East/West directions. While minimal straightening was able to be performed in the East/West direction, the column was straightened in the North/South direction by pushing the actuators in the positive, or South, direction. A spacer was placed between the actuator and column to ensure that the straightening load that was applied to the column would not relax. Because this spacer was present during the repair of the column, there was a small lateral load present during the repair of the column.

Columns #2 and #3 were primarily straightened in only the East/West direction. While some deformations may be present in the North/South direction, the

deformations were deemed minimal. Straightening in the East/West direction for Columns #2 and #3 was performed by attaching a chain between the column cap and the reaction wall. A hydraulic jack was used to apply a tensile force to the chain, which pulled the column in the direction of the strong wall. The load was applied and released several times until the column appeared to be visibly straightened. Columns #2 and #3 were repaired under a condition of zero horizontal force.



Figure 4.15. Column Straightening Setup For Columns #2 and #3

4.7.2. Removal of Loose Concrete. The “rapid repair” procedure began when loose concrete was removed from the damaged columns. Loose concrete was removed with a chisel and hammer until light tapping with the hammer on the chisel would not cause further concrete to be removed. The dense crack networks caused by the severe damage could have allowed for more concrete to be removed with more aggressive hammering, but given the large amount of concrete that was removed with only light hammering, the research group determined that removal of additional concrete would not have been advantageous. Additionally, if damaged or opened ties were in position to interfere with the placement of formwork, they were removed at this time. Figure 4.16 shows the conditions of Columns #1, #2, and #3 after removal of the loose concrete.



Figure 4.16. Columns After Removal of Loose Concrete

After the loose concrete was removed from the damaged columns, the remaining concrete dust was removed by vacuuming the concrete surface, followed by blowing the remaining dust off the surface with compressed air, and followed by once again vacuuming the concrete surface. Water was then applied to the surface of original concrete that would come into contact with the repair mortar to achieve a saturated, surface dry (SSD) condition as specified in the instructions for placement of LA40 Repair Mortar.

4.7.3. Placement of Repair Mortar. After the loose concrete was removed and the concrete surface had achieved an SSD condition, the formwork was applied around

the column. Multiple types of formwork were used for the column repairs: custom plywood forms, custom plexiglass forms, segmental steel forms, or a combination of those materials. The repair mortar was placed in lifts so that the consolidation of the placed mortar could be visually monitored.

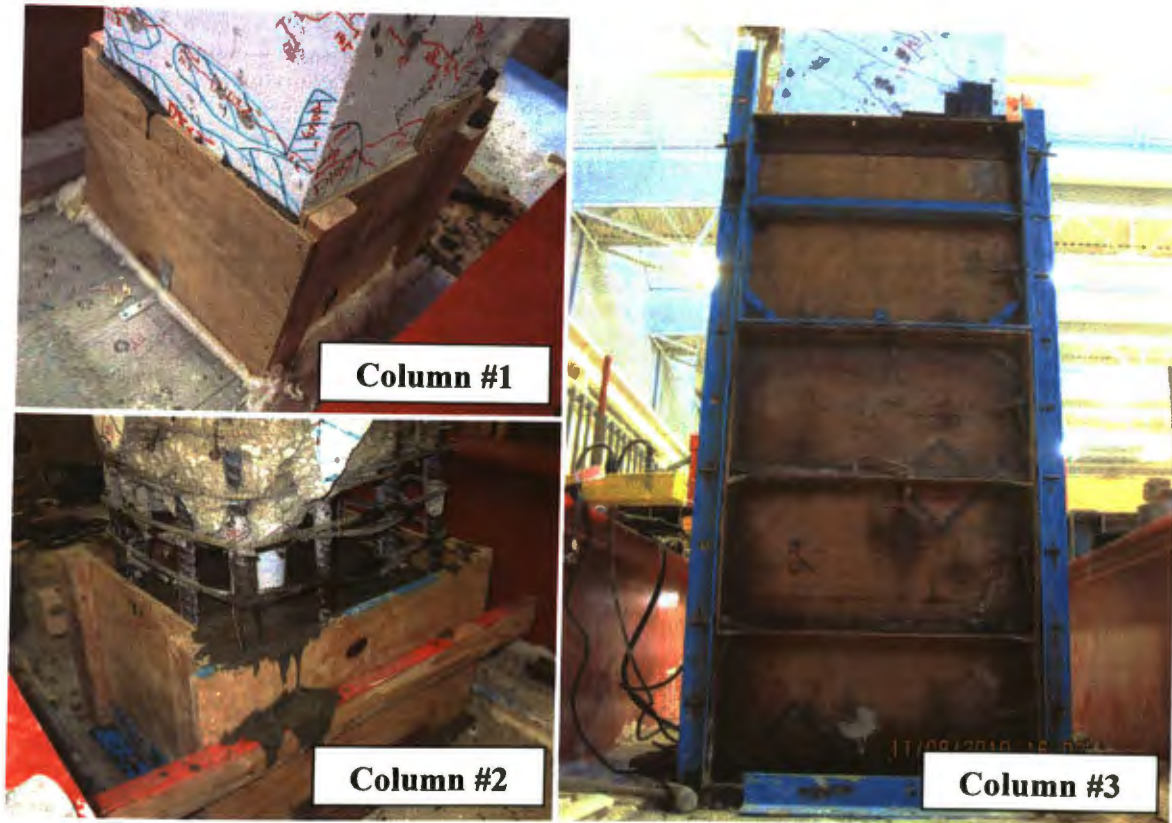


Figure 4.17. Columns With Formwork Placed Around Exterior

Per the recommendation of a representative of the repair mortar manufacturer, the forms were stripped from the column approximately 12 hours after the last lift of mortar was poured. This was done to maximize the concrete surface's air exposure time in an attempt to minimize the surface moisture content of the concrete.

4.7.4. Concrete Surface Preparation. Concrete surface preparation began just a few hours after stripping the forms. All areas of the cast repair mortar or existing concrete that were to be overlaid with CFRP were prepared as described in this section, including those areas on the footing that were covered with CFRP. First, the concrete surface was prepared with the combination of a power concrete surface preparation tool

recommended by the CFRP system manufacturer and a diamond cup wheel. For Columns #1 and #2, the corners of the columns were rounded to a radius of approximately 1 in. with a diamond cup wheel. For Column #3, quarter sections of 3 in. diameter PVC pipe were placed in the corners of the formwork so that the corner radii were cast in place. Figure 4.18 shows the concrete surface preparation tool being used.



Figure 4.18. Concrete Surface Preparation

After surface preparation was completed, dust was removed from the faces of the column by first vacuuming the surface, followed by blowing compressed air over the surface in several passes, followed again by vacuuming the surface. Once it was determined that the dust had been fully removed from the surface, the CFRP system was immediately applied.

The grooves for the U-Anchors were also created during this stage of the column repair process. The grooves were realized by using a jackhammer to create $\frac{3}{4}$ in. wide and $\frac{3}{4}$ in. deep grooves at the column-to-footing interfaces on the East and West sides of

Columns #2 and #3. The walls of the grooves were flattened by using a small electric chisel and cleaned of dust using the same procedure described for the concrete surface.

4.7.5. Installation of FRP. After the surface preparation, the first step in the installation process of the MBrace[®] CF 130 Composite Strengthening System was the application of MBrace[®] Primer to the faces of the column and footing that were to be overlaid with CFRP. The Primer was mixed per manufacturer's recommendations and applied to the surface using a 3/8 in. nap roller. Application of MBrace[®] Primer is shown in Figure 4.19.



Figure 4.19. Application of MBrace[®] Primer

After the Primer became tacky on the concrete surfaces, MBrace[®] Putty was mixed per manufacturer's recommendation and applied to the surface using drywall taping knives. The Putty was applied lightly to all surface to fill the small voids. In some cases where a larger discontinuity in the flat concrete surface was present, the Putty was applied more liberally to flatten the surface. Application of MBrace[®] Putty is shown in Figure 4.20.



Figure 4.20. Application of MBrace[®] Putty

For Column #1, Concreative[®] LPL Paste was used in lieu of MBrace[®] Putty. This was done per the recommendation of the manufacturer's representative. However, the set time for Concreative[®] LPL Paste was much longer than that of MBrace[®] Putty, and the column repair had to be extended one additional day to allow the Paste to set. After the Paste was allowed to set for approximately 18 hours, normal CFRP installation proceeded.

For Columns #2 and #3, quartz sand was mixed into the MBrace[®] Putty to thicken the mix per the recommendation of the manufacturer's representative. Mixing the quartz sand into the Putty mixture allowed for larger voids to be filled without the "sag" of normally mixed Putty.

About 30 minutes after the Putty was applied to the column, CFRP layup began. Longitudinal (vertically oriented) CFRP sheets were installed first using a "wet lay-up" process. "Wet lay-up" was performed by impregnating the fibers in a bath of MBrace[®] Saturant before placing the CFRP sheets on the column surface. Prior experience with

the CF 130 Composite Strengthening System showed that “wet lay-up” was more effective in impregnating the fibers and creating a sound bond between the CFRP system and concrete surface. Transverse (horizontally oriented) CFRP sheets were installed using a “dry lay-up” process, which involved impregnating the fibers as they were laid on the concrete surface. “Dry lay-up” was used with the transverse CFRP sheets because initial attempts to wrap the column with “wet” sheets resulted in damage to some of the fibers. In both the “wet” and “dry” processes, Saturant was applied on top of and beneath the CFRP sheets using a 3/8 in. nap roller. The fibers were then impregnated using a grooved aluminum FRP roller.

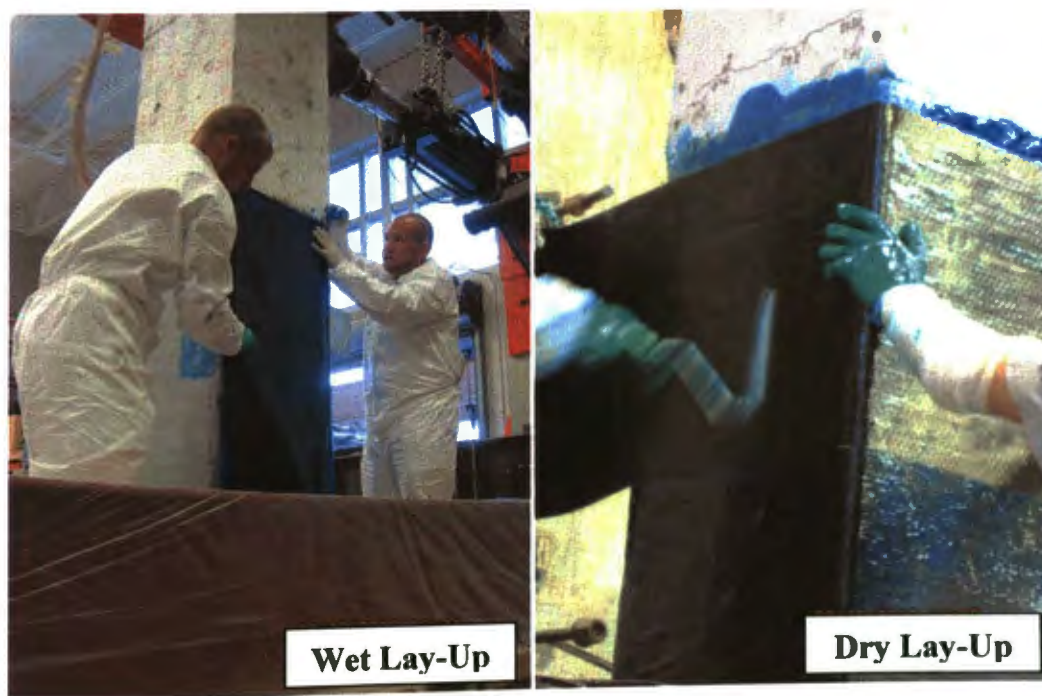


Figure 4.21. Installation of CF 130 Carbon Fiber Sheets

For Columns #2 and #3, the longitudinal CFRP was pressed into the U-Anchor grooves using a steel bar at the time of their “wet lay-up” process. The grooves, which received a coat of Primer prior to the CFRP placement, were filled with Saturant after CFRP placement.

After all of the CFRP sheets had been placed around the column, the system was allowed to cure until the start of testing. Curing of the CFRP for Columns #1 and #2

involved placing small space heaters around the column due to the low ambient temperature of the laboratory. Heaters were not used for the curing of the CFRP on Column #3 because the ambient lab temperature was sufficiently warm.

4.7.6. Installation of Anchorage. While the CFRP system remained “wet” and uncured, the anchorage plates were temporarily set into place on the footing. A thick layer of Saturant was placed over the area on the footing onto which the anchorage plate would be set. This was done to ensure a uniform bearing surface between the anchorage plate and the concrete surface, as well as to minimize the gap between the column-to-footing joint and the quarter-pipe portion of the anchorage system. A thin plastic sheet was placed between the anchorage system and the Saturant to ensure that the steel plate did not bond to the concrete surface via the epoxy Saturant. The photo in Figure 4.22 shows the temporary placement of the anchorage plate over the “wet” FRP system.



Figure 4.22. Temporary Placement of Anchorage Over “Wet” Saturant

After the FRP system was allowed to cure for about 24 hours, the anchorage plate and the thin plastic sheet were removed. The anchorage plate was then replaced in the same position so that the holes for the anchor rods could be drilled. The anchor rod holes were drilled to an embedment depth of 9 in. using a hammer drill and a 1-1/8 in. drill bit. After the holes were drilled, the anchorage plate was removed and concrete dust was removed from the holes by first blowing the holes out with compressed air, followed by

cleaning the holes with a wire brush, then vacuuming out the holes. This process was repeated until blowing compressed air into the holes resulted in clean, dust-free air to be expelled from the holes.

After the holes were sufficient cleaned, Hilti HIT-RE Epoxy Adhesive was injected into the holes using a static mixer. Once a sufficient amount of epoxy was injected into the holes, the threaded steel anchor rods were inserted by simultaneously twisting the rods and pushing them into the hole until they reached their full embedment depth. Figure 4.23 shows the injection of Hilti HIT-RE 500 epoxy into an anchor rod hole.

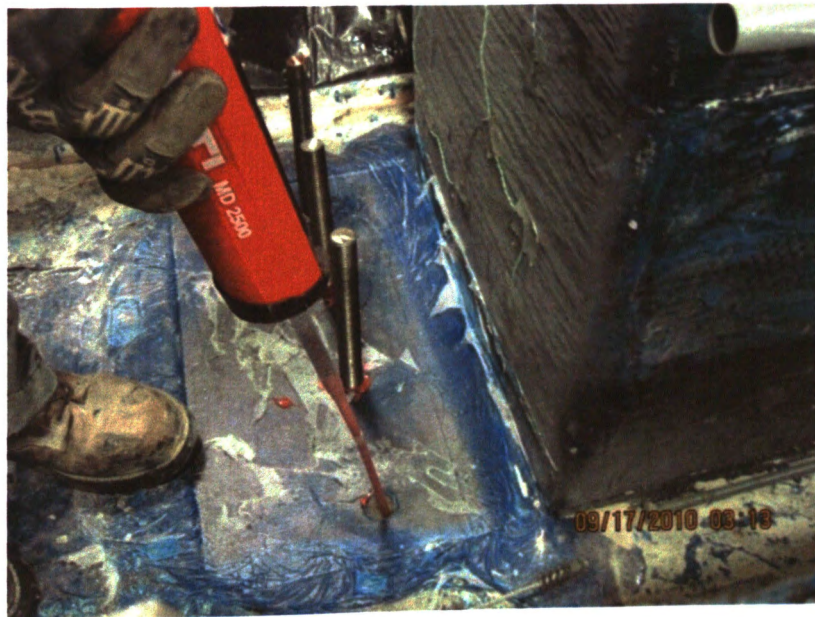


Figure 4.23. Injecting Epoxy Into Anchor Rod Holes

The anchorage plates were placed back into their final position while the anchoring epoxy was still “wet”. The anchorage epoxy was allowed to cure for at least 14 hours before the anchorage plate was fastened to the concrete by tightening nuts on the anchor rods. The 14 hour cure time allowed was in excess of the recommended cure time for the Hilti HIT-RE 500 Epoxy Adhesive Anchoring System at an ambient temperature of 68° F. The plates were finally fastened to the concrete just before the testing procedure began by tightening the nuts on the anchor rods with a wrench. Throughout the testing procedure, the nuts were monitored visually to ensure that no

slippage occurred which would have resulted in the release of the tensile force in the anchor rods.

A detailing issue that led to the premature failure of the anchorage system in the testing of Column #1, which is discussed in Chapter 5, led to a slight deviation in this procedure for the installation of the novel anchorage system in Columns #2 and #3. Because the plates were placed too close to the face of the column during the repair of Column #1, bearing of the column onto the anchorage plates caused undesirable results. Therefore, a $\frac{1}{4}$ in. gap was left between the CFRP and the anchorage plate in Columns #2 and #3. Figure 4.24 shows the installed anchorage systems for all three columns. Note that the anchorage system for Column #1 contains a setup used to monitor the loads in the anchor rods using load cells. This load cell setup is discussed in Section 4.8.

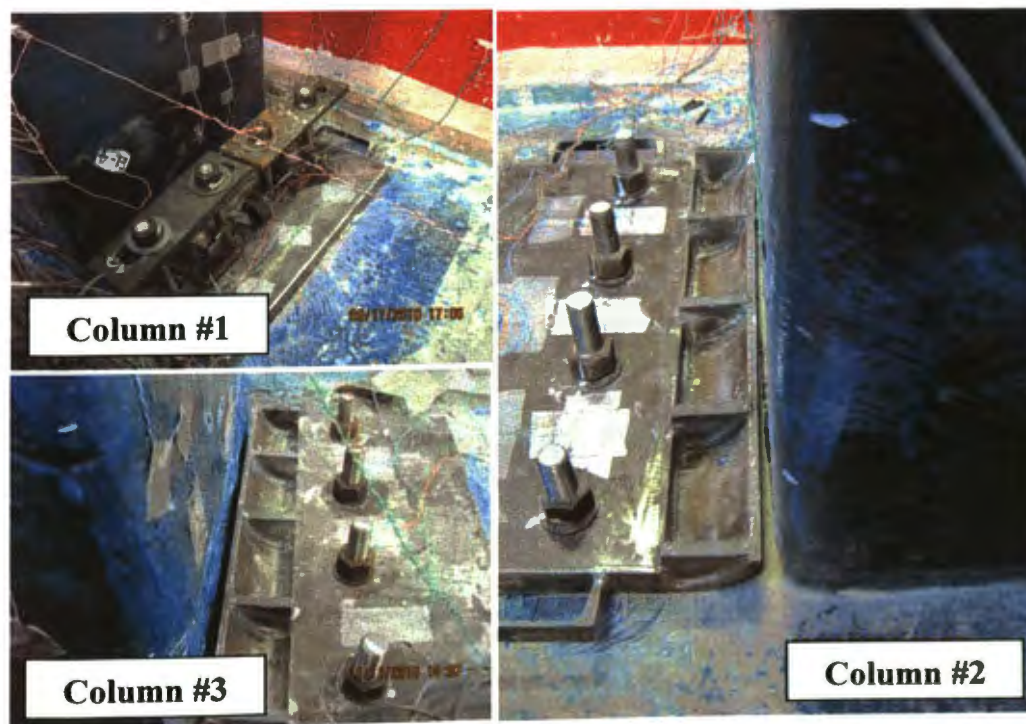


Figure 4.24. Installed Novel Anchorage System

4.8. INSTRUMENTATION AND TESTING PROCEDURE

While a significant amount of instrumentation was used on the repaired columns in order to evaluate their behavior, only a limited amount of that instrumentation was relevant in evaluating the behavior of the novel anchorage system. Therefore, only the

instrumentation relevant to the evaluation of the novel anchorage system is presented in this section. Other instrumentation placed on the column that is not included in this section includes string transducers, demountable mechanical strain (DEMEC) gauges, transverse (horizontally oriented) strain gauges, direct current variable displacement transducers (DCVTs), tilt sensors, and a load cell monitoring the axial load placed on the column. This section presents only the strain gauges that measured longitudinal (vertical) strain on the surface of the CFRP, surface strain gauges on the novel anchorage system, and load cells used to monitor the forces in the anchor rods. All strain gauges were uniaxial electrical resistance gauges of Type EA-06-250BG-120/LE from Vishay Micromasurement. All instrumentation was installed on the column after the epoxy resin of the FRP system had set, but before the initiation of testing. The instrumentation details mentioned in this section are for Columns #1, #2, and #3 only. Finally, details regarding the testing setup and procedure are also discussed.

4.8.1. Longitudinal Strain Gauges. Longitudinal, or vertically oriented, strain gauges were mounted to the surface of the outermost layer of CFRP on the columns. Figure 4.25, Figure 4.26, and Figure 4.27 show the longitudinal strain gauge locations for Columns #1, #2, and #3. Strain gauge names shown inside a box indicate those that malfunctioned before or during the testing procedure.

4.8.2. Strain Gauges on Novel Anchorage System. Strain gauges were mounted on the top face of the novel anchorage system in order to evaluate the bending of the steel plate caused by the reactions depicted in Figure 4.9. These strain gauges were mounted on the steel plate in line with the anchor rod holes. Figure 4.28 shows the locations of strain gages placed on the novel anchorage system. Some strain gauges on the novel anchorage system malfunctioned before or during the test. Table 4.7 lists the strain gauges for each column test. Malfunctioning strain gauges are highlighted in gray.

4.8.3. Load Cells on Novel Anchorage System. Load cells were installed only for Column #1 on the novel anchorage system in order to monitor the loads in the anchor rods. Anchorage load cells were not used on Columns #2 and #3 because the data used from the Column #1 anchorage load cells could be used to develop a relationship between the strain measured in the anchorage plate and the load in the anchor rods. The anchorage load cell setup for Column #1 is depicted in Figure 4.29.

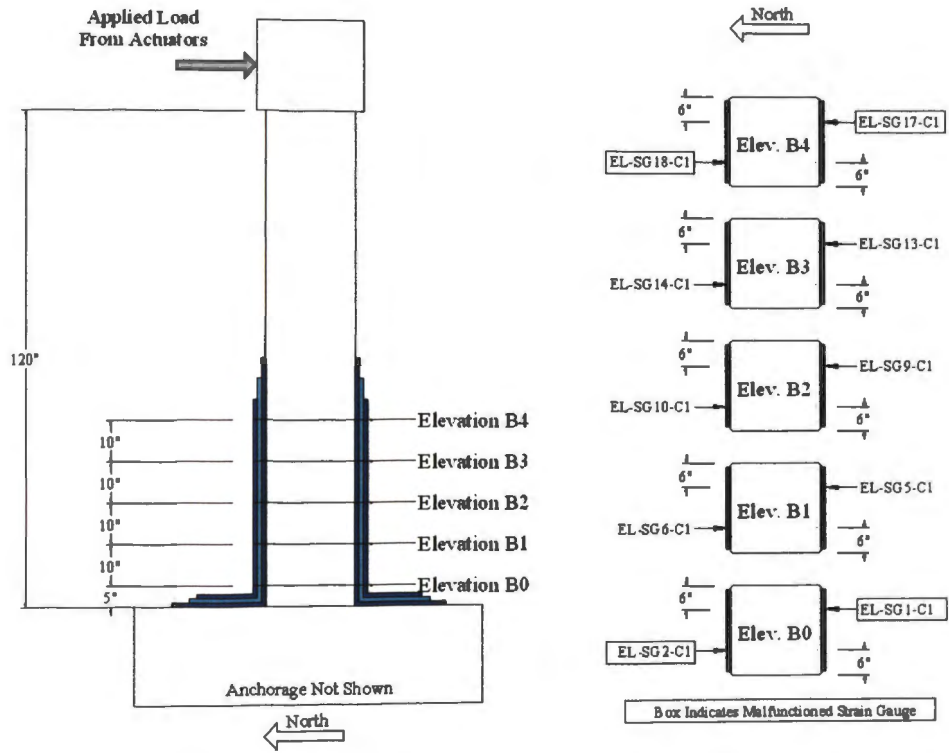


Figure 4.25. Longitudinal Strain Gauge Locations on Column #1

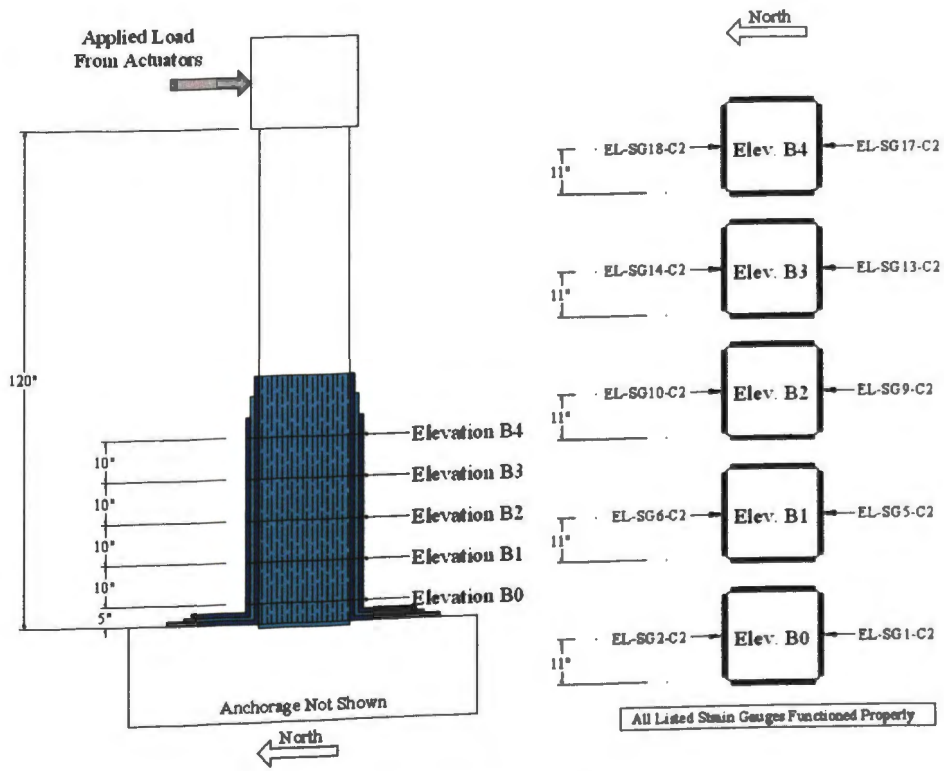


Figure 4.26. Longitudinal Strain Gauge Locations on Column #2

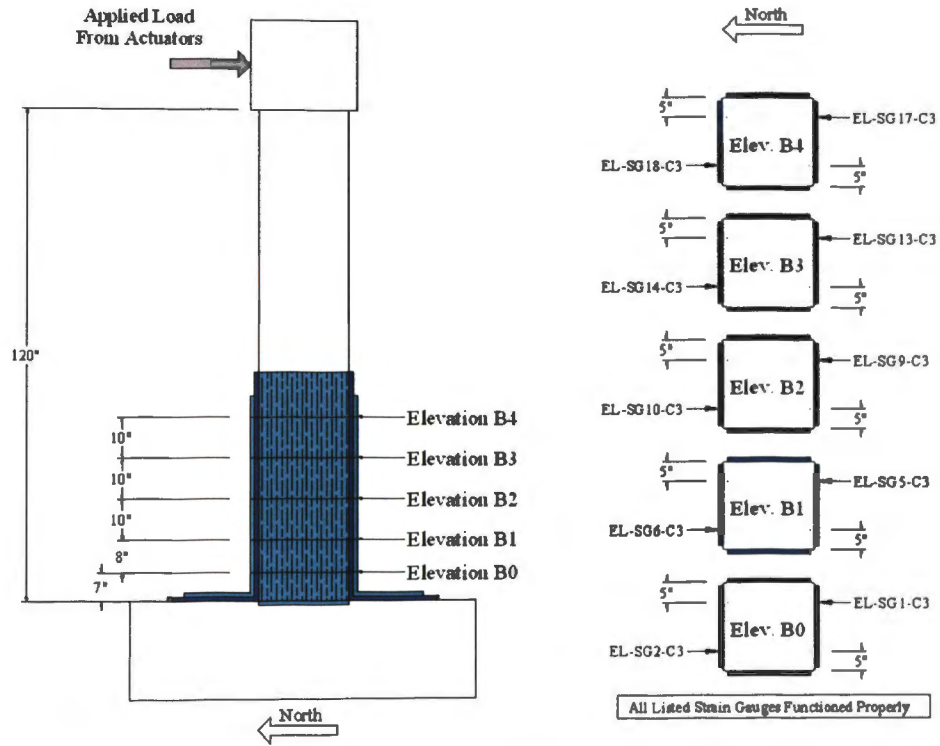


Figure 4.27. Longitudinal Strain Gauge Locations on Column #3

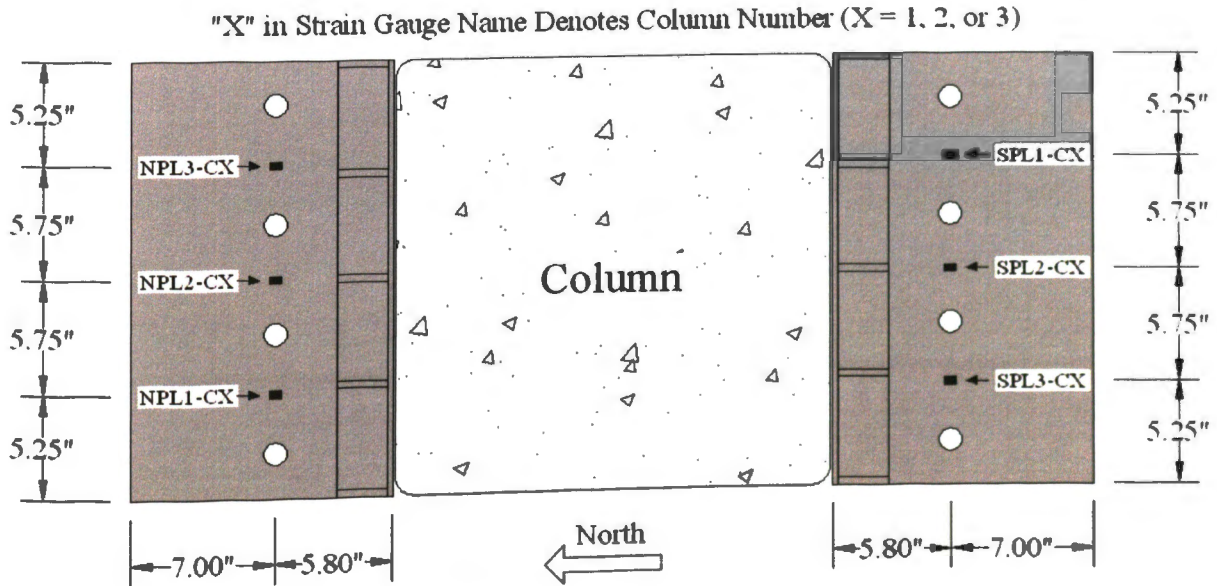


Figure 4.28. Strain Gauge Locations on Novel Anchorage System

Table 4.7. Functional Strain Gauges on Novel Anchorage System

| Column ID No. | North Anchorage | | | South Anchorage | | |
|---------------|-----------------|---------|---------|-----------------|---------|---------|
| | 1 | 2 | 3 | 1 | 2 | 3 |
| 1 | NPL1-C1 | NPL2-C1 | NPL3-C1 | SPL1-C1 | SPL2-C1 | SPL3-C1 |
| 2 | NPL1-C2 | NPL2-C2 | NPL3-C2 | SPL1-C2 | SPL2-C2 | SPL3-C2 |
| 3 | NPL1-C3 | NPL2-C3 | NPL3-C3 | SPL1-C3 | SPL2-C3 | SPL3-C3 |

Gray Highlights Indicate Malfunctioned Strain Gauge

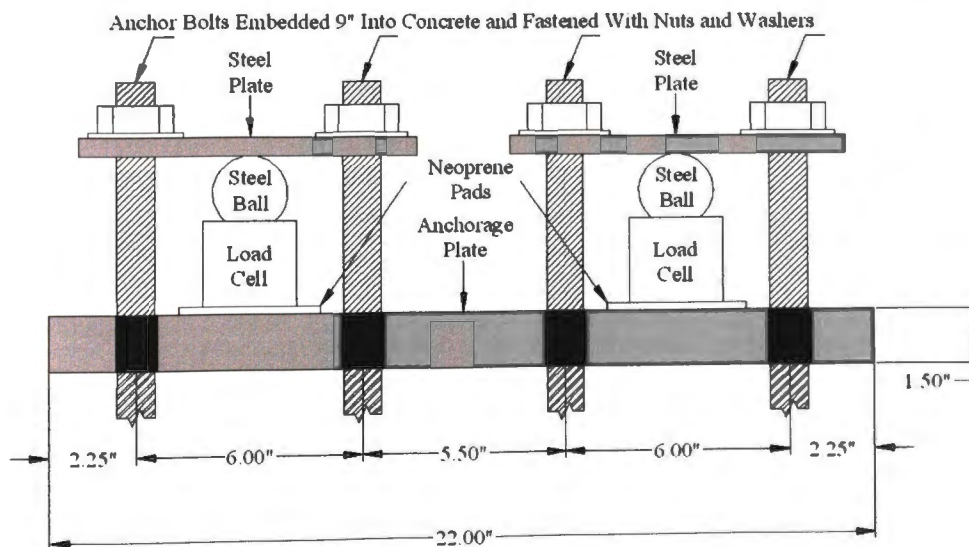


Figure 4.29. Load Cells Used on Novel Anchorage System for Column #1

4.8.4. Test Setup. The testing setup that was used to provide fixity of the footing during the column tests involved a test bed made of reinforced concrete. The column specimens were placed into the test bed. Because gaps existed between the test bed and the footing, Hydrostone[®] was cast in those gaps to eliminate the potential for movement. Hydrostone[®] is a gypsum cement with a high compressive strength that has a fluid consistency when cast. Two steel wide flange beams were placed over the surfaces of the footing and the test bed to resist the forces generated by the rotation of the footing when a lateral force was applied to the top of the column. These wide flange beams reacted against a double-channel built-up steel section placed on each end of the test bed, which transferred the reaction to the reaction floor using four dywidag bars on each end. Hydrostone[®] was also cast under the wide flange beams to ensure a uniform bearing surface on the beam flanges. Resistance to shear and torsion forces applied to the

columns was provided by two dywidag bars that ran through each end of the test bed and into the reaction floor.

Lateral loads were applied to the column using two hydraulic actuators that each had a force capacity of 220 kips in both directions and a total stroke of 30 in. (approximately 15 in. in each direction). The actuators were mounted at the height of the column cap and reacted against a reaction wall. The axial load was applied to the column by running seven steel prestressing strands through a PVC pipe in center of the column. The strands were fixed at the top of the column cap and at the bottom of footing. The axial load was applied using a hydraulic jack. The test setup is shown in Figure 4.30.

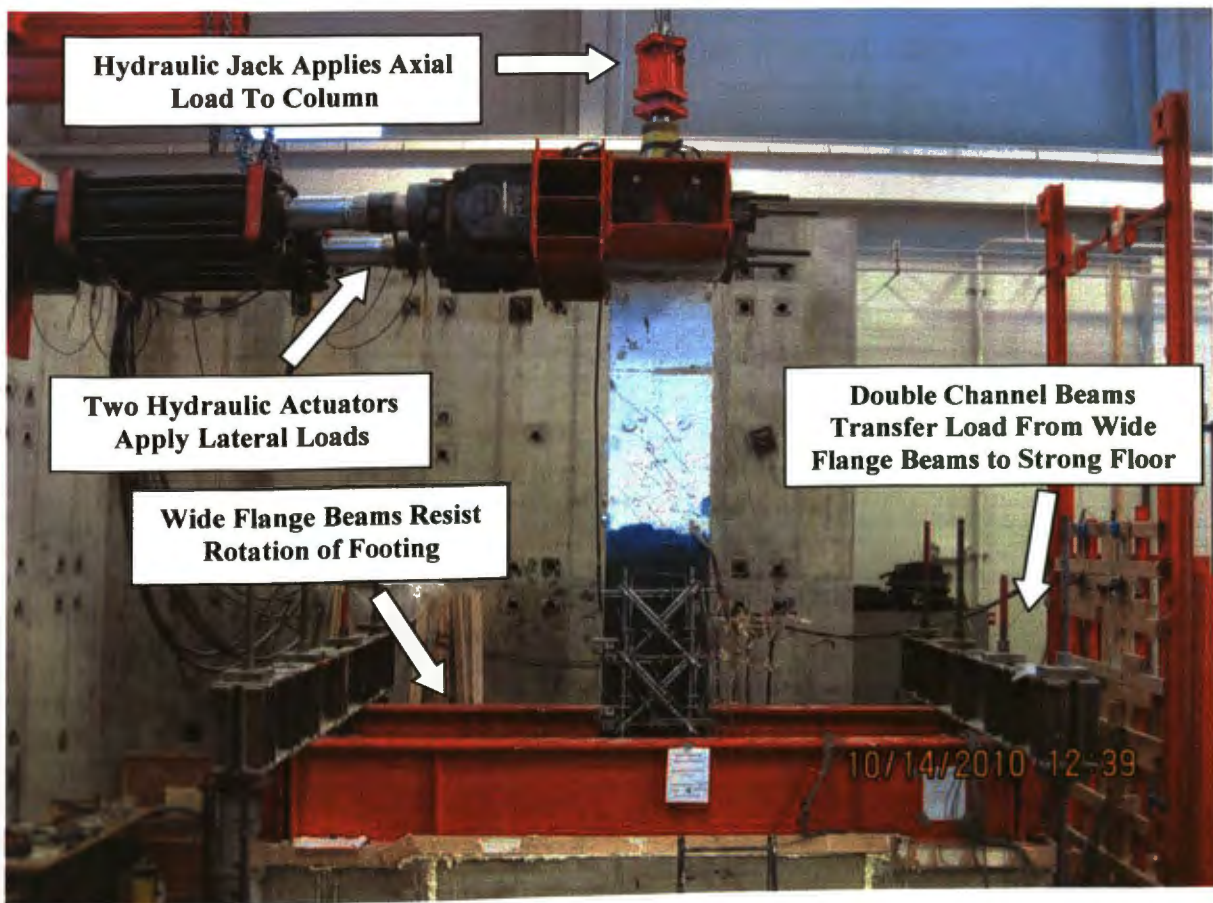


Figure 4.30. Column Testing Setup

When lateral loads were applied to the column, a positive shear force and bending moment was defined as when the actuators were pushing the column in the south

direction. Likewise, a negative shear force and bending moment was defined as when the actuators were pulling the column in the north direction. Applied torsion was defined as positive when the applied lateral forces from the actuators caused a counterclockwise rotation to the column as the column is viewed in plan. Likewise, applied torsion was defined as negative when the applied lateral forces from the actuators caused a clockwise rotation to the column as the column is view in plan. The definitions of the positive and negative torsion, shear, and flexural forces are clarified by the drawing shown below in Figure 4.31.

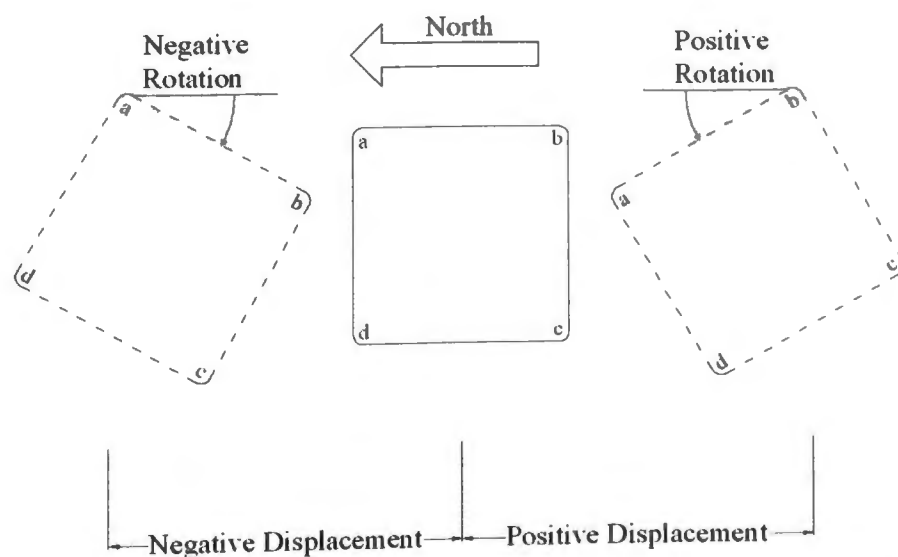


Figure 4.31. Definitions of Positive and Negative Forces (Plan View)

4.8.5. Testing Procedure. Loads were applied to the column cyclically maintaining the specified T/M ratio. The testing procedure was initiated in “force control” and was stepped up in small increments until the applied load neared 90% of the estimated yield load. At this point, the testing procedure was continued in “displacement control”. Measured values of the column stiffness obtained in “force control” loading were used to determine the applied displacements that would keep the T/M ratio constant during “displacement control”. Results and observations from the testing of Columns #1, #2, and #3 are presented in Chapter 5.

5. EXPERIMENTAL RESULTS AND DISCUSSION

5.1. GENERAL

This chapter presents the results of the experimental program. As mentioned in Chapter 4, the results that are presented are limited to those of Columns #1, #2, and #3. Results of Columns #4, #5, and #6 are not discussed since the anchorage systems used at the base of Columns #1, #2, and #3, which are the focus of the experimental portion of this thesis, were not included for Columns #4, #5, and #6.

Section 5.2 presents an overview of the overall behavior of the repaired columns. Additionally, their behavior is compared with the behavior of the original, undamaged columns. Section 5.3 discusses the performance of the anchorage systems used for the repairs of Columns #1, #2, and #3. The main focus of this section is the comparison between the predicted and actual behavior of the anchorage. Finally, Chapter 5 concludes with design recommendations for the anchorage systems tested in this study.

5.2. OVERALL BEHAVIOR OF REPAIRED COLUMNS

This section presents an overview and brief discussion of the overall behavior of the repaired columns. The discussion is limited to Columns #1, #2, and #3. It is important to note that the overall behavior of the repaired columns is not the focus of this thesis and therefore is not evaluated to the fullest possible extent. However, some discussion of the overall behavior of the columns is certainly relevant to the evaluation of the performance of the anchorage systems used at their bases.

5.2.1. Overall Behavior. The repaired columns were tested under the loading program described in Section 4.2.1. Testing began three days following the initiation of the column repair process, unless noted otherwise. The tests for Columns #1 and #2 were started and finished during the same day, while the test of Column #3 was interrupted during the first day of testing and completed over the course of two days.

During the test of Column #1, very little observable behavior occurred during the entirety of “force control” testing and also during the beginning stages of “displacement control” testing. It was observed, however, that while the test was being conducted in “force control”, equal bending moments applied to the column in both directions would

result in a larger displacement during the negative cycle than the positive cycle. As the testing procedure was changed to “displacement control”, larger displacements were applied in the negative cycle than the positive cycle in an attempt to maintain the same bending moment in both directions of the cycle.

After several cycles of “displacement control” testing had occurred, some unusual shear cracks were observed on the east and west vertical faces of the footing, directly beneath the column. These cracks were observed during the cycle that contained applied bending moments of 452.7 kip-ft and -349.25 kip-ft, and corresponding displacements of 1.9 in. and -2.2 in. A picture of the shear cracks during testing is shown in Figure 5.1.

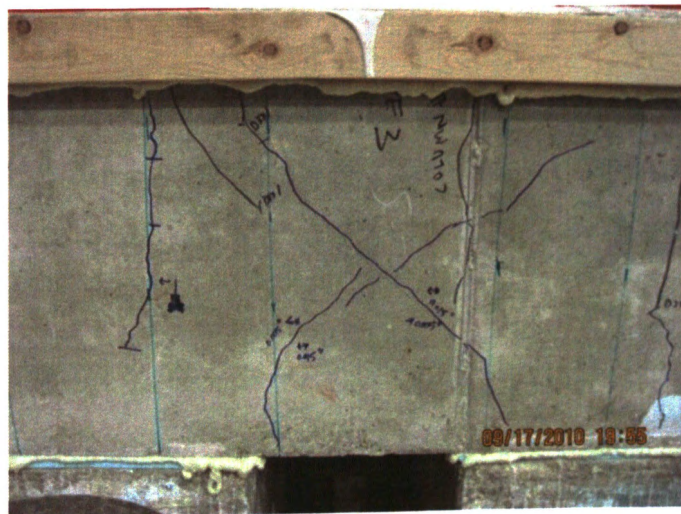


Figure 5.1. Shear Cracking in Footing Observed During Column #1 Testing

The shear cracks continued to open wider until applied bending moments of 514.8 kip-ft and -402.1 kip-ft and corresponding displacements of 2.6 in. and 2.9 in. were reached. At this point the cracks stopped opening and closing when the loading cycles were applied and reversed, and further opening of the cracks was not observed for the remainder of the test. Also, during the same load cycle, the load being measured on the anchorage load cells on both sides of the column decreased significantly and did not continue to carry any additional load through tension in the anchor rods for the remainder of the test. Strain gauges on the anchorage also stopped measuring increases in strain at this time as well.

As the test progressed, it was observed that the CFRP near the base of the column was coming into contact with the novel anchorage system. As the column deflected toward the novel anchorage, the top of the quarter-pipe section contacted the adjacent CFRP. A picture of this situation is shown in Figure 5.2.



Figure 5.2. Contact Between CFRP and Novel Anchorage in Column #1 Test

At the same time that contact between CFRP and the anchorage was being observed, tapping on the CFRP surface revealed that the CFRP directly above the anchorage had debonded from the surface of the column. The debonding appeared to worsen during the portion of the cycle that put it into compression. Therefore, it was determined that this debonding was due to compression-induced buckling of the CFRP and possibly due to concrete crushing within the cross-section, rather than due to one of the tensile debonding failure modes depicted in Figure 1.1.

The CFRP system ultimately failed by rupture of the CFRP due in large part to the bearing of the corner of the novel anchorage system on the FRP. On both sides of the column, CFRP rupture was noted at the same height as the contact between the anchorage and the CFRP. Debonding failure continued to progress slowly from the base of the column to about 18 in. from the base. Splitting of the transverse CFRP on the east and west sides of the column was also observed prior to failure; however, this was not surprising since there was no longitudinal CFRP present on those sides, and since the CFRP sheets have no tensile strength in the direction perpendicular to their fiber

direction. The test was ultimately stopped when the lateral load-carrying capacity had diminished. This occurred after a sound was heard coming from the column that seemed to be the rupture of a longitudinal reinforcing bar. Figure 5.3 shows the northwest corner of Column #1 at failure. Rupture of CFRP can be seen adjacent to the quarter-pipe section of the anchorage, while splitting of the transverse CFRP is shown on the west face.

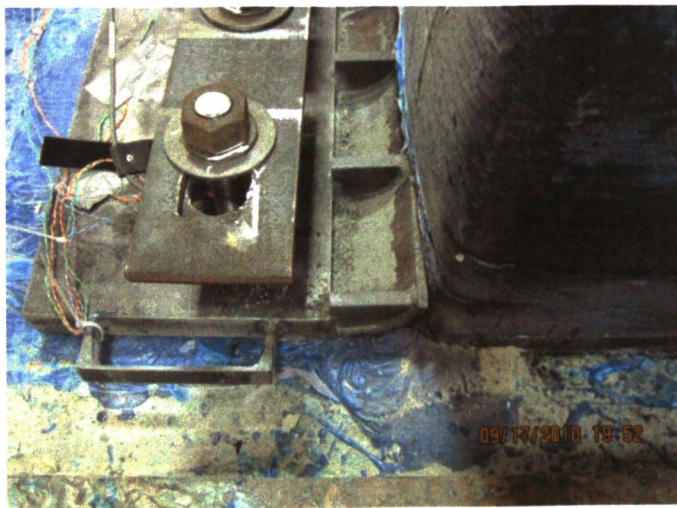


Figure 5.3. Failure of Column #1 by Rupture of CFRP at Anchorage

Testing of Column #2 proceeded with no failures or unusual observations until some pullout of the U-Anchors on the east and west faces of the column was observed on the last cycle of “force control”, corresponding to an applied moment of 542.1 kip-ft and torsion of 108.0 kip-ft. Although the first observation of U-Anchor pullout was observed at those load levels, it is likely that the U-Anchors failed prior to this observation. Their actual failure load could not be determined since the Saturant cover over the U-Anchors obstructed view of the anchorage. Pullout failure of the U-Anchors is shown in Figure 5.4.

Buckling and compression debonding of the CFRP on the north and south column faces were observed after the first cycle of displacement controlled loading. As the column was loaded cyclically, the CFRP on the compression face of the column began to buckle. Buckling started just above the height of the novel anchorage, or about 3 in. from the column base, and progressed up the height of the column as testing continued. Also

during the first cycle of displacement controlled loading, local rupture of the transverse CFRP was noted at the northwest corner of the column. The ruptured CFRP extended only about 1.5 inches from the footing, while the rest of this transverse CFRP sheet remained intact. Figure 5.5 shows the local rupture of the transverse CFRP at the base of Column #2.



Figure 5.4. Pullout Failure of U-Anchors for Column #2



Figure 5.5. Rupture of Transverse CFRP at Base of Column #2

As testing continued, the FRP continued to buckle and debond when placed under compression. The buckled portion of the CFRP bulged out from the column, extending over the quarter-pipe section of the novel anchorage even though the anchorage had been placed approximately 1/4 in. away from the face of the column. Ultimately, the CFRP on the north and south faces of the column failed by rupture of the buckled CFRP. The CFRP on the south face of the column ruptured first at a height of about 4 in. from the footing, followed shortly thereafter by rupture of the CFRP on the north face of the column at a height of about 3.5 in. from the footing. It was not clear whether the CFRP rupture was due to extensive buckling, tensile loading, or the combination of cyclic buckling and tensile loading. Figure 5.6 shows the rupture of CFRP on the south face of Column #2. CFRP rupture on the north face of the column was visually identified; however, attempts to photograph the rupture were unsuccessful due to the small width of the rupture.

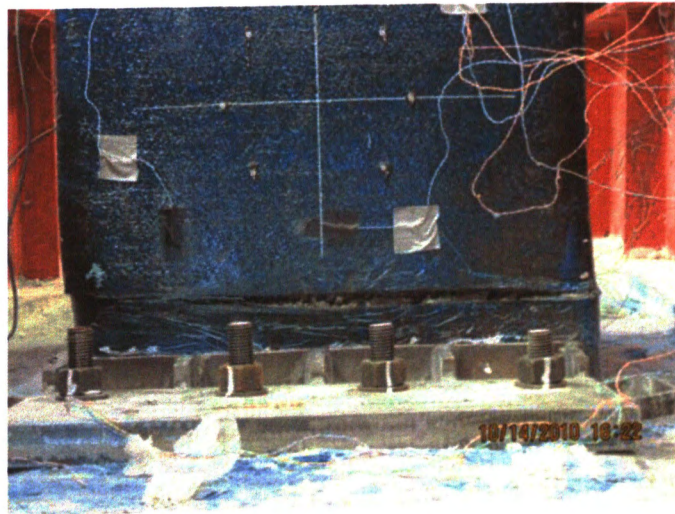


Figure 5.6. Rupture of CFRP on South Face of Column #2

After testing, the debonded areas of CFRP were located by tapping the CFRP with a hammer and marking the areas in which tapping produced a hollow sound. The heights of the debonded regions extended 29 in., 34 in., 21 in., and 28 in. on the north, south, west, and east faces, respectively. These debonded areas are shown in Figure 5.7. The white hatched areas represent the observed debonded regions.



Figure 5.7. Debonded Areas of CFRP on Column #2 After Testing

Testing of Column #3 proceeded with no unusual observations until some flexural cracks were noticed developing on the top surface of the footing after an applied moment of 184.8 kip-ft and a torsion load of 71.6 kip-ft. Throughout the initial stages of loading, existing cracks in the concrete located directly above the repair height were observed to open and close with the loading cycles. These cracks became excessively wide during the final cycle of force controlled loading, corresponding to an applied moment of 525.8 kip-ft and a torsion load of 206.0 kip-ft. These cracks are shown in Figure 5.8.

Prior to the observation of these cracks, it was observed that the concrete cover had spalled just above the repair height, although it is not clear when spalling initiated. In the cycles immediately following the observation of the severe cracks, the concrete

cover just above the repair height began to fall off of the column. The cover continued to progressively fall off of the column until testing was completed. After much of the concrete cover had fallen off, the transverse CFRP on the southwest corner of the column ruptured locally, with the rupture extending about 5 in. from the top of the uppermost layer of CFRP, as shown in Figure 5.9.

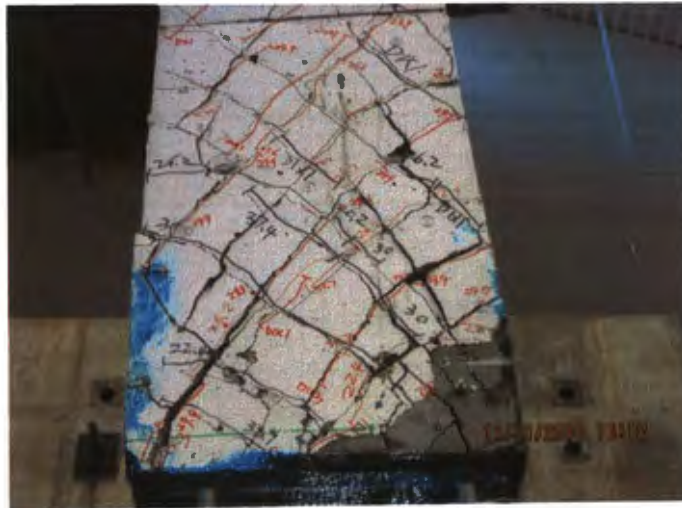


Figure 5.8. Concrete Cracking Above CFRP on West Face of Column #3



Figure 5.9. Rupture of Transverse CFRP on Southwest Corner of Column #3

A similar rupture extending about 2 in. from the top of the uppermost layer of transverse CFRP was also observed on the northeast corner of the column. Testing of Column #3 was ultimately stopped because the orientation of the actuators prevented further rotation of the column. This may have also influenced the applied forces measured in the actuator load cells, as discussed in Section 5.2.2. No visual or audible observations were made during the test that indicated failure of the novel anchorage, U-Anchors, or longitudinal CFRP near the base of the column. Figure 5.10 shows the damaged sustained to Column #3 during the final cycle of testing.

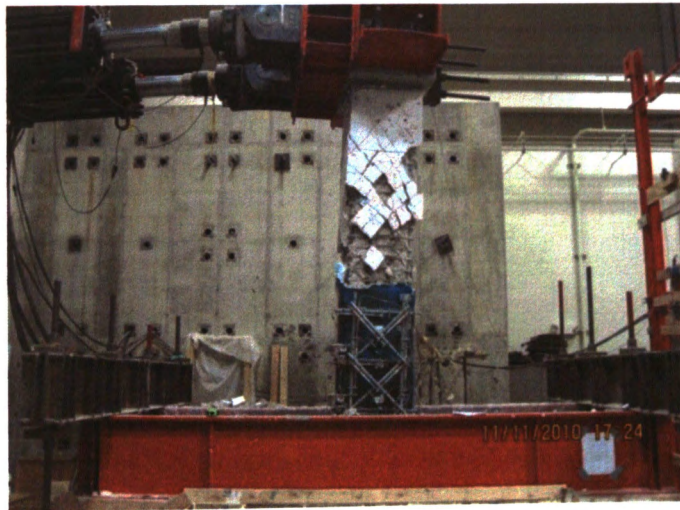


Figure 5.10. Column #3 During Final Cycle of Testing

5.2.2. Comparison to Original Column Behavior. Figure 5.11, Figure 5.12, and Figure 5.13 show the relationship between the applied bending moment and average actuator displacement for Columns #1, #2, and #3, respectively. Figure 5.14 and Figure 5.15 show the relationship between applied torsion and the angle of twist for Columns #2 and #3, respectively.

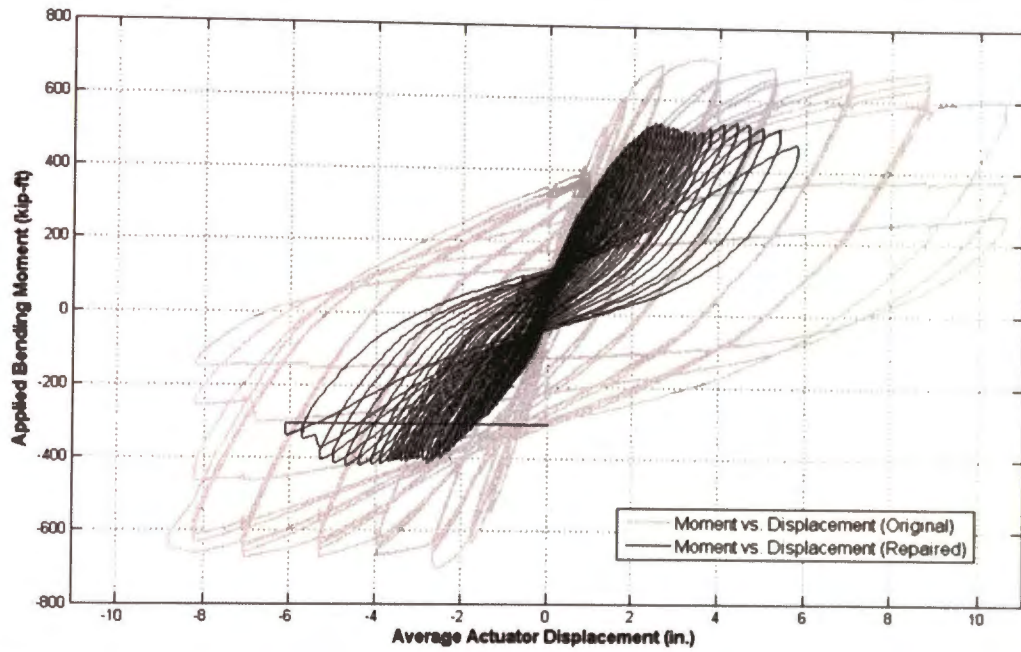


Figure 5.11. Bending Moment Versus Average Actuator Displacement for Column #1

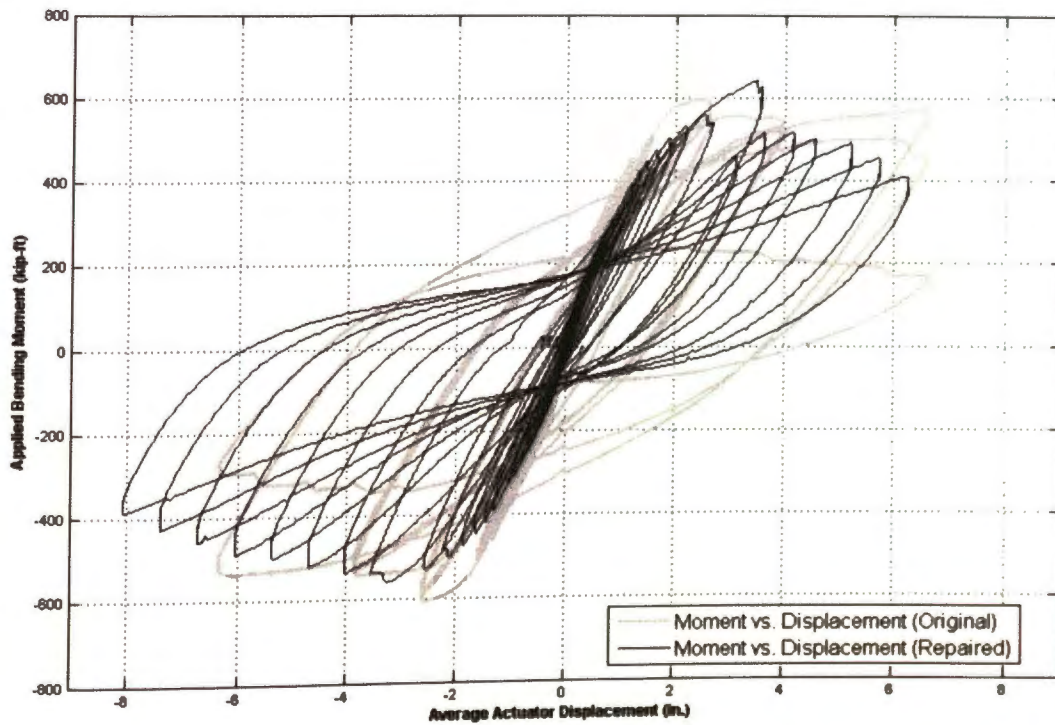


Figure 5.12. Bending Moment Versus Average Actuator Displacement for Column #2

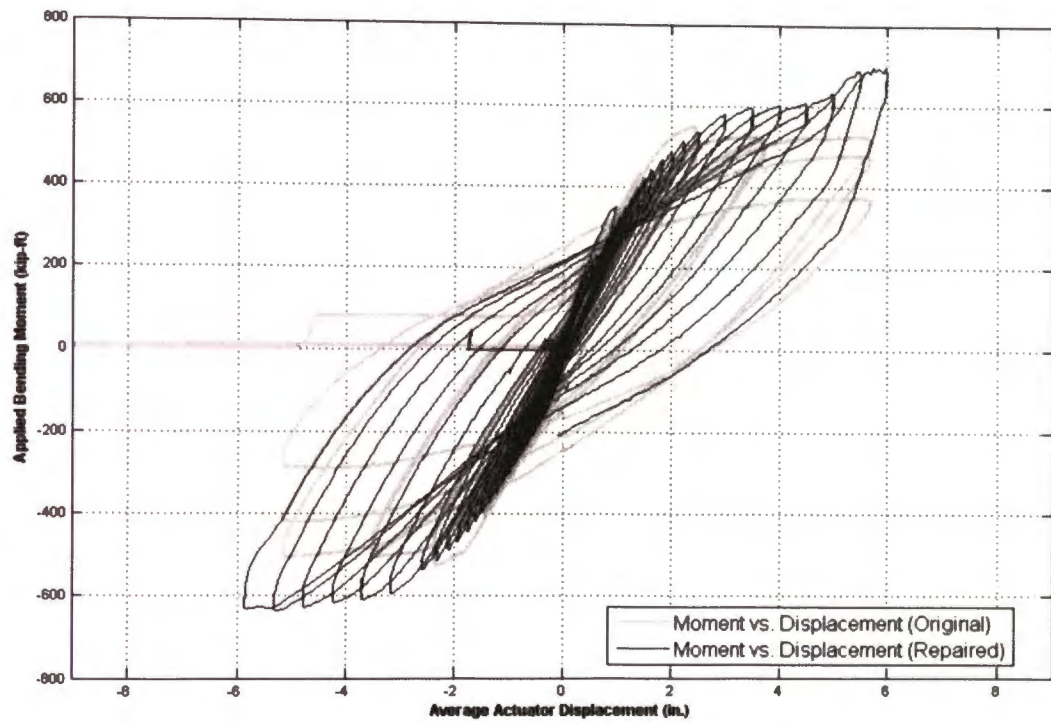


Figure 5.13. Bending Moment Versus Average Actuator Displacement for Column #3

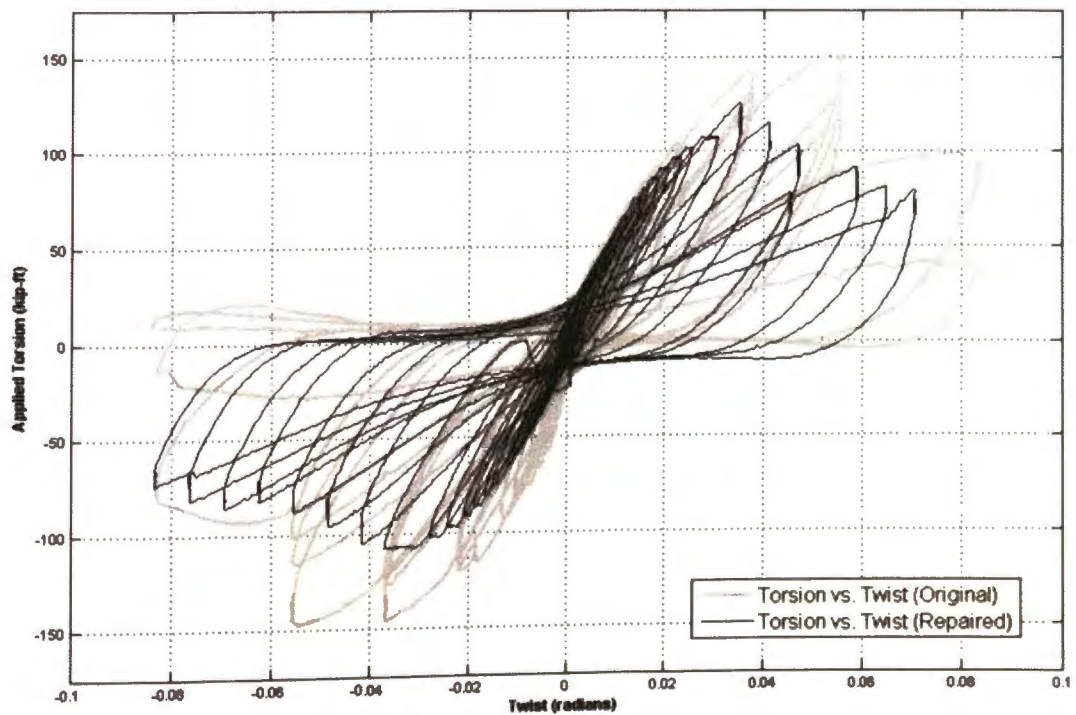


Figure 5.14. Torsion Versus Twist for Column #2

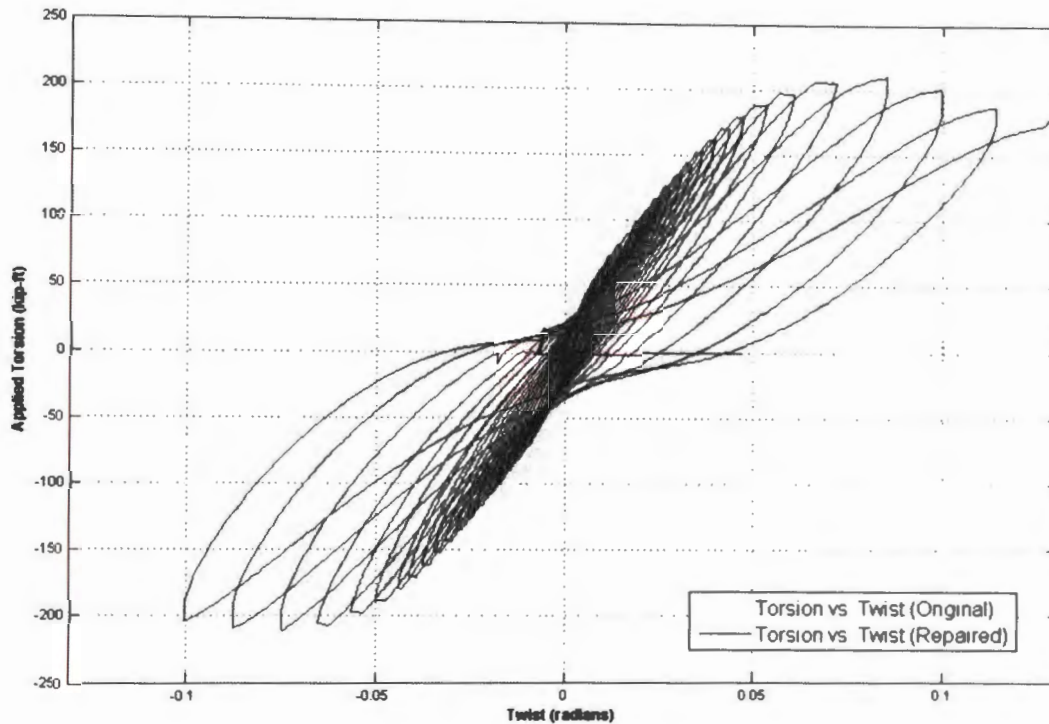


Figure 5.15. Torsion Versus Twist for Column #3

Column #1 resisted peak applied bending moments of 535.7 kip-ft and -420.8 kip-ft, corresponding to 75% and 60% of the original column's peak moment resistances in the positive and negative directions. However, it is clear from the plot in Figure 5.11 that the repaired column suffered a significant loss in ductility when compared to the originally tested column. Column #2 resisted peak applied moments of 640.5 kip-ft and -557.6 kip-ft, corresponding to 108% and 92% of the original column's peak moment resistances in the positive and negative directions. Column #3 resisted peak applied bending moments in excess of the original column's peak moment resistances of 548.3 kip-ft and -526.9 kip-ft. However, near the end of the testing program for Column #3, the large rotations caused by the torsion loads caused the swivels on the actuator heads to become bound. The binding of these swivels may have caused false readings in the internal actuator load cells to occur resulting in measured loads that may have been higher than the actual applied loads. Since the onset of binding was not apparent during testing, determining a peak applied bending moment for Column #3 from the measured data may not be accurate.

Column #2 resisted peak applied torsion loads of 125.8 kip-ft and -107.9 kip-ft, corresponding to 82% and 74% of the original column's peak torsional resistances in the positive and negative directions. Column #3 resisted peak torsion loads that were similar to or in excess of the original column's peak torsional capacities of 192.8 kip-ft and -200.1 kip-ft. As described in the preceding paragraph, it was not possible to determine peak torsion loads for Column #3 due to the possibility of false actuator load cell readings near the end of the testing program resulting from binding of the swivels on the actuators.

5.3. PERFORMANCE OF ANCHORAGE SYSTEMS

In this section, data collected from the experimental program are used to evaluate the performance of the novel anchorage system and transverse wrapping anchorage used for the repair of Columns #1, #2, as well as the #3 and the U-Anchor system used for the repair of Columns #2 and #3.

5.3.1. Novel Anchorage System. In order to evaluate the novel anchorage system's performance and create design recommendations for future use, it was desirable to evaluate several aspects of the anchorage system's behavior. These aspects included the transfer of force from the anchor rods to the concrete, the bending of the plate about the centerline of the anchor rods, and the force transfer from the CFRP at the base of the column to the anchorage plate.

It is important to note that the effects of the torsional loading on the novel anchorage of Columns #2 and #3 were not considered. While the presence of torsion in Columns #2 and #3 may have resulted in higher longitudinal stresses in the CFRP at the base of the column, the effects were considered to be minimal at this location. Since the presence of additional torsion tended to shift the plastic hinge away from the base of the column, it was expected that the torsional loading would not significantly increase the stress in the CFRP at the base of the column. Additionally, the effects of the torsional loading on the novel anchorage system were not easily quantified using the instrumentation scheme used on either of the columns.

This section contains many plots of data measured during the tests. These data are plotted as a function of time. The inclusion of a time variable in these plots is

intended only to serve as a reference point for the comparison of plotted data among other plots of data for the test column test. In each plot, long delays in the testing program in which zero force was being applied to the column were eliminated; therefore, the total time duration shown in the figures is much shorter than the actual duration of the testing procedure. Additionally, the applied bending moment is plotted on a secondary vertical axis in some plots. Again, the inclusion of this data is meant to serve as a reference, as well as to make the trends between anchorage, CFRP behavior, and overall column behavior more apparent. Finally, the plots in this section are envelope curves of the measured data. Since testing was performed cyclically, it is easier to observe data trends through envelopes, which display the high values, or the greatest positive values generated during each half-cycle of the loading program, and the low values, or the greatest negative values generated during the opposite half-cycle of the loading program.

5.3.1.1 Behavior of Novel Anchorage for Column #1. In order to evaluate the anchoring forces being transferred from the anchorage plate to the anchor rods, load cells were included during the testing of Column #1. This load cell setup is depicted in Figure 4.29. While valuable data were recorded from the load cells during the testing of Column #1, a decision was made not to include the load cells in the testing of Columns #2 and #3. This decision was made because the load cell setup allowed for the possibility of slipping or movement of the load cell, which would have resulted in a loss of function of the entire anchorage system. Figure 5.16 shows a plot of the load cell readings over the course of the Column #1 testing program. Compressive forces measured in the load cells are plotted as negative values in the plots that follow.

This plot reveals that the loads in the anchor rods began to increase significantly after applied bending moments of approximately 200 kip-ft and -150 kip-ft. These loads continued to increase until moments near the peak applied moments were reached, which occurred at a test duration of about 10600 seconds. After this point, the loads measured in the load cells were reduced significantly and did not continue to carry additional load after the reduction. Therefore, anchor failure occurred during the cycle in which the peak applied bending moments reached 533.9 kip-ft and -410.9 kip-ft. The anchors on both sides of the column failed in the same cycle. After the tensile failure of the anchor rods, the repaired column continued to resist additional loads, which was inconsistent with the

anticipated behavior of the longitudinal CFRP and the novel anchorage strengthening systems.

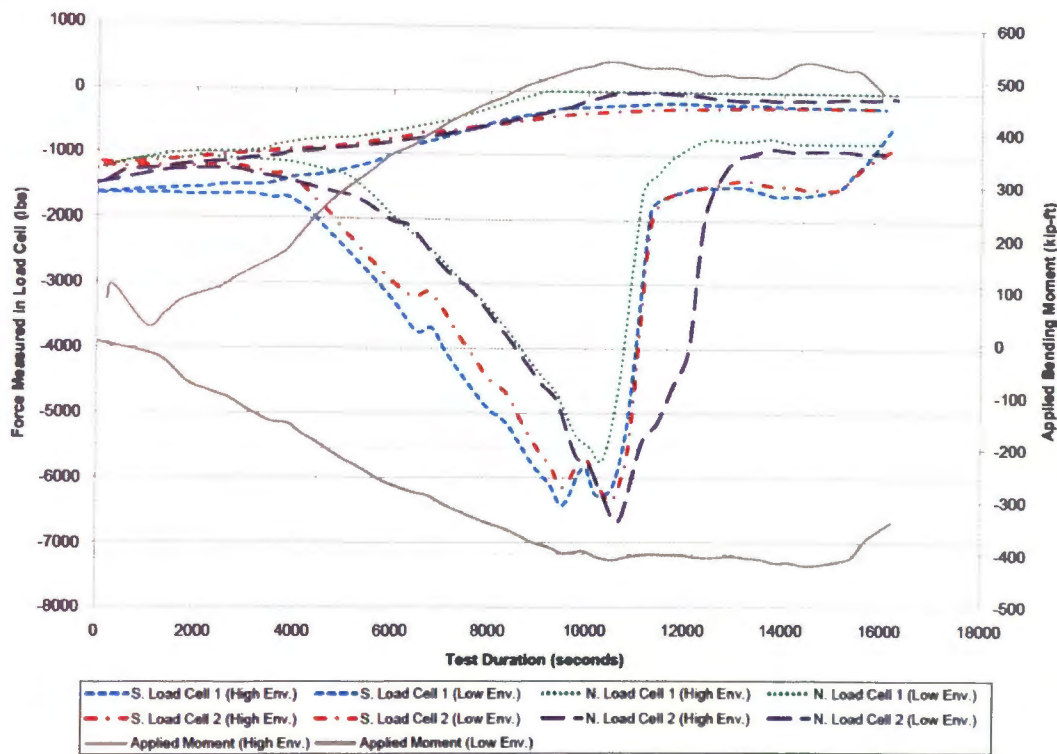


Figure 5.16. Load Cell Readings and Bending Moment Versus Time for Column #1

The average load carried by a single anchor rod can be estimated by dividing the sum of the forces measured in the two load cells on one side of the column by four, the total number of anchor rods on each side of the column. Thus, the average failure loads for the anchor rods were 3.10 kips and 3.20 kips for the north and south anchorage systems, respectively. These failure loads are significantly less than the predicted failure load of 15.38 kips based on yielding of the anchorage plate and 41.64 kips based on failure of the anchor rods. This large discrepancy could be due to one or a combination of the follow factors: additional shear induced on the anchor rods due to poor detailing of the novel anchorage system; or a difference in the assumed behavior of the force transfer mechanism between the CFRP at the column-to-footing joint and the novel anchorage system.

As previously noted, poor detailing of the anchorage plate system at the base of the column resulted in the corner of the quarter-pipe portion of the anchorage coming into

contact with the column during testing. Deformation of the column under the applied loads led to bearing of the column onto the anchorage plate system, which created two undesirable reactions. First, as previously discussed, the bearing of the CFRP onto the anchorage plate led to premature rupture of the CFRP. This resulted in the ultimate failure of the column by rupture of the longitudinal CFRP. Second, the bearing of the face of the column onto the anchorage plate also led to undesirable shear forces being transferred to the anchor rods. These shear forces likely caused the cracking in the footing shown in Figure 5.1, evidenced by the fact that these cracks did not continue to open and close after the anchor rods failed. Because the Hilti HIT-RE 500 Epoxy Adhesive Anchoring System is not intended for use in cracked concrete, the cracking in the footing most certainly resulted in a reduction in the anchor rods' ability to transfer shear and tensile forces to the concrete in the footing. Additionally, the shear forces induced on the anchor rods from the bearing of the column face on the anchor plates were not considered in the design of the anchorage system. These additional shear forces further reduced the tensile capacity of the anchor rods based on the shear-tension interaction equation given in Section RD.7 of *ACI 318-08*.

Measurement of the strain in the CFRP at or near the column-to-footing joint could be used to determine the force developed in the CFRP. Knowing the force in the CFRP at this joint would allow for an evaluation of the force transfer mechanism between the CFRP and the novel anchorage system. However, longitudinal strain gauges were mounted on the CFRP only as shown in Figure 4.25, with the nearest functional strain gauge to the anchorage located 15 in. above the column-to-footing joint. The envelopes of the strain measured by the longitudinal strain gauges on the north and south faces of Column #1 are shown in Figure 5.17 and Figure 5.18, respectively. Tensile strain is shown as positive in the figure.

Inspection of Figure 5.17 and Figure 5.18 does not reveal any trends that could be used to interpolate for an estimate of the strain in the longitudinal CFRP at the column-to-footing interface. This is due to the presence of local effects when measuring the strain in longitudinal CFRP.

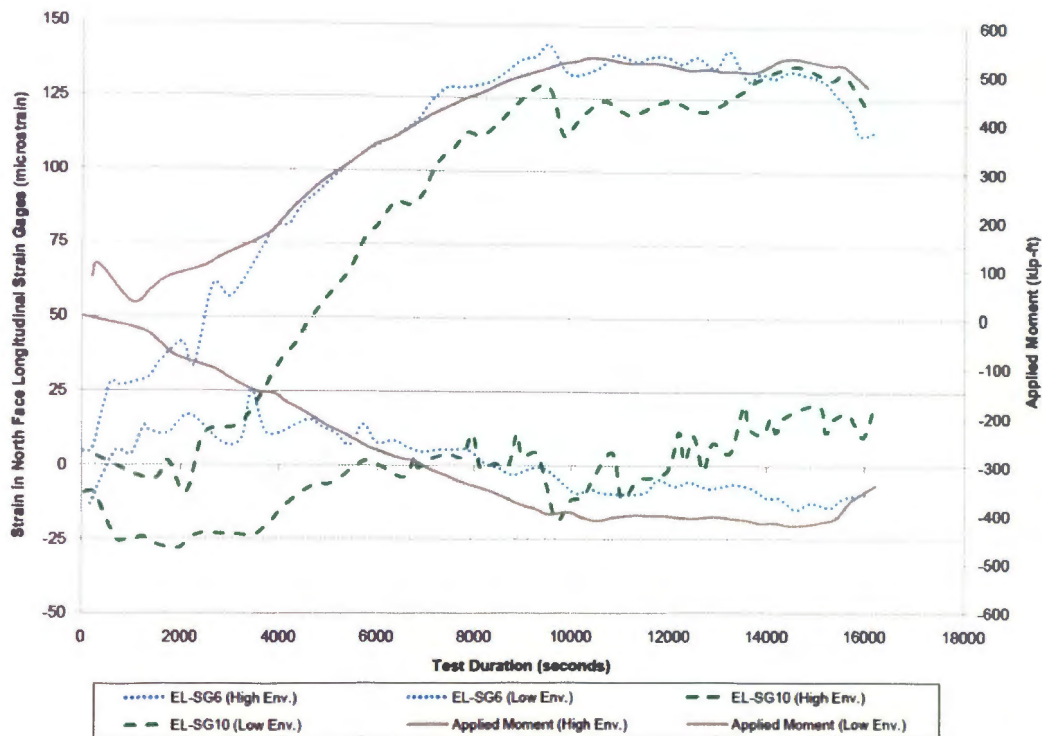


Figure 5.17. Longitudinal Strain Measurement in North Face of Column #1

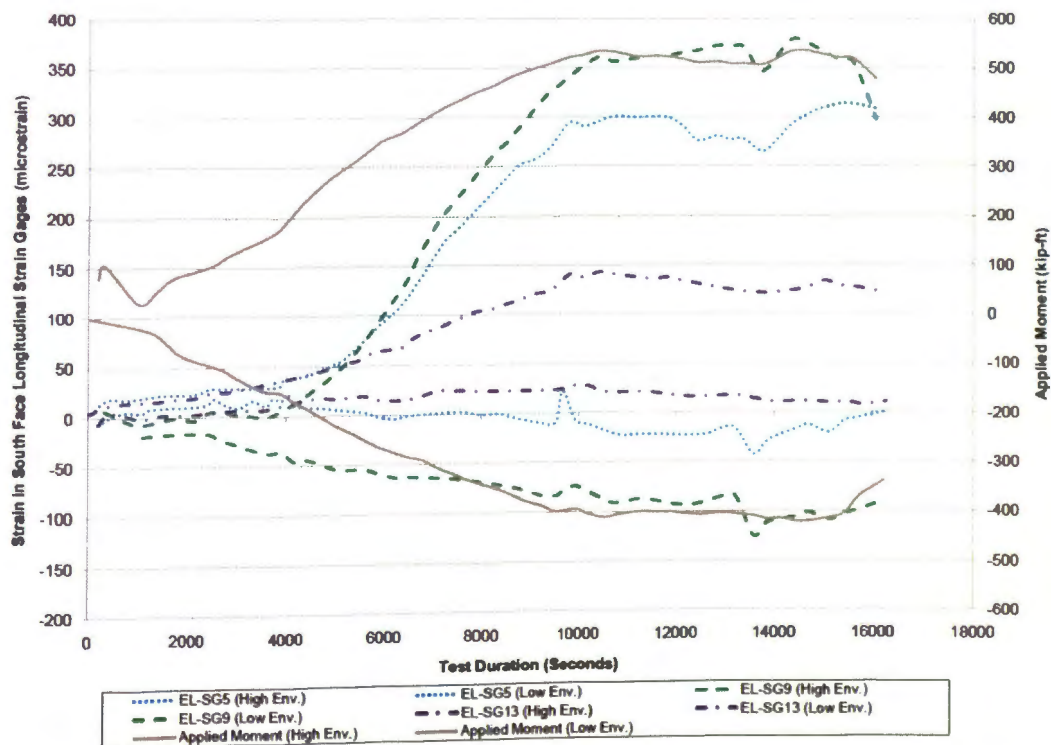


Figure 5.18. Longitudinal Strain Measurement in South Face of Column #1

Since no experimental data could be used to determine the strain in the CFRP at the column-to-footing interface, a program written by Ruili He, a doctoral student at Missouri S&T who worked on other aspects of this study, that uses moment-curvature analysis to predict the level of strain and subsequently the tensile force developed in the longitudinal CFRP was used. This program was modified specifically for Column #1 and took into account the effects of the ruptured and buckled longitudinal reinforcing bars. It also assumed perfectly anchored CFRP at the column-to-footing interface. The results of this program are shown in Figure 5.19.

Based upon this analysis, the theoretical maximum bending moment capacity of the repaired column was 707.8 kip-ft, and the governing failure mode would be rupture of the longitudinal CFRP fibers in tension.

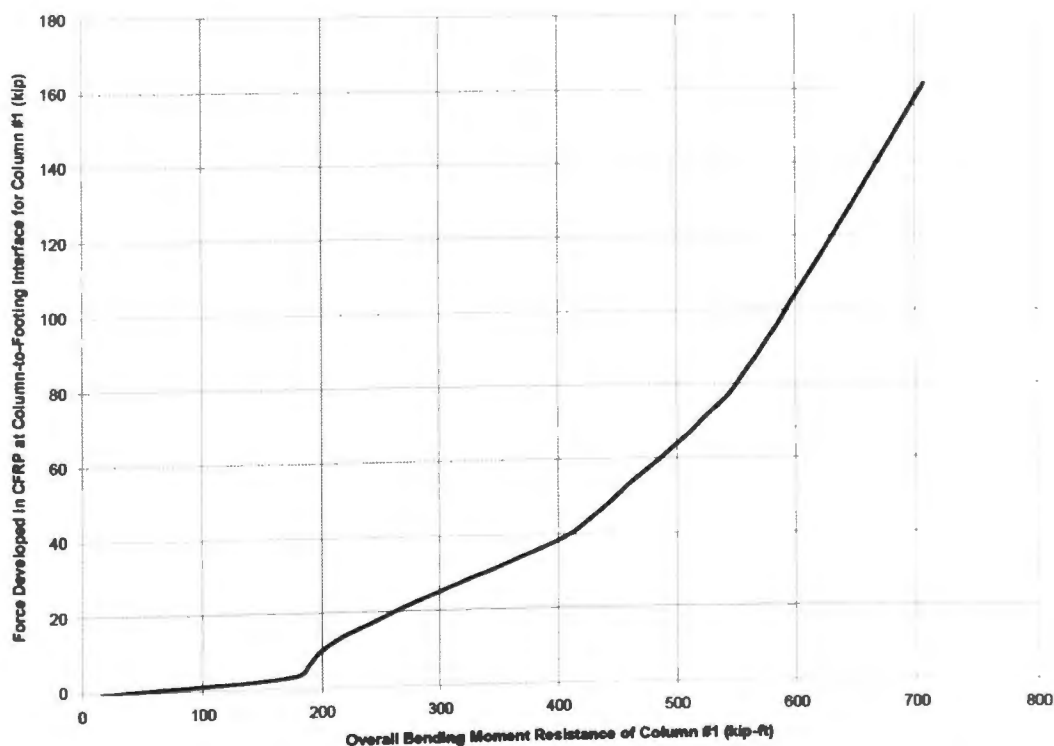


Figure 5.19. Prediction of Force in CFRP at Column-to-Footing Interface of Column #1

From this analysis, it can be determined that the theoretical forces developed in the longitudinal CFRP at the peak loads of 535.7 kip-ft and -420.8 kip-ft are 74.6 kips and 42.5 kips, respectively. Both of these loads are in excess of the predicted maximum force $F_{F,y}$ of 40.8 kips capable of being developed in the longitudinal CFRP at the

column-to-footing interface when the failure mode is yielding of the anchorage plate. However, inspection of the levels of strain measured on the anchorage plate does not indicate that yielding of the plate occurred. The envelopes of the strains measured in the anchorage plate by the strain gauges in line with the anchor rods are plotted in Figure 5.20. Compressive strains in the anchorage plate, which are reported as negative strains, indicate that the longitudinal CFRP on that side of the column was being stressed in tension.

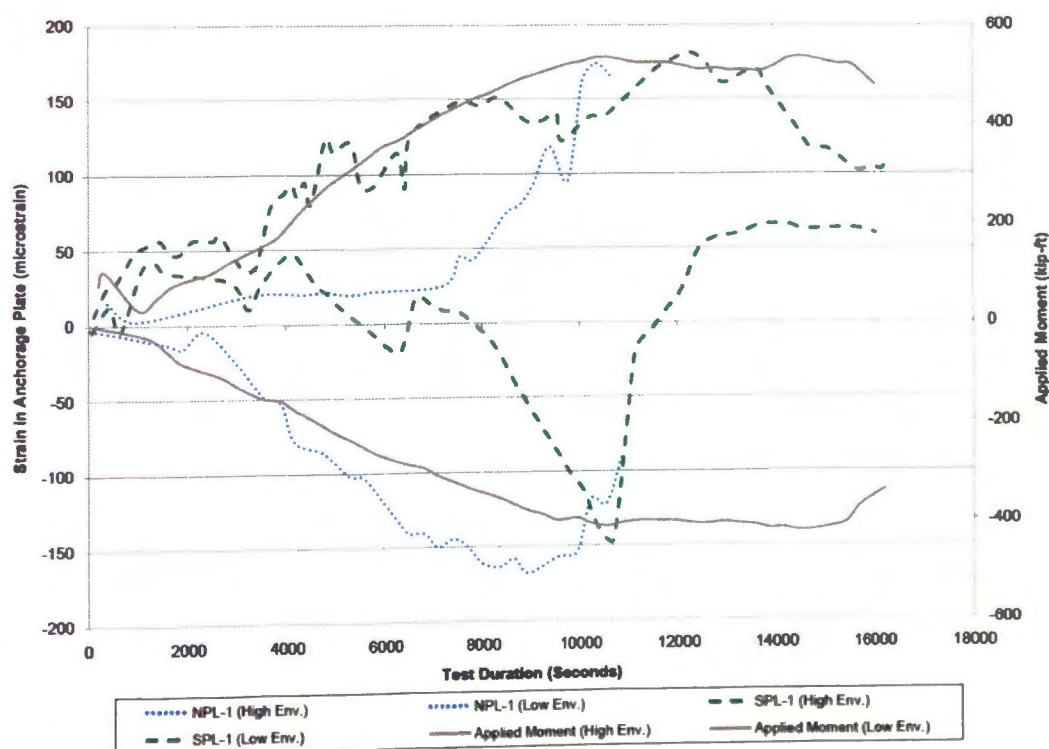


Figure 5.20. Strains Measured in Anchorage Plate for Column #1

Based on these data, the strains reached in the anchorage plate at the time of failure of the novel anchorage system were -168 microstrain on the north anchorage and -146 microstrain on the south anchorage. These values correspond to 13.5% and 11.7% of the plate's yield strain for the north and south plates, respectively. The high levels of tensile strain in the anchorage plate are not particularly of interest since they occurred during the half of the loading cycle in which the longitudinal CFRP was in compression. These tensile strains are most likely due to the bearing of the column onto the anchorage

plate during the compression cycle due to poor detailing of the anchorage plate, as previously discussed. This is supported by the lack of these high tensile strains for Column #2 and #3 after the detailing problem was addressed.

An additional discrepancy between the expected and actual behavior of Column #1 with regard to overall performance and the novel anchorage system's performance stems from the column's ability to continue resisting additional applied bending moments after the tensile failure of the anchor rods. Since the longitudinal CFRP is not capable of improving the column's flexural capacity without some form of anchorage at the column-to-footing interface, the novel anchorage system must have been capable of providing anchorage to the longitudinal CFRP after the tensile failure of the anchor rods. This evidence supports the claim that the assumed force transfer mechanism from longitudinal CFRP to the novel anchorage system shown in Figure 4.9 is incorrect. Thus, a secondary force transfer mechanism must have occurred after the anchor rods stopped carrying tensile forces.

Because pull-out of the anchor rods was not observed, it is possible that while they lost their ability to carry tensile loads, they were still capable of transferring shear loads to the footing. Additionally, the CFRP bonded to the footing could provide some vertical anchorage forces by means of the pull-off bond strength, which was determined using the testing procedure prescribed by *ASTM D7234* and described in Section 4.4.1. A conceptual schematic of this secondary force transfer mechanism is shown in Figure 5.21. However, due to the complexity of these reactions and the lack of available instrumentation, it is not possible to determine or verify the distribution or locations or the reactions.

While a limited amount of experimental data exist to verify the experimental performance of the novel anchorage, the following conclusions can be drawn about its performance during the testing of Column #1:

1. Tensile failure of the anchor rods occurred under measured loads that were significantly less than expected. This may have been due to the tensile force interaction with unexpected shear loads that were induced on the anchor rods, cracking of the concrete in the footing, or a combination of both.

2. Poor detailing of the novel anchorage system resulted in additional shear loads being transferred to the anchor rods and contributed to the ultimate failure of the column.
3. Measured strains in the anchorage plate resulting from bending of the plate were lower than expected, indicating that the assumed force transfer mechanism between the longitudinal CFRP and the novel anchorage system was incorrect.
4. A secondary force transfer mechanism must have existed that allowed the longitudinal CFRP to contribute to the column's flexural capacity after tensile failure of the anchor rods.

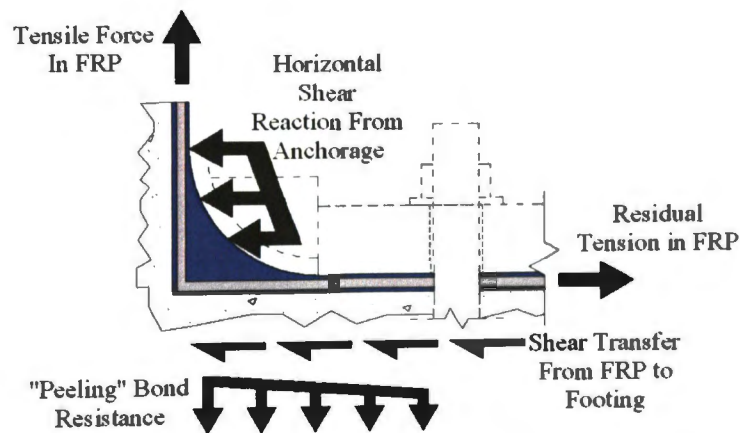


Figure 5.21. Possible Secondary Force Transfer of Novel Anchorage (Conceptual)

5.3.1.2 Behavior of Novel Anchorage for Columns #2 and #3. Since no failures of the novel anchorage systems were observed during the testing of Columns #2 and #3, the analysis of their behavior is limited. Additionally, no load cells were used to monitor the tensile forces developed in the anchor rods during the testing of Columns #2 and #3. The only instrumentation available to evaluate the performance of the novel anchorage system for the tests of Columns #2 and #3 were the strain gauges mounted to the top surface of the anchorage plate, as shown in Figure 4.28. The plots shown in Figures 5.22, 5.23, and 5.24 present the measured strain in the anchorage plates used for the repair of Columns #2 and #3.

Only two of the six strain gauges applied to the anchorage plate for the testing of Column #2 functioned properly, and those two gauges read significantly different levels of strain. Strain gauge NPL-2 measured a peak strain of -214 microstrain, corresponding to 17% of yield strain. Strain gauge SPL-3 measured a peak strain of -76 microstrain, corresponding to 6% of yield strain. While no experimental data exist to explain the large differences in measured strain between the two gauges, it is possible that the torsion loading may be responsible. No visible or audible failure of the anchorage system was noted during testing, and review of the strain gauge data for Column #2 does not necessarily show a clearly defined point of failure.

Strain gauges on the north anchorage plate used for the repair of Column #3 measured peak strains in strain gauges NPL-1, NPL-2, and NPL-3 of -129 microstrain (10% of yield), -130 microstrain (10% of yield), and -50 microstrain (4% of yield), respectively. Strain gauges on the south anchorage plate used for the repair of Column #3 measured peak strains in strain gauges SPL-1 and SPL-3 of -107 microstrain (9% of yield) and -222 microstrain (18% of yield). As with Column #2, no visible or audible failure of either novel anchorage system was noted during the testing of Column #3. However, a significant reduction in measured strain occurred on the north anchorage plate at a time of about 17700 seconds into the test and under a bending moment of 452.0 kip-ft and on the south anchorage plate at a time of about 21800 seconds into the test under a bending moment of -536.9 kip-ft. Based on observations from Column #1, it is reasonable to assume the anchor rods failed, losing their tensile capacity after these loads.

As was observed in the results of Column #1, the bending moment in the anchorage plate induced by the reaction of the longitudinal FRP onto the novel anchorage was far from being large enough to cause yielding of the anchorage plate. Therefore, failure of Column #3 must have occurred in the anchor rods. As previously mentioned, no load cells were included in the instrumentation of Columns #2 and #3. However, a relationship between the measured strain in the anchorage plate and the tensile forces measured in the anchor rods was determined using data from Column #1. This relationship is detailed in Appendix C. Predicted anchor rod forces from strain gauge data are plotted in Figure 5.25 and compared with the measured forces for the load cells during the testing of Column #1.

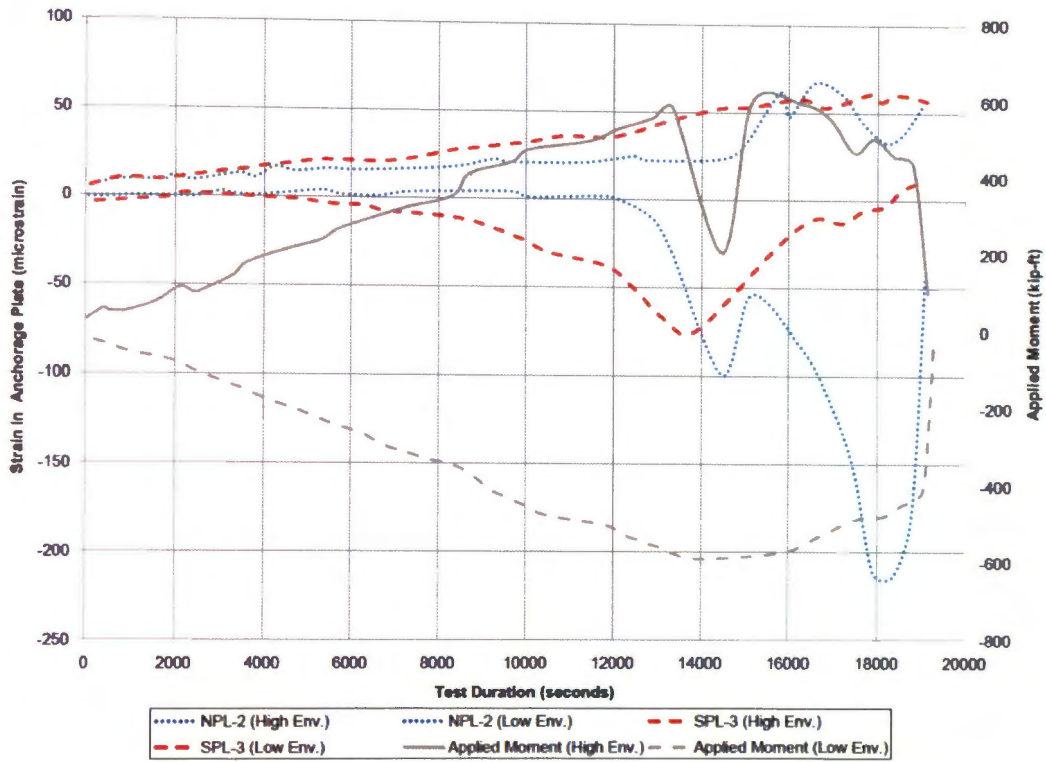


Figure 5.22. Strains Measured on Anchorage Plates for Column #2

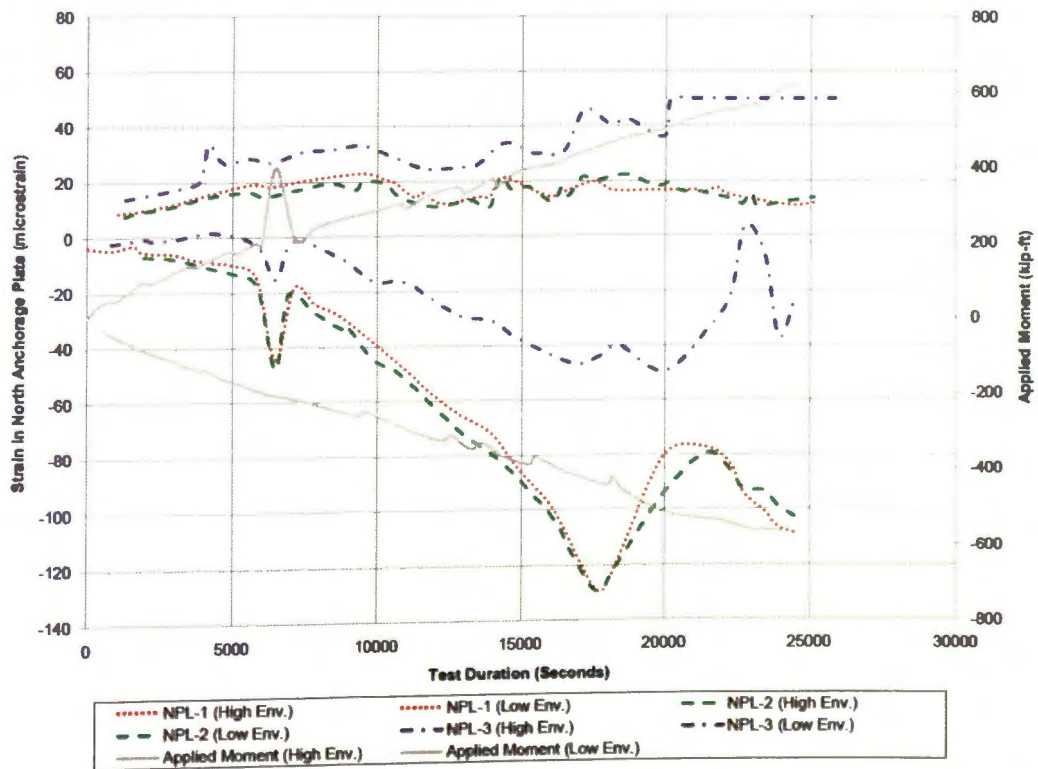


Figure 5.23. Strains Measured on North Anchorage Plate for Column #3

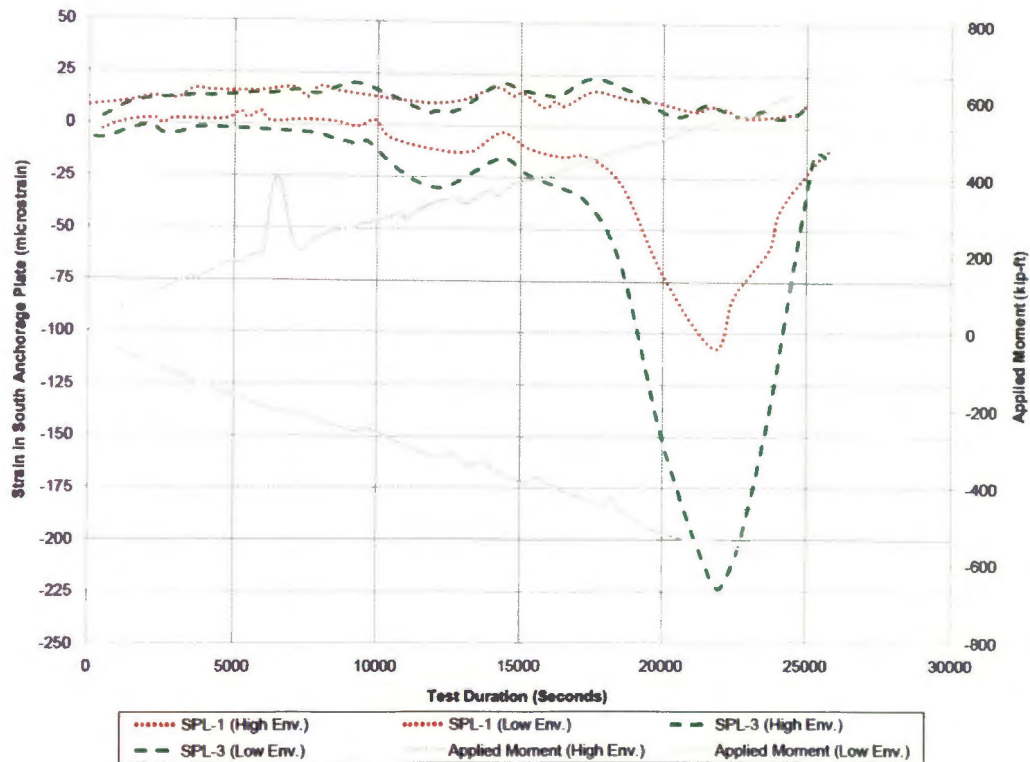


Figure 5.24. Strains Measured on South Anchorage Plate for Column #3

It is clear from Figure 5.25 that the peak anchor rod loads predicted from the strain gauge data match well with the actual load cell readings. Thus, the model can be used to estimate the tensile forces in the anchor rods for Columns #2 and #3. Figure 5.26 and Figure 5.27 show the predicted tensile forces in a single anchor rod for Columns #2 and #3, assuming a pre-applied force of 550 lbs resulting from initial tightening of the nut on the anchor rod.

While it appears that the anchor rods failed due to loss of their tensile capacity in Column #3, the loads in the anchor rods at the presumed point of failure are significantly less than the calculated anchor rod capacities. Additionally, no bearing of the column face on the anchorage plate was observed which would indicate that no additional shear was induced on the anchor rods. No significant cracking in the footing that would reduce the capacity of the anchor rods was observed during the test of Column #3, although it is possible that cracks developed in the concrete that were not visible during testing. Finally, no rupture of the longitudinal CFRP occurred during the testing of Column #3. Therefore, the cause of failure of the anchor rods used on Column #3 is not apparent.

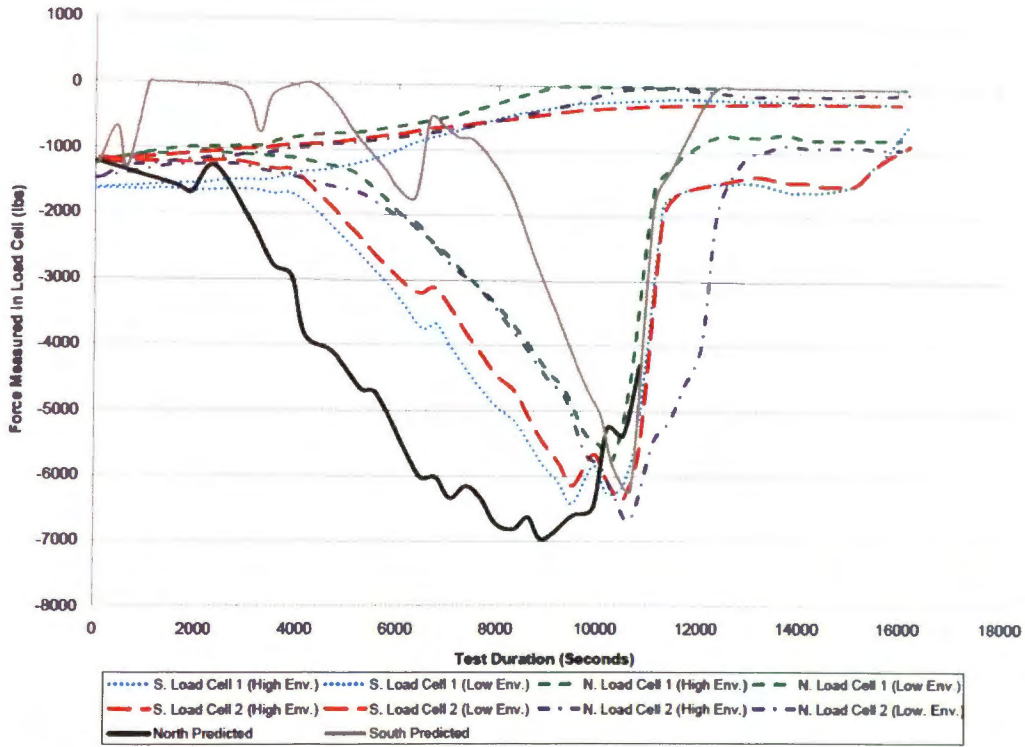


Figure 5.25. Prediction of Anchor Rod Loads From Strain Gauge Data for Column #1

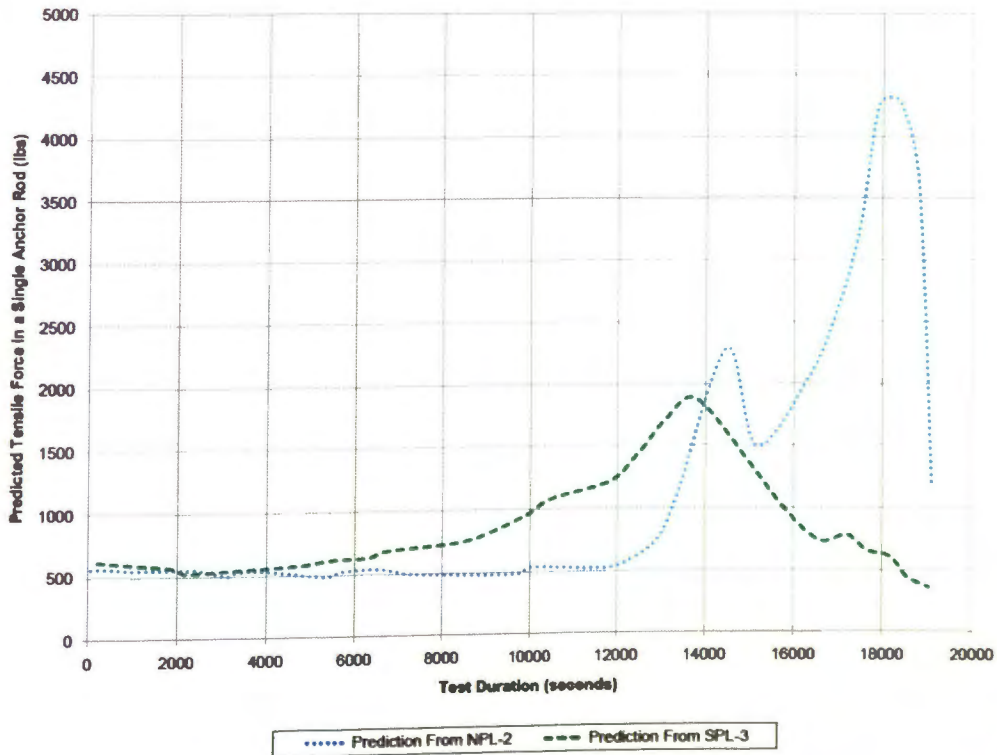


Figure 5.26. Prediction of Anchor Rod Loads From Strain Gauge Data for Column #2

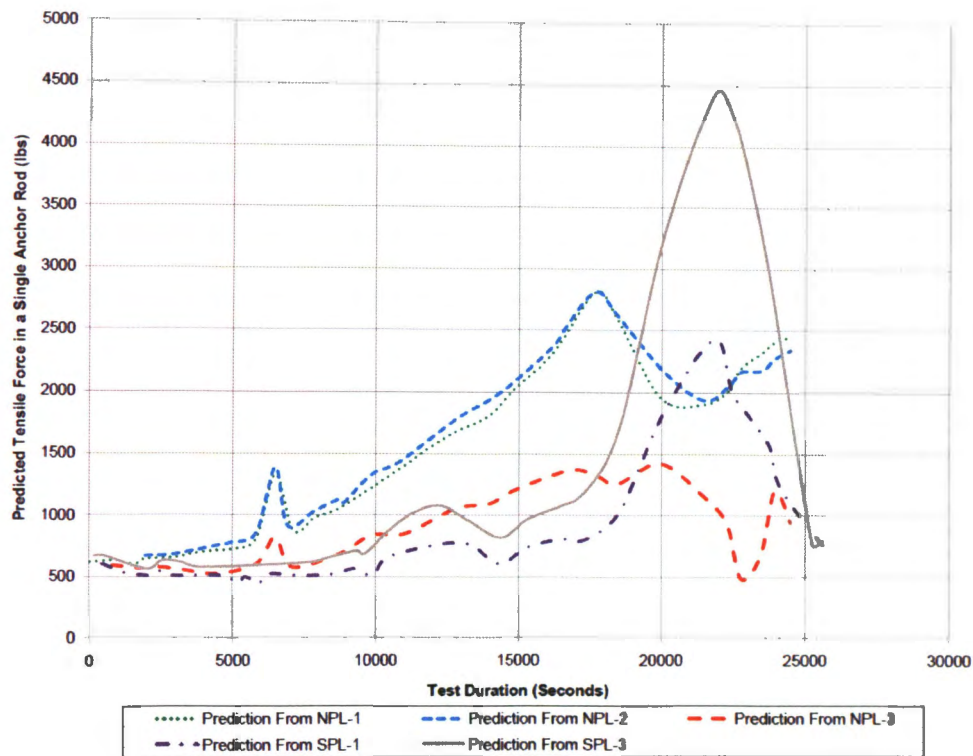


Figure 5.27. Prediction of Anchor Rod Loads From Strain Gauge Data for Column #3

The strains measured in the longitudinal CFRP during the testing of Columns #2 and #3 did not provide sufficient information that could be used to determine the tensile force developed in the CFRP at the column-to-footing interface. As mentioned in the discussion of the behavior of Column #1, the longitudinally-oriented strain gauges were likely to be influenced by local behavior of the CFRP. Therefore, it is difficult to evaluate the force transfer mechanism from the longitudinal CFRP at the column-to-footing interface to the novel anchorage system. Measurements from the longitudinally-oriented strain gauges installed on Columns #2 and #3 are plotted as envelopes in Figures 5.28, 5.29, 5.30, and 5.31.

The behavior of Column #3 is also similar to that of Column #1 in that after the anchor rods failed by losing their tensile capacity, the column was able to resist additional bending moment. This may have been due to a secondary force transfer mechanism such as the one shown in Figure 5.21; however, since Column #3 did not contain any ruptured bars, its flexural capacity was not as severely diminished before the inclusion of longitudinal CFRP.

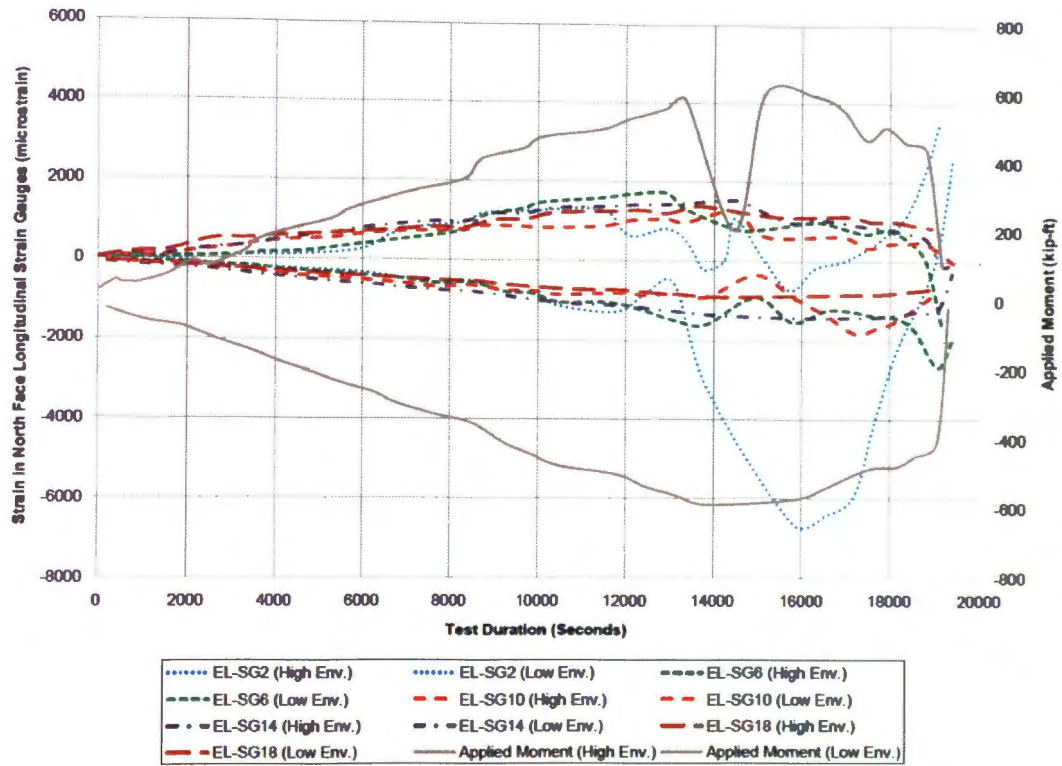


Figure 5.28. Longitudinal Strain Measurement in North Face of Column #2

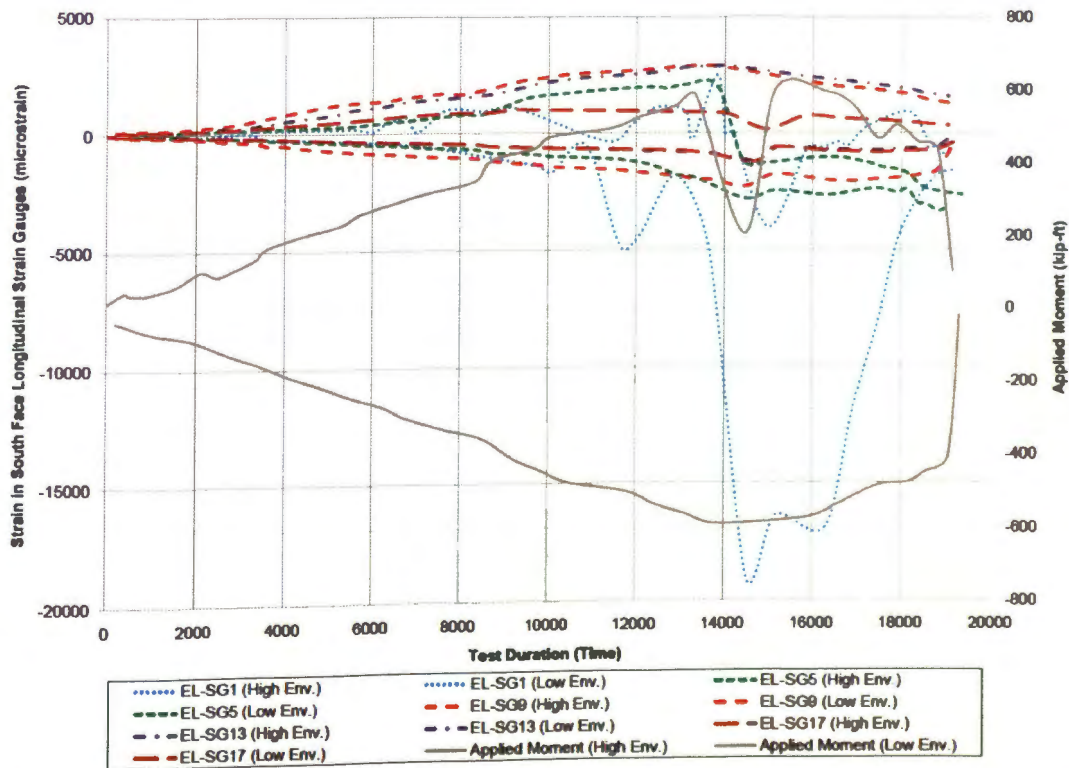


Figure 5.29. Longitudinal Strain Measurement in South Face of Column #2

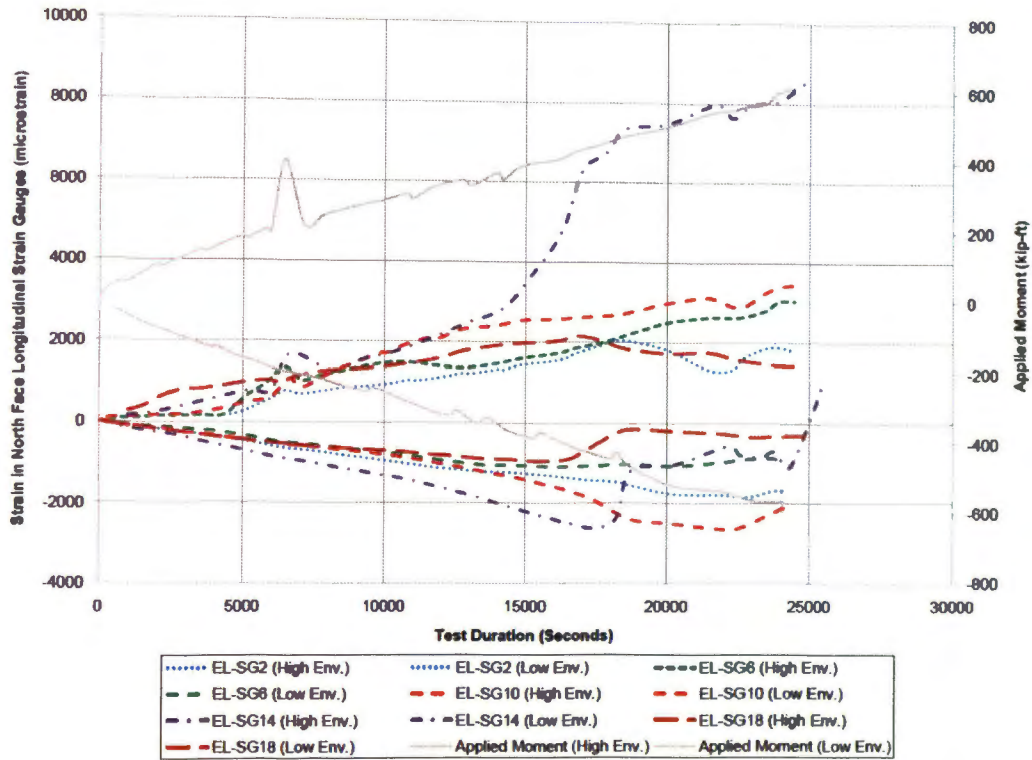


Figure 5.30. Longitudinal Strain Measurement in North Face of Column #3

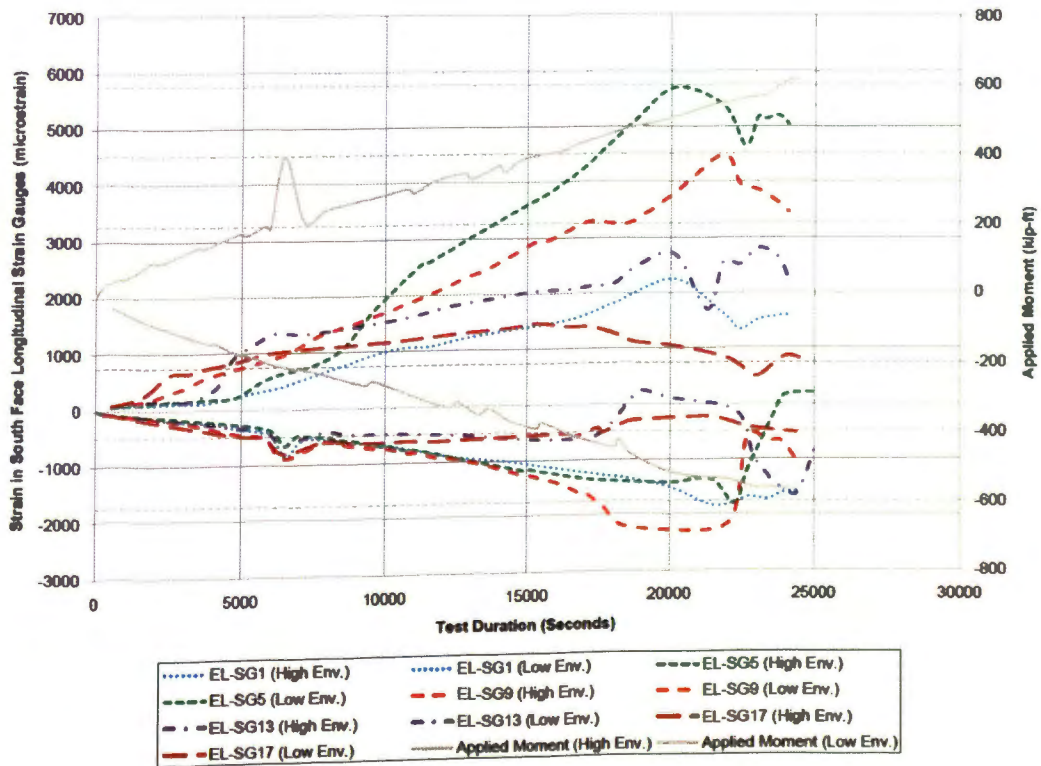


Figure 5.31. Longitudinal Strain Measurement in South Face of Column #3

5.3.1.3 Summary of Novel Anchorage Behavior. It is apparent from the behavior of the novel anchorage system used on Columns #1, #2, and #3 that the behavioral model in Figure 4.9 used for the design of the anchorage plate and anchor rods was not accurate. Designing the anchorage using this model resulted in an overdesign of the plate thickness. Additionally, the early failure of the anchor rods in Column #1 and #3 suggests that unexpected shear loads were transferred from the column, through the novel anchorage, and into the anchor rods. The effects of improper detailing were also observed, as placement of the novel anchorage in Column #1 was a factor in causing the ultimate failure of the longitudinal CFRP.

While a determination of the force in the longitudinal CFRP at the column-to-footing interface would have been advantageous in evaluating the force transfer mechanism from the CFRP to the novel anchorage, the instrumentation scheme of the column did not facilitate the acquisition of such data. Therefore, only general conclusions about the anchorage behavior can be drawn from the test results.

The overall contribution of the novel anchorage to the moment capacity of the repaired columns can be determined by finding the induced tensile reaction in the anchor rods and multiplying that force by the length of its moment arm about the centerline of the column. A free-body diagram showing this contribution is depicted in Figure 5.32.

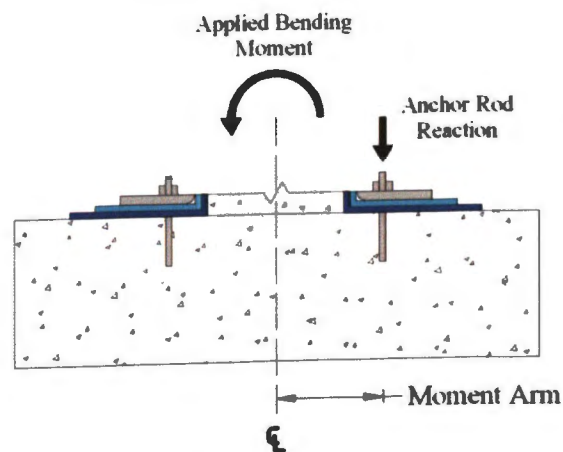


Figure 5.32. Free-Body Diagram of Anchor Rod Contribution to Moment Capacity

For all three columns, the induced tensile reaction is equal to the tensile force in the anchor rods measured or predicted minus the pre-tightening tension load of 550 lbs.

Since the tensile force in each anchor rod was not explicitly measured during testing, this force is taken as the average of the forces measured in the load cells for each side of Column #1 and the average of the predicted forces for Columns #2 and #3. The anchor rods on the north side of Column #1 provided a maximum contribution to the column's moment resistance of 12.5 kip-ft during the positive-direction loading, while the rods on the south side of Column #1 provided a maximum contribution of 14.4 kip-ft during negative-direction loading. The anchor rods on the north side of Column #2 provided a maximum contribution to the column's moment resistance of 20.9 kip-ft during the positive-direction loading, while the rods on the south side of Column #1 provided a maximum contribution of 7.4 kip-ft during negative-direction loading. Finally, the anchor rods on the north side of Column #3 provided a maximum contribution to the column's moment resistance of 10.1 kip-ft during the positive-direction loading, while the rods on the south side of Column #1 provided a maximum contribution of 16.1 kip-ft during negative-direction loading. These contributions represent only a few percent of the total moment resistance of the repaired column; therefore, an additional method of moment transfer must have been present to provide the flexural resistance that allowed the repaired columns to perform as they did.

5.3.2. U-Anchors. There was no instrumentation present on Columns #2 and #3 that allowed for an evaluation of the U-Anchor performance. However, after the testing was completed, the failed U-Anchors were removed from their groove in the concrete for inspection. The U-Anchors on both Column #2 and #3 had failed at some point during testing as discussed in Section 5.2.1. When removed from their groove, each U-Anchor was found to have failed via breakout of the concrete substrate in the groove. A layer of concrete between 1/8 in. and 1/4 in. remained bonded to the walls of the U-Anchor. A photo of a U-Anchor after removal from its groove is shown in Figure 5.33.

5.3.3. Transverse Wrapping Anchorage. The transverse wrapping anchorage provided by the transverse CFRP reinforcement was effective in preventing debonding of the longitudinal CFRP at the end of the sheet bonded to the column face. While evaluation of the transverse wrapping was not a priority of this study, it is useful to note that for each column, no debonding or slipping failures of the longitudinal CFRP were observed at the end of the longitudinal CFRP sheet opposite the novel anchorage system.



Figure 5.33. Failed U-Anchor After Removal From Groove

5.4. DESIGN RECOMMENDATIONS

Since no definite conclusions could be made regarding the behavior of the load transfer mechanism from longitudinal CFRP to the novel anchorage plate, it is not possible to recommend specific behavioral design guidelines for use of the novel anchorage. However, the small amount of bending that took place in the anchorage plate indicates that the vertical force transferred from the longitudinal CFRP to the anchorage was overestimated. Additionally, the failure of the anchor rods under tensile load levels that were smaller than expected may indicate that unexpected shear forces may have been present. Therefore, one possible change to the assumed behavior model in Figure 4.9 is to reduce the angle of action, measured from a horizontal axis, that F_F follows. This will, in turn, reduce both the plate size and required tensile strength of the anchor rods. An additional force transfer mechanism should also be considered since the contribution of the anchor rods to the overall flexural capacity of the column was minimal. These additional forces may be due to the novel anchorage's ability to resist a debonding force orthogonal to the plane of the column, or due to the CFRP's bond strength on the footing. Possible modifications to the assumed behavioral model of the novel anchorage system are presented in Figure 5.34.

Additionally, the possible secondary force transfer mechanism discussed in Section 5.3.1.1 should be evaluated to determine its applicability to the behavior of the novel anchorage system after the failure of the anchor rods.

When selecting anchor rods to fasten the anchorage plate to the footing, only those anchors that are certified for use in cracked concrete should be chosen. While the anchor rods were placed a distance away from the column to avoid having to place them in cracked concrete, it was observed that the concrete surrounding the embedded anchor rods in at least one of the three column tests had cracked rather significantly.

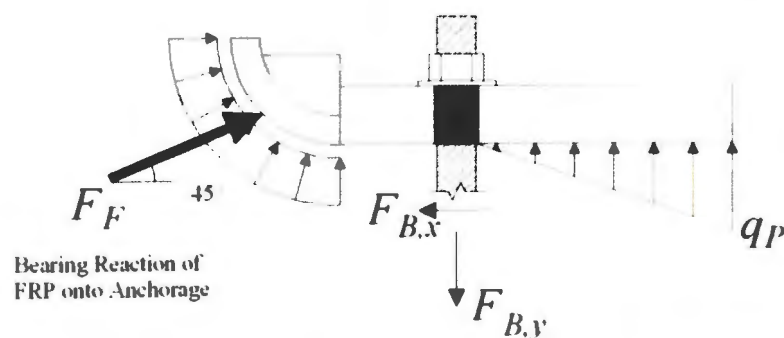


Figure 5.34. Possible Modifications to Assumed Behavioral Model for Novel Anchorage

Future construction of this novel anchorage system should take into account the possibility for deformation of the column when designing the details of the anchorage plate placement. The novel anchorage should be placed at least 1/4 in. away from the face of the structural member to avoid bearing of the column face and FRP onto the anchorage as the column bends and dilates. Additionally, instead of including a quarter-pipe section on the end of the anchorage plate, a half-pipe section should be included to avoid bearing of the CFRP onto the sharp corner of the quarter pipe section. While it is not necessary to use the full half-pipe section, simply using the half-pipe section should allow for ease of fabrication. Some method should be taken to reduce the potential for corrosion of the novel anchorage system. The entirety of the anchorage system should be fabricated from stainless steel, galvanized, or encapsulated in an innovative way. Similarly, a non-corrosive barrier such as a sheet of GFRP should be installed between the novel anchorage and CFRP to prevent contact of the two conductive materials.

Finally, since the portion of the CFRP that was bonded to the footing seemed to perform well and provide an additional method of force transfer from the CFRP to the footing, the design procedure describe in Section 4.6.3 used in for determining the length of CFRP to bond to the footing should be used. While this approach uses a rather conservative effective bond length model, the critical nature of Type III anchorage systems warrants such conservatism. The design recommendations made in this section are summarized in Figure 5.35.

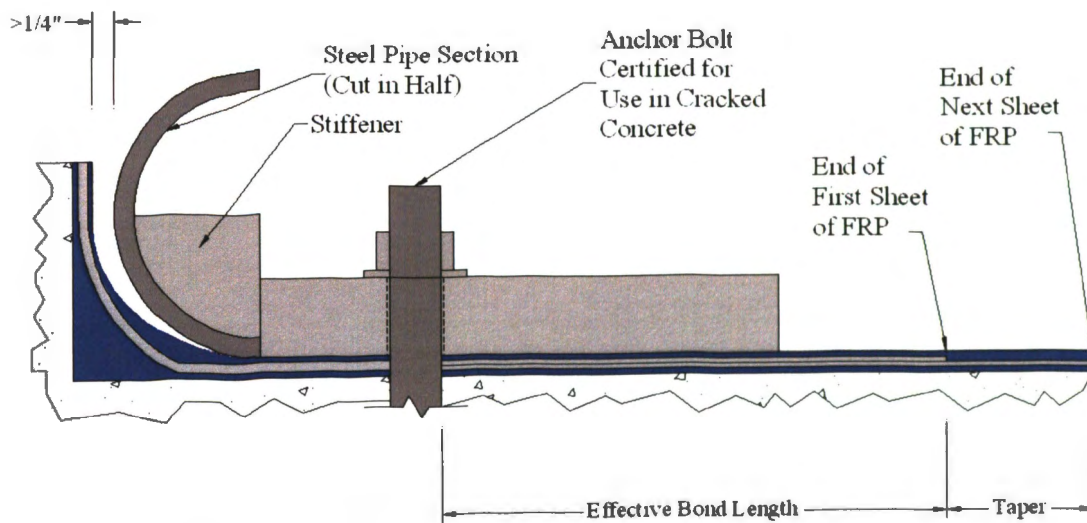


Figure 5.35. Design Recommendations Summary for Novel Anchorage

6. SUMMARY AND CONCLUSIONS

6.1. SUMMARY OF RESEARCH PERFORMED

Externally-bonded FRP has been used for the strengthening of reinforced concrete elements for several decades. Despite promising developments in FRP research and widespread field implementation, the challenge of anchoring FRP to achieve higher design strengths has not been addressed sufficiently. Existing anchorage research has been sparse and very few researchers have taken a systematic approach to evaluating new anchorage systems. Additionally, the selection of an anchorage device for a particular application is difficult due to the lack of centralization of anchorage system information, especially anchorage system design procedures.

In an attempt to facilitate better understanding of anchorage system behavior and applicable testing procedures, three anchorage system categories were developed based on the intended application of the system and its behavior. This categorization system should aid in the selection of an anchorage system for a particular application, as well as promote systematic testing of FRP anchorage systems. Existing anchorage devices reported upon in literature were categorized according to this new system. The studies in which independent anchorage testing was performed were focused upon, and their testing programs related to the applicable anchorage categories.

In the experimental portion of this thesis, several anchorage systems were chosen for use in a project involving the “rapid repair” of severely-damaged bridge columns subjected to combined loading effects. The main focus of this thesis was the evaluation of a novel anchorage system used to provide Type III anchorage to the longitudinal CFRP at the column-to-footing interface. Test results were used to evaluate the behavior of this device and to provide design recommendations for future use.

Based upon the information contained in this thesis, several conclusions have been made and are presented in Section 6.2. Details regarding ongoing studies related to this project are discussed in Section 6.3. Finally, recommendations are given for future research regarding general FRP anchorage systems as well as the novel anchorage system developed in this study.

6.2. CONCLUSIONS

1. Based on the review of anchorage systems in Chapter 2, it is apparent that research on anchorage systems for externally-bonded FRP is limited. While many different types of anchorage systems have been tested and evaluated, design procedures based that have been verified experimentally are essentially nonexistent for most anchorage system types. Additionally, existing design guidelines such as *ACI 440.2R-08* provide minimal information regarding anchorage system use, selection, behavior, or design.
2. The anchorage categorization system developed in Chapter 3 should help advance future FRP anchorage research by promoting a better understanding of anchorage system behavior, aiding in the selection of an anchorage system for a particular FRP strengthening application, and specifying proper testing procedures for certain types and applications of anchorage systems.
3. The novel anchorage system tested in the experimental program did not perform as expected. The force transfer mechanism between the CFRP sheet at the column-to-footing interface did not transfer load to the anchor rods as assumed in the original behavioral model. A different method of force transfer must have occurred in order for the CFRP to contribute to the column's flexural capacity.
4. After failure of the anchor rods in the novel anchorage system occurred during the testing of Column #1 and #3, the repaired columns continued to resist additional bending moment. This indicates that the CFRP was still anchored at the column-to-footing interface despite the failure of the anchor rods. Therefore, a secondary force transfer mechanism must have been present to resist load after the failure of the anchor rods.
5. Improper detailing of the novel anchorage system used for the repair of Column #1 contributed to the ultimate failure of the repaired column by longitudinal CFRP rupture. The rupture was induced by bearing of the column face on the quarter-pipe portion of the novel anchorage. This problem was addressed by leaving a small gap between the novel anchorage and the column face during the repairs of Columns #2 and #3. Because of this change, no problems due to improper detailing were observed in Columns #2 or #3. Future detailing of the

novel anchorage at the column-to-footing interface should be performed similar to the anchorage detailing for Columns #2 and #3.

6. Despite the inclusion of a significant amount of instrumentation during testing of the repaired columns, only a small amount of the acquired data can be used to evaluate the performance of the novel anchorage system. Therefore, it was not possible to provide specific design instructions for the novel anchorage system. Independent tests of the novel anchorage system including as few variables as possible are needed to evaluate the basic behavior of the anchorage plate.

6.3. ONGOING STUDIES

As previously mentioned, the anchorage evaluation contained in this thesis was performed as a part of a larger study entitled “Rapid Repair of Severely Damaged Columns Under Combined Loading Effects” and funded by the University of Missouri Research Board. Testing of the six repaired columns mentioned in this thesis constituted the entirety of the experimental work involved in this project. These tests were performed between September 2010 and March 2011. At the time of the publication of this thesis, experimental data obtained during the tests were being analyzed in order to address the objectives stated in Section 4.3 of this thesis.

6.4. RECOMMENDATIONS FOR FUTURE RESEARCH

Additional research on anchorage systems for externally bonded FRP is needed to facilitate implementation of anchorage systems into readily available design guidelines for strengthening reinforced concrete structures with FRP. Existing anchorage systems that show promise for use in field applications should be scrutinized under both independent testing and representative testing. Independent testing should be performed systematically and should include a minimal number of variables so that the most basic performance of the anchorage systems can be evaluated. Ideally, application-specific representative testing should follow independent testing so that the contribution of the anchorage system to the overall FRP strengthening scheme can be evaluated. Representative testing should also allow for effects due to scale and detailing to be evaluating. Using a systematic approach similar to the one shown in Figure 3.8 will

allow for design guidelines to be published in readily available documents such as journals, committee reports, and proprietary design specifications. Additionally, the creation of a communal database of containing test data and important variables has the potential to advance current state of knowledge on FRP anchorage systems.

Because the novel anchorage system mentioned in this thesis was tested only under large-scale representative testing, many complex variables affected its performance. Some of these variables were unexpected; therefore, the instrumentation necessary to evaluate their influence on the behavior of the novel anchorage was not included in the tests. Because the novel anchorage system provided a significant contribution to the restoration of strength in the repaired columns, it shows promise for use as a Type III anchorage system. As with any other anchorage system, future research should include independent testing of the novel anchorage system. The independent testing results can be verified with the representative testing results contained in this thesis, or with representative testing results for other Type III applications. Future use of the novel anchorage system should consider the design recommendations presented in Section 5.4.

APPENDIX A
PHOTOS OF DAMAGED COLUMNS PRIOR TO REPAIR

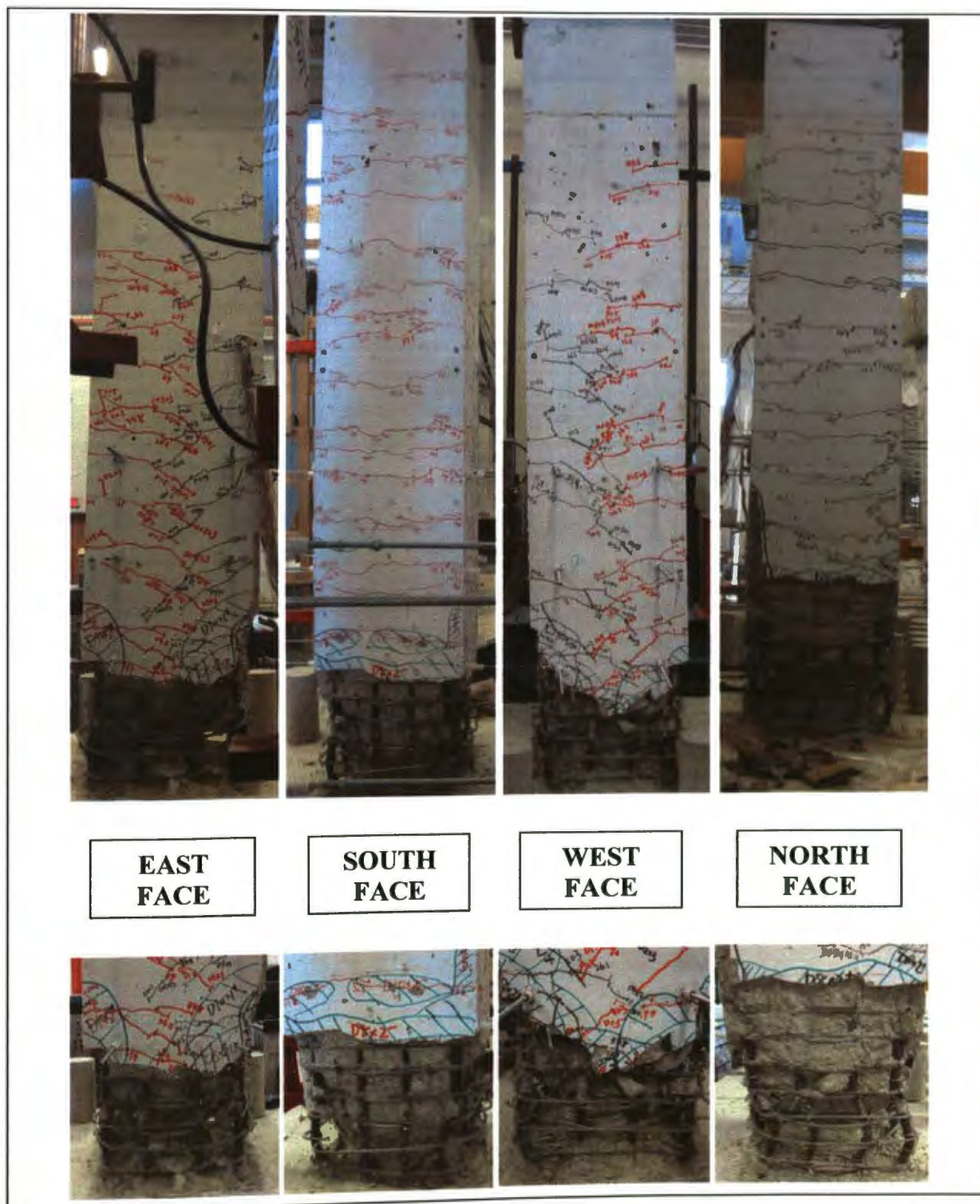


Figure A-1. Damage Photos of Column #1 Prior to Repair

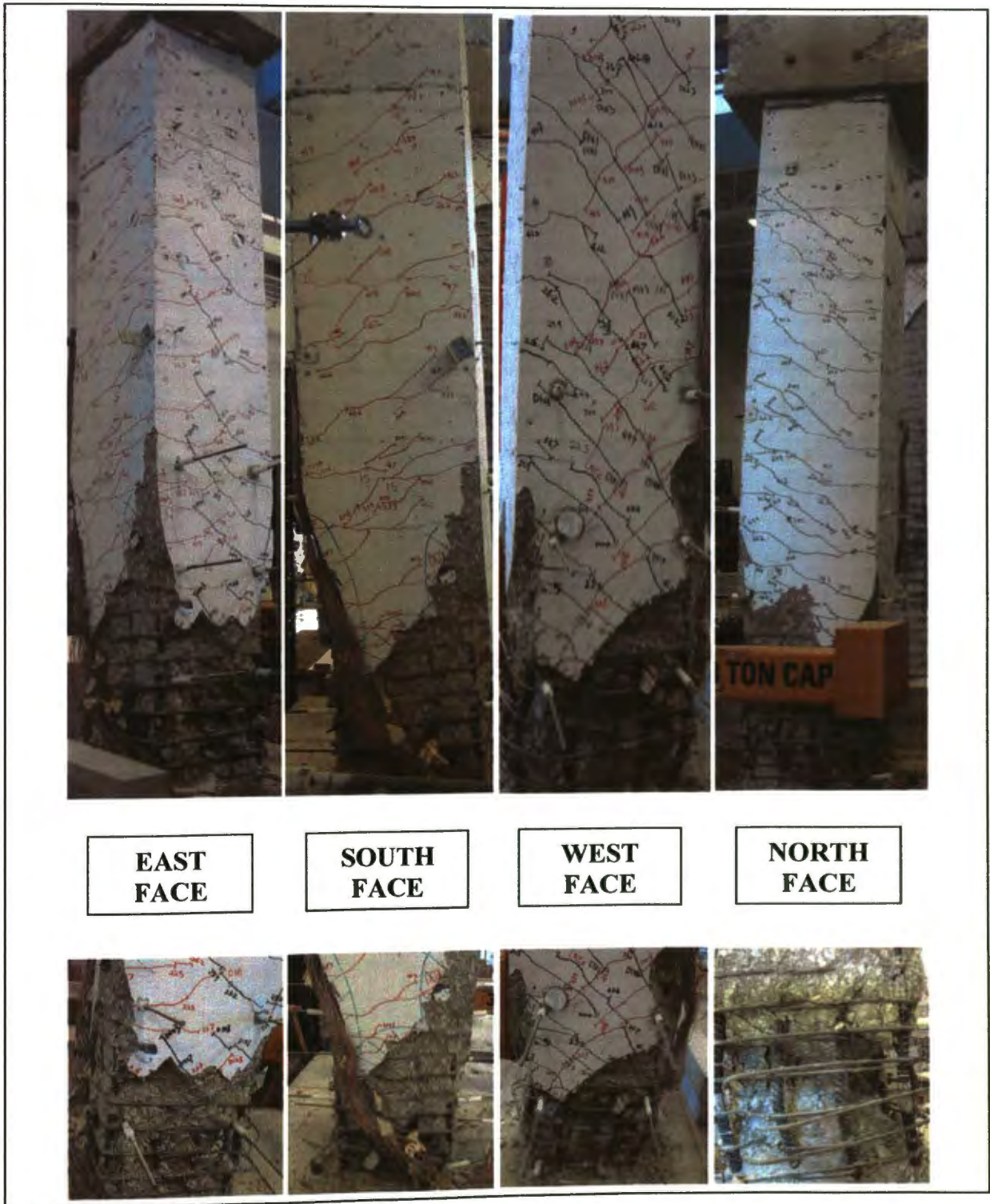


Figure A-2. Damage Photos of Column #2 Prior to Repair

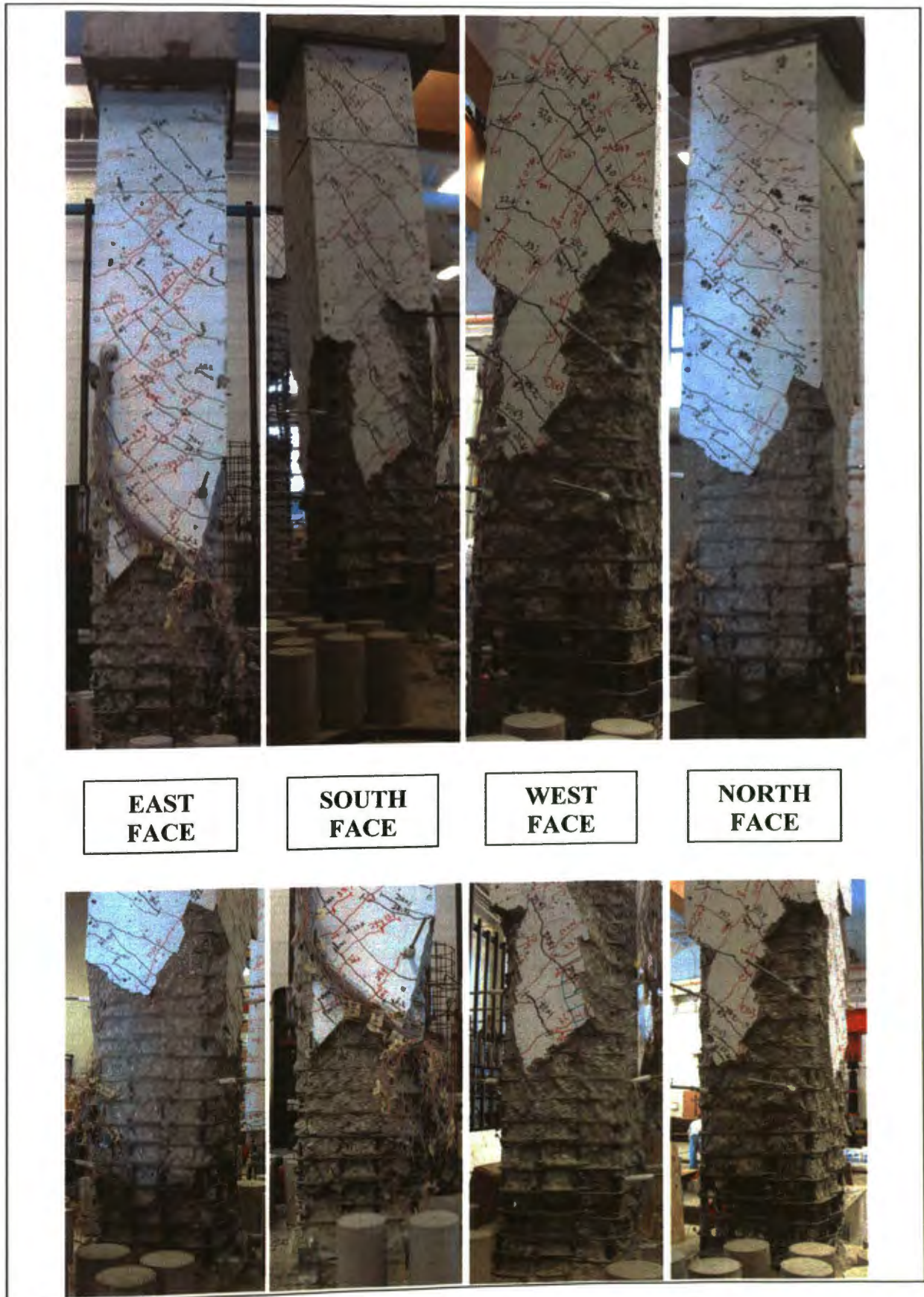


Figure A-3. Damage Photos of Column #3 Prior to Repair

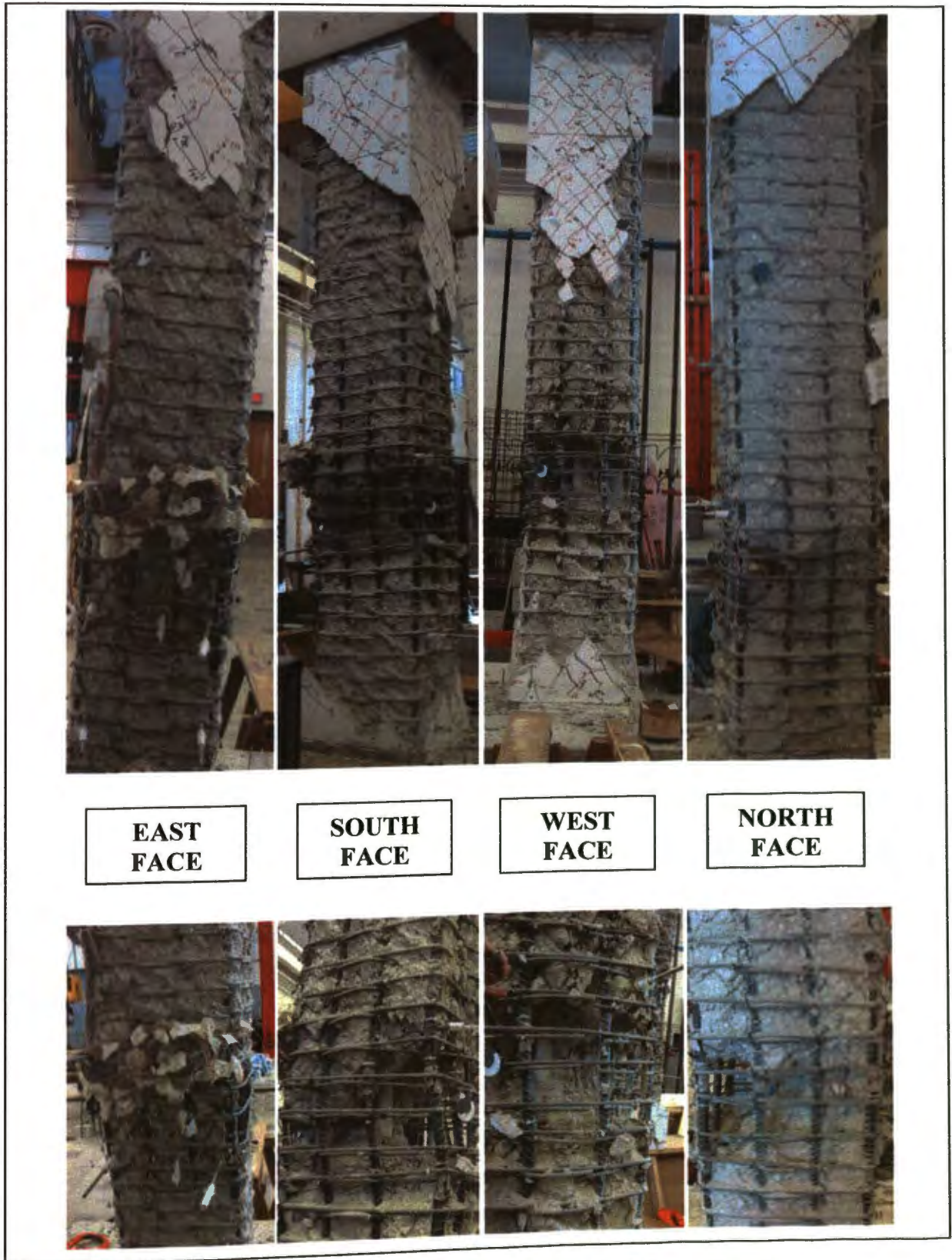


Figure A-4. Damage Photos of Column #4 Prior to Repair

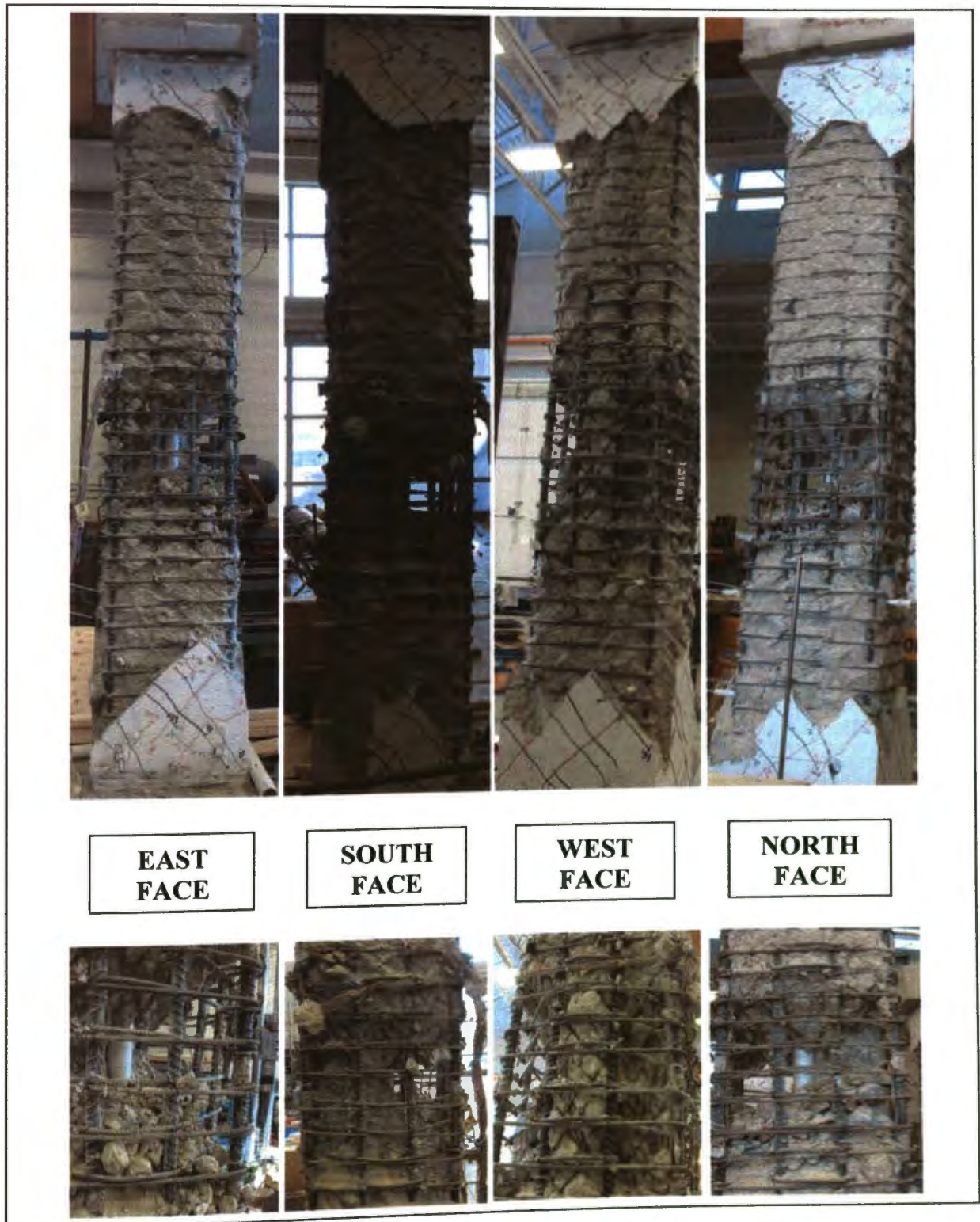


Figure A-5. Damage Photos of Column #5 Prior to Repair



Figure A-6. Damage Photos of Column #6 Prior to Repair

APPENDIX B
DESIGN AND STRENGTH CALCULATIONS FOR NOVEL ANCHORAGE

Two failure modes of the novel anchorage were considered: yielding of the anchorage plate along the centerline of the anchor rods; and failure of the anchor rods due to the interaction between shear and tensile forces. Because it was desired that the bolts should fail before the plate so that the novel anchorage system could be reused, initial design calculations were carried out with the intent of determining the maximum vertical force that could be carried in the anchored CFRP. Once this was determined, the required plate thickness could be calculated. Because the tests were being performed in a laboratory environment, all designs used a safety factor of 1.0.

Referring to the variables defined in Figure 4.9, the anchorage system would initially have the following properties:

$$d_T / 2 = 2.78 \text{ in.}$$

$$l_{P1} = 2.44 \text{ in.}$$

$$l_{P2} = 6.44 \text{ in.}$$

$$d_H = 1.13 \text{ in.}$$

These values were arrived upon for a combination of reasons, including material availability and constructability. Additionally, it was determined that four 1 in. nominal diameter *ASTM A 193 B7* anchor rods would be used to anchor the plate to the concrete along with the Hilti HIT-RE 500 Epoxy Adhesive Anchoring System. Embedment depth was selected as 9 in., which was less than the maximum embedment depth of anchors with a minimum spacing of 5.5 in. From Table 4.6, the concrete in Columns #1, #2, and #3 had a 28-day compressive strength in excess of 4000 psi. Since the Hilti Product Technical Guide (2008) only provides anchor capacities for 28-day concrete compressive strengths of 2000 psi and 4000 psi, the 4000 psi capacities would be used to determine the anchor strengths. From the Hilti Product Technical guide, the ultimate bond/concrete capacities of one anchor were, before spacing reductions:

$$N_n \text{ (no spacing reduction)} = 69,645 \text{ lb}$$

$$V_n \text{ (no spacing reduction)} = 95,160 \text{ lb}$$

Since the anchors were to be spaced at a minimum spacing of 5.5 in., this required the above values to be reduced by f_A , the spacing load adjustment factor for tension and shear loads. The Hilti Product Technical guide contained a figure that was used to

determine f_A . Therefore, the ultimate capacities for each anchor rod for independent tensile and shear forces were determined to be:

$$N_n = 50,710 \text{ lb}$$

$$V_n = 44,180 \text{ lb}$$

It is important to note that V_n had to be further reduced from its ultimate bond/concrete capacity in shear since the ultimate shear strength of the *ASTM A193 B7* steel rods controlled the design. Because both shear and tensile loads would be present on the anchors, their interaction must be considered. Section RD.7 of *ACI 318-08* gives the following equation for shear-tension interaction:

$$\left(\frac{N_{ua}}{N_n}\right)^{5/3} + \left(\frac{V_{ua}}{V_n}\right)^{5/3} \leq 1.0$$

Based on Figure 4.9, N_{ua} for the novel anchorage should be equal to $F_{B,y}$ just as V_{ua} should be equal to $F_{B,x}$. In order to solve this equation, a relationship must be drawn between $F_{B,x}$ and $F_{B,y}$. Using equations [4.1], [4.2], and [4.3] and the given properties of the novel anchorage, the following relationships can be determined:

$$q_p = (0.157/\text{in})(F_{B,y})$$

$$F_{F,y} = 0.494F_{B,y}$$

$$F_{F,x} = F_{B,x} = F_{F,y}$$

Therefore, the following relationship can be established:

$$F_{B,x} = 0.494F_{B,y}$$

Substituting variables relevant to the novel anchorage into the interaction equation gives:

$$\left(\frac{F_{B,y}}{N_n}\right)^{5/3} + \left(\frac{F_{B,x}}{V_n}\right)^{5/3} \leq 1.0$$

Finally, substitutions can be made so that the above equation can be solved for $F_{B,y}$. In doing so, the values of N_n and V_n should be the full capacity of the set of four anchor rods used in each novel anchorage system. This gives:

$$\left(\frac{F_{B,y}}{202,840 \text{ lb}}\right)^{5/3} + 0.309\left(\frac{F_{B,y}}{176,720 \text{ lb}}\right)^{5/3} \leq 1.0$$

Solving this equation gives:

$$F_{B,y} \leq 166,559 \text{ lb}$$

Substitution the maximum permissible $F_{B,y}$ (shown above) into Equations [4.1], [4.2], and [4.3] results in:

$$F_{F,y} = F_{F,x} = F_{B,x} = 82,280 \text{ lb}$$

Neglecting any moment caused by the eccentricity of the $F_{F,x}$ force, the resulting moment about the centerline of the anchor rods is 475,990 in-lb. Bending stress in a member is given by the following equation, where M is the moment in the member at a given location, c is the distance from the neutral axis to the point of interest, and I is the moment of inertia about the centroidal axis:

$$\sigma_B = \frac{Mc}{I}$$

For the anchorage plate at the bolt centerline, I is calculated as follows, where t_{PL} is the plate thickness to be calculated:

$$I = \frac{1}{12} [22 \text{ in.} - (4 \times 1.13 \text{ in.})] t_{PL}^3$$

$$I = (1.458 \text{ in.}) t_{PL}^3$$

Because the neutral axis of the plate's cross section lies at half the plate thickness and it is necessary to determine the bending stress on the tensile face of the plate, c is equal to half of t_{PL} . It is also known that f_y , or the yield strength of the plate, is 36 ksi. Thus, substituting 36 ksi for σ_B and solving for t_{PL} should result in a plate that yields at the same time as anchor rod failure. Substituting these values gives:

$$36,000 \text{ psi} = \frac{(475,990 \text{ in-lb})(t_{PL} / 2)}{(1.458 \text{ in.})(t_{PL})^3}$$

Solving for t_{PL} gives:

$$t_{PL} = 2.1 \text{ in.}$$

Thus, the calculated plate thickness required to simultaneously allow for yielding of the plate about the centerline of the anchor rods and failure of the steel anchor rods due to the interaction of shear and tension is 2.1 in. However, after discussing the feasibility of obtaining a steel plate in excess of 2.1 in. and fabricating a novel anchorage system out of it, it was determined that a smaller thickness of plate should be used. The use of a

smaller thickness of plate was also justified because the research team was not convinced that such large loads could be transferred from the FRP to the novel anchorage. Therefore, a plate thickness of 1.5 in. was selected in part due to the aforementioned reasons, but also due to local material availability.

With a 1.5 in. thick plate, the moment that results in yielding of the plate is calculated as 236,200 in-lb. This results in the following maximum vertical reaction of the FRP onto the novel anchorage:

$$F_{F,y} = 40,830 \text{ lb}$$

Solving equations [4-1] and [4-2] gives:

$$q_p = (0.157 / \text{in})(F_{F,y}) = 6,410 \text{ lb}$$

$$F_{B,y} = F_{F,y} + \frac{1}{2}(q_p)(l_{P2}) = 61,470 \text{ lb}$$

Therefore, the maximum vertical force that could theoretically be developed and anchored in the longitudinal CFRP is 40.83 kips. This force would induce 40.83 kips of shear and 61.47 kips of tension to the group of four anchor rods.

APPENDIX C
DETERMINATION OF ANCHOR ROD FORCES FROM STRAIN GAUGE DATA

To determine the tensile force in the anchor rods based upon the measured strain in the anchorage plate, first determine the stress in the plate in the line of the anchor rods. Bending stress is given by

$$\sigma_B = \frac{Mc}{I}$$

The plate has a width of 22 in. and a height of 1.5 in. It also contains four bolt holes of diameter 1.25 in. Determining I for the plate gives

$$I = \frac{1}{12}bh^3 = \frac{1}{12}[(22'')(1.5'')^3 - 4(1.25'')(1.5'')^3] = 4.78 \text{ in}^4$$

Since $h = 1.5$ in. and the plate is rectangular in cross-section, $c = 0.75$ in. Based on the assumed behavior of the plate, the moment about the line of bolts in the plate is

$$M = F_{F,y}d = F_{F,y}(5.8'')$$

Substituting into the stress equation, this gives

$$\sigma_B = \frac{F_{F,y}}{1.099 \text{ in}^2}$$

Stress can be expressed as

$$\sigma_B = E\varepsilon$$

Strain data are given, so rewrite the stress equation

$$\varepsilon = \frac{F_{F,y}}{E(1.099 \text{ in}^2)} = \frac{F_{F,y}}{31871 \text{ kip}}$$

However, the force in the FRP is not necessarily of interest. The force in the anchor rods is of interest. The force in the anchor rods is given by

$$F_{B,y} = F_{F,y} + \frac{1}{2}(6.44'')(q_c)$$

Where q_c is the magnitude of the bearing force per inch at the end of the plate farthest from the column. q_c can be related to the force in the FRP by

$$q_c = (0.371 \text{ /in})(F_{F,y})$$

Substituting into the equation for $F_{B,y}$ gives

$$F_{B,y} = 2.195F_{F,y}$$

Finally,

$$F_{B,y} = (69957 \text{ kip})(\varepsilon)$$

In order to determine the total tensile force in a single anchor rod, $F_{B,y}$ must be divided by the number of anchor rods used to fasten the novel anchorage to the concrete. Additionally, the initial tensile force resulting from the tightening of the nut on the anchor rod must be subtracted from $F_{B,y}$ since $F_{B,y}$ represents the induced tensile force in the anchor rods resulting from anchoring the FRP. For this project, four anchor rods were used in each anchorage plate and an initial tension of 550 lbs. was observed. This final equation was used to predict the tensile forces in the anchor rods from the anchorage strain gauge data.

$$\text{Tension in Rods} = (17389 \text{ kips/rod})(\varepsilon) - 0.550 \text{ kips/rod}$$

BIBLIOGRAPHY

- ACI Committee 318. (2008). "Building Code Requirements for Structural Concrete (ACI 318-08) and Commentary." American Concrete Institute (ACI), Farmington Hills, MI.
- ACI Committee 355. (2007). "Qualification of Post-Installed Mechanical Anchors in Concrete and Commentary (ACI 355.2-07)." American Concrete Institute, Farmington Hills, MI.
- ACI Committee 440. (2008). "Guide for the Design and Construction of Externally Bonded FRP Systems for Strengthening Concrete Structures (ACI 440.2R-08)," American Concrete Institute, Farmington Hills, MI.
- Antonopoulos, C.P. and Triantafillou, T.C. (2003). "Experimental Investigation of FRP-Strengthened RC Beam-Column Joints," *Journal of Composites for Construction*, 7(1), 39-49.
- Applied Technology Council. (1997). "Seismic Design Criteria for Bridges and Other Highway Structures: Current and Future." *ATC-18*. Redwood City, CA.
- ASTM A193/A193M-10a. (2010). "Standard Specification for Alloy-Steel and Stainless Steel Bolting for High Temperature or High Pressure Service and Other Special Purpose Applications." ASTM International.
- ASTM A36/A36M-08. (2008). "Standard Specification for Carbon Structural Steel." ASTM International.
- ASTM C109/C109M-08. (2008). "Standard Test Method for Compressive Strength of Hydraulic Cement Mortars (Using 2-in. or [50-mm] Cube Specimens)." ASTM International.
- ASTM C39/C39M-09. (2009). "Standard Test Method for Compressive Strength of Cylindrical Concrete Specimens." ASTM International.
- ASTM D638-10. (2010). "Standard Test Method for Tensile Properties of Plastics." ASTM International.
- ASTM D695-10. (2010). "Standard Test Method for Compressive Properties of Rigid Plastics." ASTM International.
- ASTM D7234-05 (2005). "Standard Test Method for Pull-Off Adhesion Strength of Coatings on Concrete Using Portable Pull-Off Adhesion Testers." ASTM International.

- ASTM D790-10. (2010). "Standard Test Method for Flexural Properties of Unreinforced and Reinforced Plastics and Electrical Insulating Materials." ASTM International.
- Beigay, M., Young, D.T. and Gergely, J. "An Improved Composite Anchoring System," *QuakeWrap*, <<http://www.quakewrap.com/frp%20papers/An-Improved-Composite-Anchoring-System.pdf>> (7 Nov. 2010).
- Belarbi, A. and Bae, S.W. (2007). "An Experimental Study on the Effects of Environmental Exposures and Corrosion on RC Columns with FRP Composite Jackets." *Composites: Part B*, 38, 674-684.
- Ben Ouezdou, M., Belarbi, A., and Bae S.W. (2009). "Effective Bond Length of FRP Sheets Externally Bonded to Concrete." *International Journal of Concrete Structures and Materials*, 3(2), 127-131.
- Brosens, K. and Van Gemert, D. (2001). "Anchorage of Externally Bonded Reinforcements Subjected to Combined Shear/Bending Action." *FRP Composites in Civil Engineering: Proceedings of the International Conference on FRP Composites in Civil Engineering*, 12-15 Dec. 2001, Hong Kong, China, 589.
- Ceroni, F., Pecce, M., Matthys S. and Taerwe, L. (2008). "Debonding Strength and Anchorage Devices For Reinforced Concrete Elements Strengthened with FRP Sheets." *Composites: Part B*, 39, 429-441.
- Donchev, T. and Nabi, P. (2010). "Non-Bolted Anchorage Systems for CFRP Laminates Applied for Strengthening of RC Slabs." *Proceedings of the 5th International Conference on FRP Composites in Civil Engineering*, CICE, 27-29 Sept. 2010, Beijing, China.
- Eshwar, N., Ibell, T. and Nanni, A. (2003). "CFRP Strengthening of Concrete Bridges with Curved Soffits," *Proceedings of International Conference on Structural Faults and Repairs*, 1-3 July 2003, London, England.
- Foo, S., Naumoski, N. and Cheung, M. (2001). "Research and Application of Seismic Retrofit Technologies in Canada." *RPS/AES/Technology Directorate*, Public Works and Government Services Canada, Hull, Quebec, Canada.
- Galal, K. and Mofidi, A. (2009). "Strengthening RC Beams in Flexure Using New Hybrid FRP Sheet/Ductile Anchor System." *Journal of Composites for Construction*, ASCE, 13(3), 217-225.
- Hall, J.D., Schuman, P.M. and Hamilton III, H.R. (2002). "Ductile Anchorage for Connecting FRP Strengthening of Under-Reinforced Masonry Buildings." *Journal of Composites for Construction*, 6(1), 3-10.
- Hilti. (2008). "North American Product Technical Guide." Hilti, Inc., Tulsa, OK.

- Hiotakis, S. (2004). "Repair and Strengthening of Reinforced Concrete Shear Walls for Earthquake Resistance Using Externally Bonded Carbon Fibre Sheets and a Novel Anchor System." MS Thesis, Carleton University, Ottawa, Ontario, Canada.
- Holberg, A.M. (2000). "FRP/Steel Connection Strengthening of Unreinforced Concrete Masonry Shear Walls." MS Thesis, University of Wyoming, Laramie, WY, 93 pp.
- Huang, X. and Chen, G. (2005). "Bonding and Anchoring Characterization Between FRP Sheets, Concrete, and Viscoelastic Layers Under Static and Dynamic Loading." *Proceedings of the International Symposium on Bond Behavior of FRP in Structures*, 7-9 Dec. 2005, Hong Kong.
- Hwang, S-J., Tu, Y-S., Yeh, Y-H. and Chiou, T-C. (2004). "Reinforced Concrete Partition Walls Retrofitted with Carbon Fiber Reinforced Polymer." *ANCER Annual Meeting: Networking of Young Earthquake Engineering Researchers and Professionals*, ANCER, 2004.
- Kalfat, R. and Al-Mahaidi, R. (2010). "Investigation Into Bond Behaviour of a New CFRP Anchorage System for Concrete Utilising a Mechanically Strengthened Substrate." *Composite Structures*, 92(11), 2738-2746.
- Khalifa, A., Alkhrdaji, T., Nanni, A. and Lansburg, S. (1999). "Anchorage of Surface Mounted FRP Reinforcement." *Concrete International: Design and Construction*, 21(10), 49-54.
- Khan, A.A.R. and Ayub, T. (2010). "Effectiveness of U-Shaped CFRP Wraps as End Anchorages in Predominant Flexure and Shear Region." *Proceedings of the 5th International Conference on FRP Composites in Civil Engineering*, CICE, 27-29 Sept. 2010, Beijing, China.
- Kim, S.J. and Smith, S.T. (2010). "Pullout Strength Models for FRP Anchors in Uncracked Concrete." *Journal of Composites for Construction*, ASCE, 14(4), 406-414.
- Kobayashi, K., Fujii, S., Yabe, Y., Tsukagoshi, H., and Sugiyama, T. (2001). "Advanced Wrapping System With CF-Anchor – Stress Transfer Mechanism of CF-Anchor." *Non-metallic Reinforcement for Concrete Structures*, FRPRCS-5, 16-18 July 2001, London, England.
- Li, B. and Grace Chua, H.Y. (2009). "Rapid Repair of Earthquake Damaged RC Interior Beam-Wide Column Joints and Beam-Wall Joints using FRP Composites." *Key Engineering Materials*, Vols. 400-402, 491-499.
- MBrace[®] Composite Strengthening System. (2002). "Engineering Design Guidelines." 3rd Edition, *BASF Construction Chemicals – Building Systems*, Shakopee, MN.

- Micelli, F., Annaiah, R.H. and Nanni, A. (2002). "Strengthening of Short Shear Span Reinforced Concrete T Joists with Fiber-Reinforced Plastic Composites." *Journal of Composites for Construction*, 6(4), 264-271.
- Nagy-György, T., Moşoarcă, M., Stoian, V., Gergely, J. and Dan, D. (2005). "Retrofit of Reinforced Concrete Shear Walls With CFRP Composites." *Keep Concrete Attractive: Proceedings of the fib Symposium*, Hungarian Group of fib, 23-25 May 2005, Budapest, Hungary.
- Niu, H. and Wu, Z.S. (2000). "Study on the Debonding Failure Load of RC Beams Strengthened with FRP Sheets." *Journal of Structural Engineering*, JSCE, 46A, 1431-1441.
- Ortega, C. (2009). "Anchorage and Bond Characteristics of Externally Bonded FRP Laminates Used for Shear Strengthening of RC and PC Girders," MS Thesis, Missouri University of Science and Technology, Rolla, MO, 232 pp.
- Orton, S.L. (2007). "Development of a CFRP System to Provide Continuity in Existing Reinforced Concrete Buildings Vulnerable to Progressive Collapse." PhD Dissertation, University of Texas at Austin, Austin, Texas.
- Pan, J., Leung, C.K.Y., and Luo, M. (2010). "Effect of Multiple Secondary Cracks on FRP Debonding From the Substrate of Reinforced Concrete Beams." *Construction and Building Materials*, 24(12), 2507-2516.
- Piyong, Y., Silva, P.F. and Nanni, A. (2003). "Flexural Strengthening of Concrete Slabs by a Three-stage Prestressing FRP System Enhanced with the Presence of GFRP Anchor Spikes." *Proceedings of the International Conference Composites in Construction (CCC2003)*, 239-244.
- Prota, A., Manfredi, G., Balsamo, A., Nanni, A. and Cosenza, E. (2005). "Innovative Technique for Seismic Upgrade of RC Square Columns." *7th International Symposium on Fiber Reinforced Polymer for Reinforced Concrete Structures (FRPRCS-7)*, ACI, Kansas City, MO, Nov. 2005.
- Sadeghian, P., Rahai, A.R. and Ehsani, M.R. (2010). "Experimental Study of Rectangular RC Columns Strengthened with CFRP Composites Under Eccentric Loading." *Journal of Composites for Construction*, ASCE, 14(4), 443-450.
- Sadone, R., Quiertant, M., Chataigner, S., Mercier, J. and Ferrier, E. (2010). "Behaviour of an Innovative End-Anchored Externally Bonded CFRP Strengthening System Under Low Cycle Fatigue." *Proceedings of the 5th International Conference on FRP Composites in Civil Engineering*, CICE, 27-29 Sept. 2010, Beijing, China.

- Sami, Q., Ferrier, E., Michel, L., Si-Larbi, A. and Hamelin, P. (2010). "Experimental Investigation of CF Anchorage System Used for Seismic Retrofitting of RC Columns." *Proceedings of the 5th International Conference on FRP Composites in Civil Engineering*, CICE, 27-29 Sept. 2010, Beijing, China.
- Smith, S.T. and Teng, J.G. (2002). "FRP-Strengthened RC Beams. I: Review of Debonding Strength Models." *Engineering Structures*, 24, 385-395.
- Teng, J.G., Lam, L., Chan, W., and Wang, J. (2000). "Retrofitting of Deficient RC Cantilever Slabs Using GFRP Strips." *Journal of Composites for Construction*, ASCE, 4(2), 75-84.
- Teng, J.G., Cao, S.Y. and Lam, L. (2001). "Behaviour of GFRP-Strengthened RC Cantilever Slabs." *Construction and Building Materials*, 15(7), 339-349.
- Teng, J.G., Chen, J.F., Smith, S.T. and Lam, L. (2002). *FRP-Strengthened RC Structures*. John Wiley and Sons, Ltd., West Sussex, England.
- Teng, J.G., Chen, J.F., Smith, S.T., and Lam, L. (2003). "Behavior and Strength of FRP-Strengthened RC Structures: A State-of-the-Art Review." *Proceedings of the Institution of Civil Engineers – Structures and Buildings*, 156(1), 51-62.
- Vosooghi, A., Saiidi, M.S., and Gutierrez, J. (2008). "Rapid Repair of RC Bridge Columns Subjected to Earthquakes." *Proceedings of the 2nd International Conference on Concrete Repair, Rehabilitation, and Retrofitting*, ICCRRR, 24-26 November 2008, Cape Town, South Africa.
- Zhao, X.L. and Zhang, L. (2007). "State-of-the-Art Review on FRP Strengthened Steel Structures." *Engineering Structures*, 29, 1808-1823.
- Zhuo, J., Wang, F. and Li, T. (2009). "Application of FRP Strap in an Innovative Prestressed Method." *Journal of Materials in Civil Engineering*, ASCE, 21(4), 176-180.

VITA

Stephen Vincent Grelle was born in St. Louis, MO on April 17, 1987. He graduated from DeSmet Jesuit High School in Creve Coeur, MO in May 2005. In August 2005, he began attending Missouri University of Science and Technology (Missouri S&T), then called University of Missouri-Rolla. Stephen earned his Bachelor of Science degrees in Architectural Engineering and Civil Engineering from Missouri S&T in December 2009. As an undergraduate, Stephen played on the Missouri S&T Lacrosse Club Team and was a member of the Alpha Kappa Chapter of Pi Kappa Alpha, Order of Omega, and the Intercollegiate Knights Service Fraternity. Additionally, Stephen was a student member of the American Concrete Institute and the American Society of Civil Engineers.

Also as an undergraduate, Stephen performed research investigating a new enamel-coated rebar product under the advisory of Dr. Genda Chen from May 2007 to May 2008. From May until August of 2008, Stephen worked as an intern for McCarthy Building Companies in St. Louis, MO. He also worked as an intern for a subsidiary of McCarthy called MC Industrial, Inc. from May until August of 2009 in Lexington, KY.

Immediately after earning his Bachelor of Science degrees, Stephen enrolled in the Structural Engineering graduate program at Missouri S&T in January 2010. Stephen worked as a Graduate Teaching Assistant for the Spring 2010 semester, and as a Graduate Research Assistant for the entire time he was enrolled. He received the Missouri S&T Chancellor's Fellowship in May 2010 and won first place in the Chancellor's Fellowship Research Poster Competition in February 2011. Stephen also co-authored a conference paper and presented it at the ASCE Structures Congress in Las Vegas, NV in April 2011. He received his Master of Science in Civil Engineering degree in August 2011.